Trans-Tech™
Ceramics and Advanced Materials

Products for
RF/Microwave
Applications

DIELECTRIC MATERIALS

COAXIAL RESONATORS

CERAMIC FILTERS

MAGNETIC MATERIALS

Trans-Tech™
Ceramics and Advanced Materials

Trans-Tech, located in Adamstown, Maryland, provides complementary state-of-the-art RF/Microwave ceramic products. Trans-Tech designs and manufactures a complete line of RF and Microwave components that meet the stringent demands of today's commercial markets. Corporate headquarters is located in Adamstown, Maryland. Visit trans-techinc.com for more information.

65+ Years of Experience

Trans-Tech, Inc. is a world leader in technically advanced ceramics for over years, offers a complete line of High Quality, Low Cost ceramic based components for the Rf/Microwave Wireless Communication and Broadband Access markets. Our tightly controlled processes from raw materials, to firing, finishing, assembly and test, produce the highest quality and the most consistent reproducibility components available today.

Contact us

Contact us today and find out how we can work together to provide high-performance, low cost solutions designed for your specific requirement.

Visit us on the web at **www.trans-techinc.com** for new products, additional company information, application notes, product specs and so much more!

Products for
RF/Microwave Applications

This catalog lists general characteristics for Trans-Tech's Temperature stable materials.

TABLE OF CONTENTS

1

2

3

4

5

6

**A Designer's Guide to
Microwave Dielectric
Resonators**

Introduction & Applications
# for Temperature Stable Dielectric Resonators

Typical Applications

- Cellular Base Station Filters and Combiners
- PCS/PCN Filters and Combiners
- Direct Broadcast Satellite Receivers
- Police Radar Detectors
- LMDS/MMDS Wireless Cable TV
- Automobile Collision Avoidance Sensors
- Dielectric Resonator Antennas
- Motion Detectors

Introduction

Trans-Tech manufactures *millions* of dielectric resonators (DR's) each year for commercial and military markets, at frequencies from below 850 MHz to above 32 GHz. DR's fill the need for compact, temperature-stable, high Qu-factor microwave resonating elements. They are well understood and documented in engineering literature, and are commonly used in dielectric resonator oscillators (DRO's) and low-loss filters. In this catalog section, we refer to unmetallized ceramic cylinders, with or without an inner diameter, intended to operate in the $TE_{01\partial}$ mode, the most commonly used DR mode for filters and oscillators. The ceramic resonator is usually supported between a metal floor and a metal roof, sometimes (as in oscillators) with an intervening substrate attached to the metal floor. The support, when used, is a low-loss, low dielectric constant material that provides space between the DR and the metal floor. That space differs for filters and oscillators, and will be discussed later. There are usually metal sidewalls to complete a conducting boundary enclosing the DR. We call the enclosure a cavity. The cavity itself is not intended to be resonant without the ceramic DR. The important concept to grasp is that the resonant frequency of the $TE_{01\partial}$ mode DR is dependent upon not just the ceramic,

but also the cavity size and the mounting of the DR within the cavity. The same ceramic DR will give a different resonant frequency in a different cavity. The reason for this is that nearby conducting surfaces perturb the RF magnetic field of the $TE_{01\partial}$ mode, and the closer the metal is to the DR, the higher the frequency will be. This is a totally different principle of operation than TEM (coaxial) resonators, where the RF fields are contained primarily within the metallized ceramic.
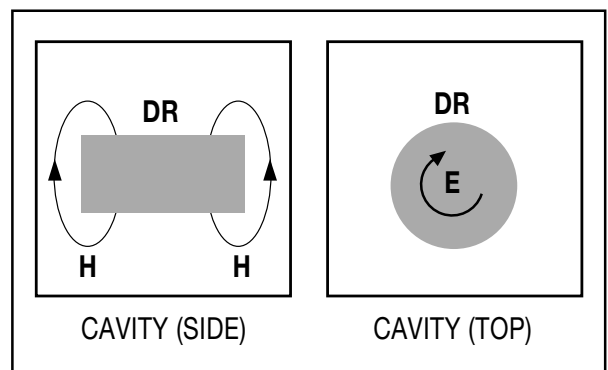
$TE_{01\partial}$ mode Dielectric Resonators

Some General Words About Trans-Tech Microwave Dielectrics

1

At Trans-Tech, we use the term dielectric constant whereas permitivity is cited in texts. In reality, dielectric constant isn't constant. It varies somewhat with the blend that's used to determine the ceramic's temperature coefficient, it varies slightly from lot to lot, and it changes perceptibly with tem-perature. We compensate for these effects by offering DR's sized to frequency, and with "custom-tailored" temperature coefficients when necessary.

Dielectric microwave materials are commonly assigned a loss tangent to permit an estimate of signal losses. But ceramic dielectric resonators operate at a specific frequency, in a specified geometry, which allows direct measurement and specification of Qu, the unloaded quality factor. Qu is a fun-damental resonator parameter which is particularly appropri-ate (and more useful than loss tangent) for filter and oscillator applications.

Ceramics don't age perceptibly. Any change in the resonant frequency of a DR over time can be attributed to change in the measurement cavity or measurement technique.

Ceramics don't absorb moisture noticeably, but moisture condensation on the surface of the DR can affect Qu. The Qu will recover when the moisture is driven off, for example, by self-heating of the DR in a transmitter filter.

The Qu of ceramic resonators can be degraded by finger oils, pencil marking, tape, and a host of other contaminants. Cleanliness is important.

Ceramics chip easily when they contact hard surfaces. Most tiny chips will not affect the electrical performance at all. Nei-ther is surface roughness particularly important: there are no currents in a ceramic dielectric resonator, only stored energy in the form of fields. Smooth surfaces are desireable from the standpoint of avoiding trapped contaminants.

Ceramics are "born" in kilns at temperatures over 1,000 C. They can stand much higher temperatures than the electronic equipment they are used with, i.e., far in excess of soldering temperatures. But ceramics conduct heat much more slowly than metals. A large enough temperature gradient through a ceramic part can cause failure due to differential expansion: we call this thermal shock. Sudden application of heat on one side of a thick ceramic part invites fracture.

Adhesives used to mount DR's must be chosen carefully. Adhesives will always degrade a DR's Qu, but Trans-Tech has developed bonding systems to minimize Qu loss while guaranteeing bond strength.

Overview by Material Type

	E'	Q x F	Relative Cost/volume	Linearity
8300	36	41,000	lowest	excellent
4300	43	43,000	low	good
4500	45	41,000	low	OK for small temp range
3500	35	70,000	moderate	excellent
8700	30	100,000	high	good
2900	30	110,000	high	good

Note: the Q x F product applies when cavity size is large enough that metal wall losses can be neglected (cavity size approximately 3 times the DR size), and somewhat below 2 GHz.

8300

Available in a wide range of temperature coefficients, 8300 is a workhorse composition that combines good Qu with low cost. Wideband filter applications benefit from E'36 for coupling that's easier to achieve than with the 4300 or 4500 series. Millions of Ku-Band LNB assemblies of 8300 material with Alumina supports have been delivered in tape-and-reel format for our customers.

4300

Popular for narrowband UMTS filter applications, the 4300 series is the correct choice for size reduction, where good linearity is required for temperature compensation.

3500

Introduced in June 2000, the 3500 series provides a Qu boost from generic E'36 ceramics, yet without the costly high Tantalum content. This material is popular in narrowband 2 GHz filter applications and in X/Ku-band satellite LNB where better phase noise performance is required.

4500

Originally developed with AMPS and GSM autotuned cellular combiners in mind, the 4500 series offers the best size reduction vs. Qu tradeoff where some non-linearity of Fo vs. temperature can be tolerated, such as moderate-bandwidth filters.
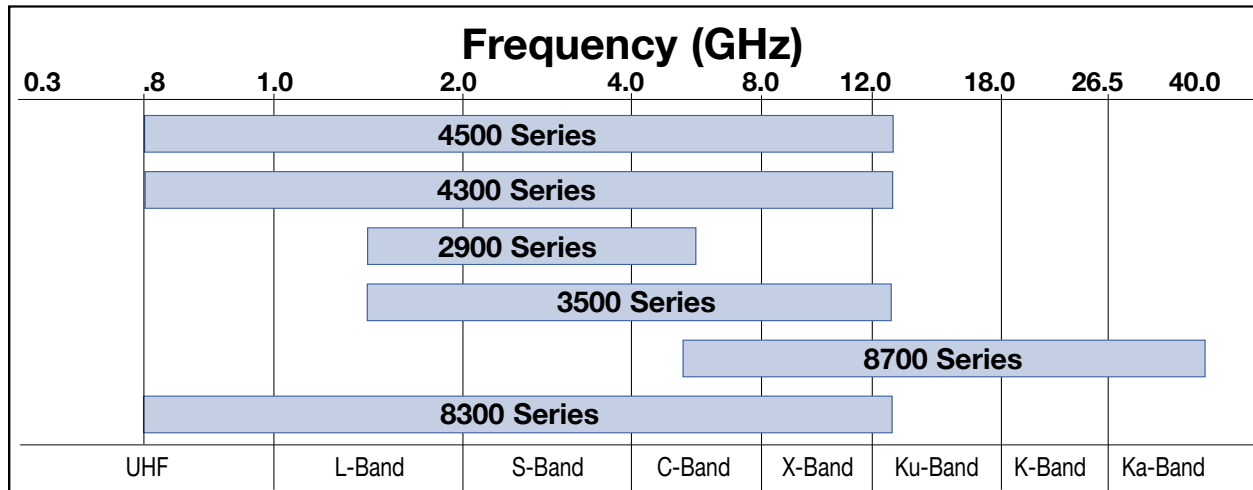
2900

Originally developed for narrow-band PCS and DCS autotuned combiners where highest Qu was paramount. This material is occasionally used in multipole filters where the highest Qu is needed for lowest losses. Sizes have been produced for applications as low as 1800 MHz, but the Tantalum additives drive cost up.

8700

Predecessor of the 2900 series, 8700 is still popular at high frequencies, generally above 4 GHz. We have produced this material for automotive collision avoidance and motion-detection DRO's near 24 GHz, and fiber-optic clock-recovery applications near 38 GHz. The low E'30 facilitates manufacturing tolerances for the highest-frequency small part sizes.

Figures present a summary overview of the temperature compensated dielectric resonator materials available from Trans-Tech.

Frequency (GHz)

0.3	.8	1.0	2.0	4.0	8.0	12.0	18.0	26.5	40.0

4500 Series

4300 Series

2900 Series

3500 Series

8700 Series

8300 Series

UHF	L-Band	S-Band	C-Band	X-Band	Ku-Band	K-Band	Ka-Band

Suggested Frequency Range for Dielectric Resonator Materials.

For cellular and PCS applications we offer customized products in 4500, 2900 and 8300 Series materials.

For high frequency applications we offer 4500, 8700 and 8300 Series materials. Tables of suggested dimensions are provided in the designated sections.

Product Characteristics		Series		
		4500	**4300**	**2900**
Dielectric Constant		44.7 - 46.2	43.0	29.0 - 30.7
Q (1/tanδ)		>9,500	>9,500	>50,000
		at 4.3 GHz	at 4.3 GHz	at 2.0 GHz
Available Frequency (MHz)	Disc Type	800-13800	800-13,800	1500-5550
	Cylinder Type	800-9010	800-9010	1500-5550
	Available τ_f (ppm/°C)	6/3/0/-3/-6	6/3/0/-3/-6	4/2/0/-2
Available τ_f Tolerance (ppm/°C)		±2 or ±1	±2 or ±1	±2 or ±1
Composition		Zr Titanium Based	Zr Titanium Based	BaZnTa Oxide

Product Characteristics		Series		
		3500	**8700**	**8300**
Dielectric Constant		34.5 - 36.5	29.5-31	35.0 - 36.5
Q (1/tanδ)		>35,000	10,000	>9,500
		at 2 GHz	at 10.0 GHz	at 4.3 GHz
Available Frequency (MHz)	Disc Type	1500-13800	5550-32150	800-13800
	Cylinder Type	1500-9010	5550-9870	800-9010
	Available τ_f (ppm/°C)	6/3/0/-3	4/2/0	9/6/3/0/-3
Available τ_f Tolerance (ppm/°C)		±2 or ±1	±2 or ±1	±2 or ±1
Composition		BaZnCoNb	BaZnTa Oxide	Titanate Based

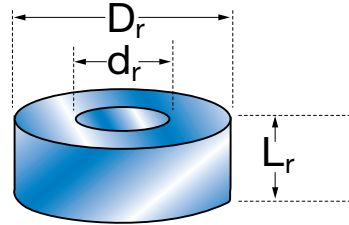*Summary of Product Characteristics of Dielectric Resonator Materials*

*All components manufactured based on capability and customer design.

Standard Dielectric Resonator Diameters and Sizes

Disks Type
Mechanical Configuration
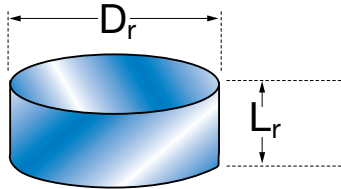
Cylinder Type
Mechanical Configuration

Disks Cylinders Assemblies

Standard Outside Diameter (D_r)

0.975 ± 0.002	0.470 ± 0.001	0.200 ± 0.001
0.905 ± 0.001	0.435 ± 0.001	0.190 ± 0.001
0.840 ± 0.001	0.405 ± 0.001	0.180 ± 0.001
0.785 ± 0.001	0.375 ± 0.001	0.170 ± 0.001
0.730 ± 0.001	0.350 ± 0.001	0.160 ± 0.001
0.675 ± 0.001	0.325 ± 0.001	0.150 ± 0.001
0.630 ± 0.001	0.305 ± 0.001	0.140 ± 0.001
0.585 ± 0.001	0.285 ± 0.001	0.130 ± 0.001
0.545 ± 0.001	0.265 ± 0.001	0.120 ± 0.001
0.505 ± 0.001	0.245 ± 0.001	0.112 ± 0.001
	0.230 ± 0.001	0.104 ± 0.001
	0.215 ± 0.001	0.096 ± 0.001
		0.089 ± 0.001
		0.082 ± 0.001
		0.076 ± 0.001

Standard Inside Diameter (d_r)

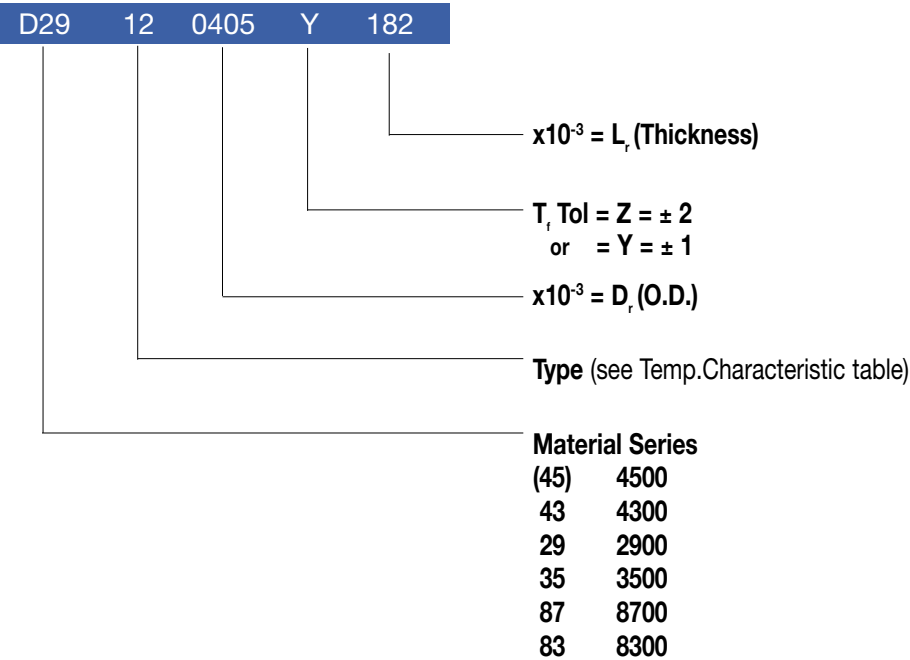| |
|---|
| 0.162 ± 0.004 |
| 0.122 ± 0.004 |
| 0.083 ± 0.004 |

We offer a broad range of standard catalog sizes which are approximately tailored for frequency. All sizes are custom, and are not to be interpreted as limitations in dimensions. The optimum DR will be uniquely sized for each application. For each diameter, we *suggest a* height range (L_r) which is 35% to 45% of the resonator's diameter. This ratio is optimum for spurious mode-free operation in the case of an *isolated* resonator (see reference article by S. Cohn), but does not guarantee mode separation where the DR enclosure influences performance.

We also offer DR's with center holes (cylinders), generally in specified inner diameters (ID's). The ID will raise the frequency above that of a solid DR by 1% to 2% if the inner hole is less than one-fourth the resonator's diameter (see reference by R. Mongia). The inner hole tends to increase separation of the $TE_{01\delta}$ mode frequency from that of higher-order modes. The more practical reason for choosing a cylindrical resonator is simply ease of mounting with a low dielectric constant non-conducting screw, such as Nylon. Supports are available with companion ID's for screw clearance. For cost-saving, the ID's of the cylindrical resonators are less critically toleranced than the outer diameters. This is no disadvantage when the DR's are properly sized for frequency, as described above.
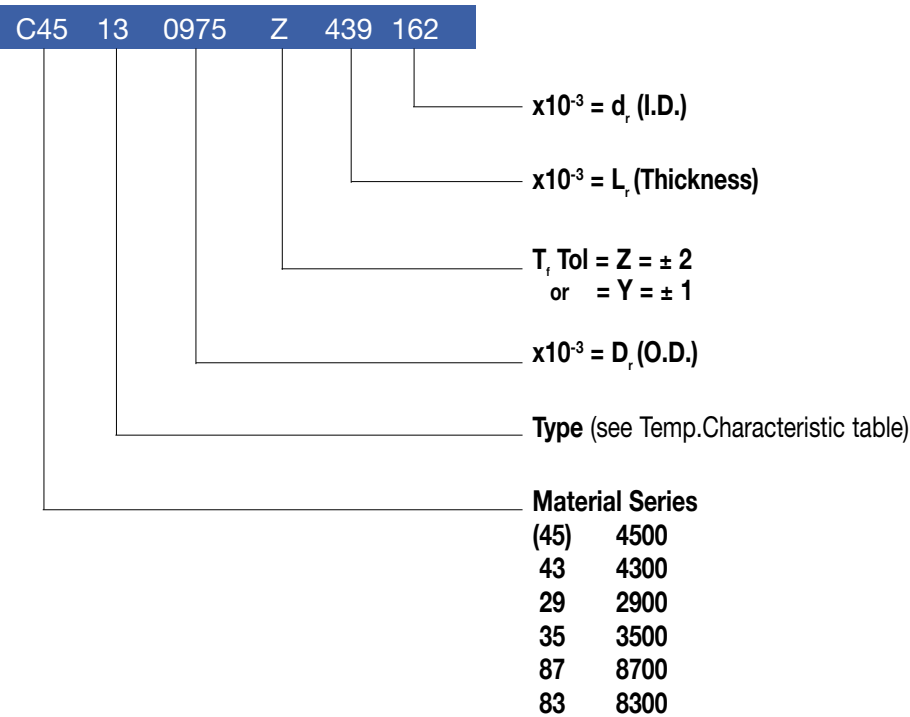
Dielectric Resonator Part Numbering

Dielectric Resonators can be ordered by dimensions only (rather than ferquency-tuned) with the following part numbering system:
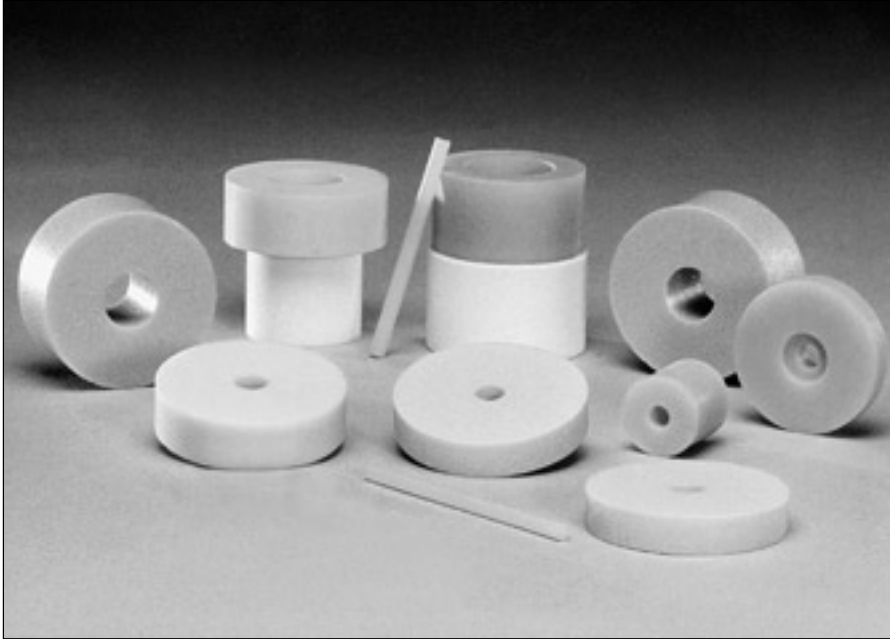
Disk Type *Example:* D2912-0405-Y-182

D29	12	0405	Y	182

$\times 10^{-3} = L_r$ **(Thickness)**

T_f **Tol = Z = ± 2**
  or   **= Y = ± 1**

$\times 10^{-3} = D_r$ **(O.D.)**

Type (see Temp.Characteristic table)

Material Series
(45)	4500
43	4300
29	2900
35	3500
87	8700
83	8300

Cylinder Type *Example:* C4512-0975-Z-439-162

C45	13	0975	Z	439	162

$\times 10^{-3} = d_r$ **(I.D.)**

$\times 10^{-3} = L_r$ **(Thickness)**

T_f **Tol = Z = ± 2**
  or   **= Y = ± 1**

$\times 10^{-3} = D_r$ **(O.D.)**

Type (see Temp.Characteristic table)

Material Series
(45)	4500
43	4300
29	2900
35	3500
87	8700
83	8300

2900 Series
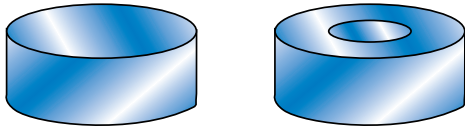# Temperature Stable Dielectric Resonators

Features
- 100,000 Qu x F product
- matching tuners available
- matching low-loss Alumin supports available

Benefits
- Lowest possible insertion loss
- Small size
- Frequency stability vs temperature

Applications
- Microwave filters
- PCS / DCS filters and combiners

Introduction

The D2900 series ceramic is optimized for high Qu in the 1800 MHz - 2000 MHz range, especially for low-loss PCS and DCS filter and combiner applications. Qu x F product is cavity-dependent, but is generally 100,000 or more. Although usually cylindrical, virtually all parts are customer-specific geometries which are unique to the application. For example, combiner resonators may have large inner diameters (ID's) to permit dielectric tuning with a moveable slug of the same or similar material. Or, the resonator may have a small hole for mounting purposes and might be tuned by a moveable ceramic disc. We recommend high-purity Alumina supports to retain the high Qu-factor, and we provide custom resonator/ support assemblies bonded with proprietary adhesives. Resonators or resonator/support assemblies are sized to frequency, typically +/-5 MHz tolerance, in customer-specified cavities, and 100% inspected. Please contact our factory with specific requirements.

Typical Sizes

PCS: 1.20" OD x 0.6" ID x 0.6" height   (2000 MHz)
DCS: 1.33" OD x 0.6" ID x 0.6" height   (1834 MHz)
Custom sizes available for 1500-5550 MHz

Material Characteristics

Dielectric Constant 29.0-30.7
Temperature Coefficient of Resonant Frequency
   (τf) (ppm/°C) . . . . -2 to +4
Q (1/tan δ) min . . . .~50,000 at 2.0 GHz
Thermal Expansion
(ppm/°C) (20-°C) . . . . >10
Thermal Conductivity
(cal/cm sec°C) @ 25°C . . . .~0.006
Specific Heat (cal/g °C) 0.07
Density (g/cc) . . . . >7.6
Water Absorption . . . . <0.01
Composition . . . . Ba, Zn, Ta-oxide
Color . . . . .Yellow

Temperature Characteristics

| Series	Type	Dielectric Constant	Temperature Coefficient of f_o (τ_f)$\pm$2	Q at 2.0 GHZ
D/C29	14	30.7 $\pm$ 1	+4 ppm/°C	~50,000
D/C29	12	30.4 $\pm$ 1	+2 ppm/°C	~50,000
D/C29	00	30.0 $\pm$ 1	0 ppm/°C	~50,000
D/C29	02	29.0 $\pm$ 1	-2 ppm/°C	~50,000

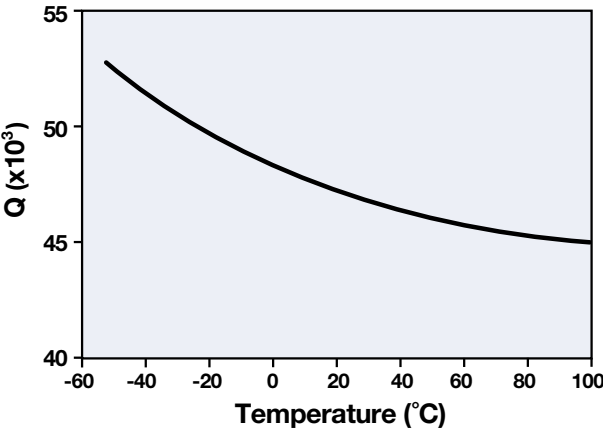*Note: Contact factory for custom τ_f and other tolerances.*

2900 Series
Temperature Stable Resonator

1

Typical Q vs Frequency

Typical (ε_r) vs Frequency

Courtney Parallel Plate Method
Measurement Accuracy 0.5%
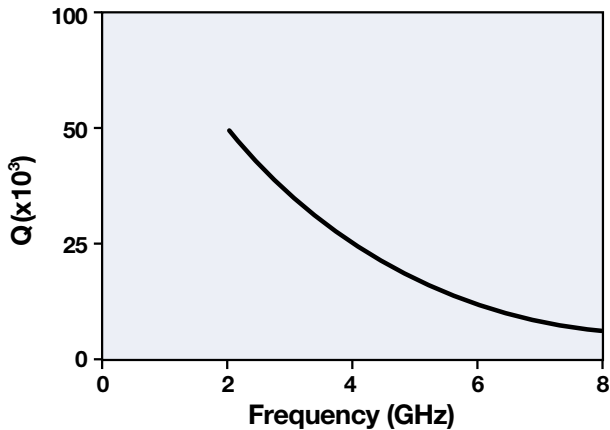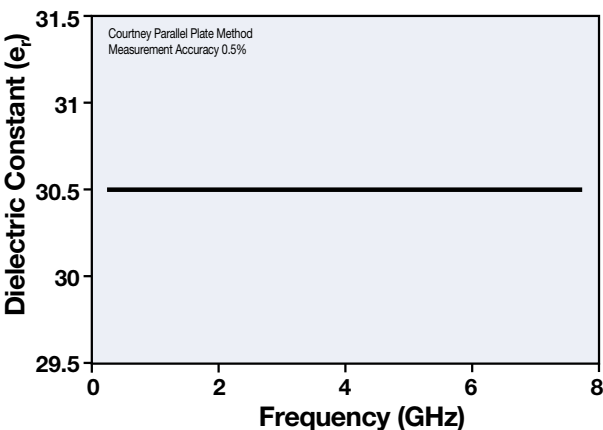
Typical Q vs Temperature @ 2 GHz

4300 Series
Temperature Stable Dielectric Resonators
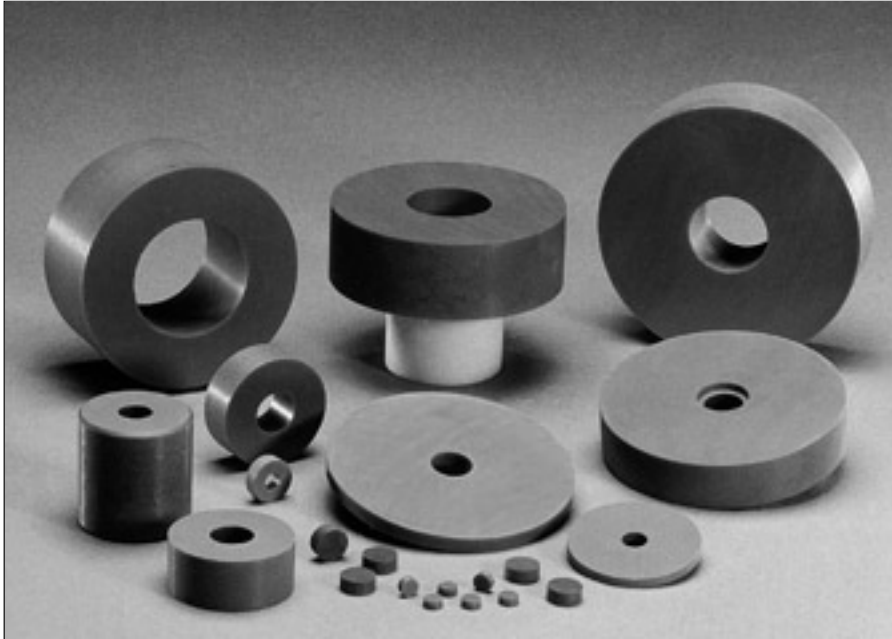
Features
- High ε'
- High Q
- Wide range of τ_f
- High Q assemblies available

Benefits
- Small size
- Repeatability of design
- Low insertion loss
- High stability DRO design
- Ease of compensation for temperature drift
- Linear temperature coefficient

Applications
- Basestation filters and combiners
- Microwave filters and oscillators
- All cellular & PCN platforms
- DRO's for LNB's

Introduction

The 4300 series is designed for frequency operation from 1500 MHz to 13.8 GHz. This series offers a reduced size while maintaining high Q. Custom temperature coefficients are available.

Material Characteristics

Dielectric Constant . . . . 43.0 $\pm$ 0.75
Temperature Coefficient of Resonant Frequency
  (τ_f) (ppm/°C) . . . . -6 to +6
Q (1/tan δ) min . . . . 35,000 at 850 MHz
. . . . 9,500 at 4.3 GHz
Thermal Expansion
(ppm/°C) (20-200°C) 6.5
Thermal Conductivity
(cal/cm sec°C) @ 25°C . . . . ~0.005
Non-Linear Coefficient ($\tau_{f'}$)(ppm/°C^2) . . . . -0.01
Specific Heat (cal/g °C) . . . . ~0.15
Density (g/cc) 5.00
Water Absorption . . . . <0.01
Composition . . . . Zirconium Titanate Based

Temperature Characteristics

Series	Type	Dielectric Constant	Temperature Coefficient of f_o (τ_f)$\pm$2	Q at 4.3 GHZ
D/C43	16	43.0 $\pm$ 0.75	+6	>9,500
D/C43	13	43.0 $\pm$ 0.75	+3	>9,500
D/C43	00	43.0 $\pm$ 0.75	0	>9,500
D/C43	03	43.0 $\pm$ 0.75	-3	>9,500
D/C43	06	43.0 $\pm$ 0.75	-6	>9,500

Note: Contact factory for custom τ_f and other tolerances.
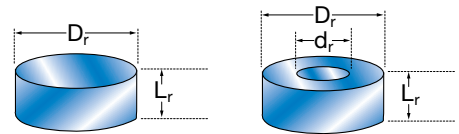
	Disk	Cylinder
Diameter Range		
D_r	0.975 - 0.160	0.975 - 0.245
L_r	35% to 45% of D_r	35% to 45% of D_r
d_r	N/A	0.162 - 0.083
Frequency Range (GHz)		
	1.85 to 13.5	1.85 to 8.01

Note: Contact factory for custom sizes.

4300 Series
Temperature Stable Resonator
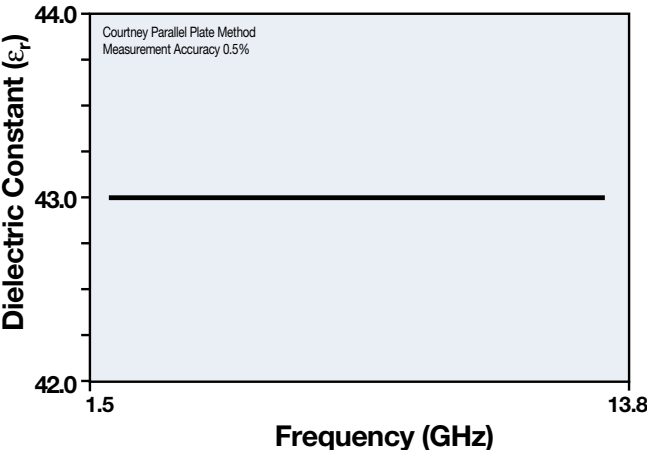
1

Typical Q vs Frequency

Typical (ε_r) vs Frequency

Courtney Parallel Plate Method
Measurement Accuracy 0.5%

Q vs Temperature (Typical)

Q @ 850MHz

Q @ 4.3 GHz
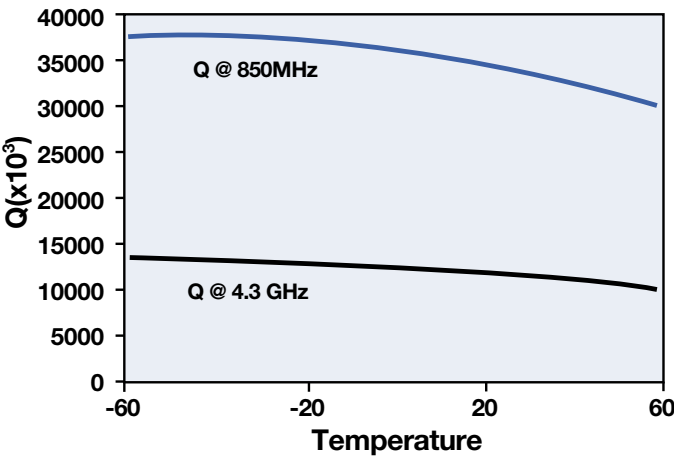
4500 Series
Temperature Stable Dielectric Resonators

Features
- High ε'
- High Q
- Wide range of τ_f
- High Q assemblies available

Benefits
- Small size
- Repeatability of design
- Low insertion loss
- High stability DRO design
- Ease of compensation for temperature drift

Applications
- Microwave filters and oscillators to 13.5 GHz
- DRO's for LNB's
- Cellular and PCN basestation filters and combiners

Introduction

4500 is designed for cellular radio filters and combiners, and offers an excellent compromise of Q, dielectric constant and cost, with a wide range of temperature coefficients. It is available as an assembly, with an alumina support, with customized thermal and electrical parameters, for high power applications.

Material Characteristics

Dielectric Constant 44.7- 46.2
Temperature Coefficient of Resonant Frequency
  (τf) (ppm/°C) .... -6 to +6
Q (1/tan δ) min .... 35,000 at 850 MHz
  .... 9,500 at 4.3 GHz
Thermal Expansion
(ppm/°C) (20-200°C) 6.5
Thermal Conductivity
(cal/cm sec°C) @ 25°C .... ~0.005
Specific Heat (cal/g °C) .... ~0.15
Density (g/cc) 4.95
Water Absorption .... <0.01
Composition .... Zirconium Titanate Based
Color .... Brown

Temperature Characteristics

Series	Type	Dielectric Constant	Temperature Coefficient of f_o (τ_f) ±2	Q at 4.3 GHZ
D/C45	16	46.2 ± 1.5	+6 ppm/°C	>9,500
D/C45	13	45.7 ± 1.5	+3 ppm/°C	>9,500
D/C45	00	45.2 ± 1.5	0 ppm/°C	>9,500
D/C45	03	44.9 ± 1.5	-3 ppm/°C	>9,500
D/C45	06	44.7 ± 1.5	-6 ppm/°C	>9,500

Note: Contact factory for custom τ_f and other tolerances.
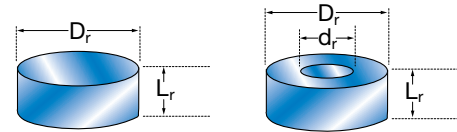
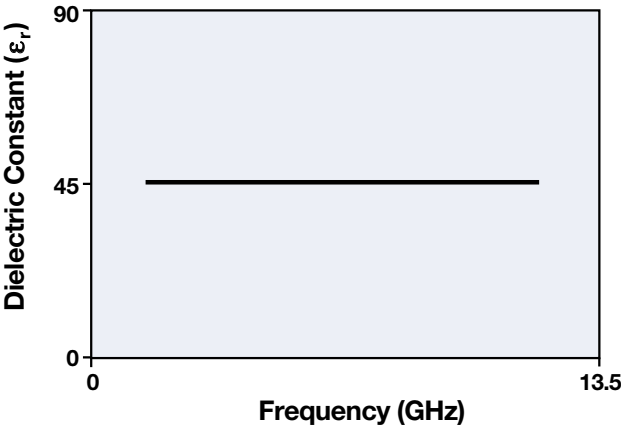|	Disk	Cylinder
	Diameter Range	
D_r	0.975 - 0.160	0.975 - 0.245
L_r	35% to 45% of D_r	35% to 45% of D_r
d_r	N/A	0.162 - 0.083
	Frequency Range (GHz)	
	1.85 to 13.5	1.85 to 8.01

Note: Contact factory for custom sizes.

4500 Series
Temperature Stable Dielectric Resonator

1

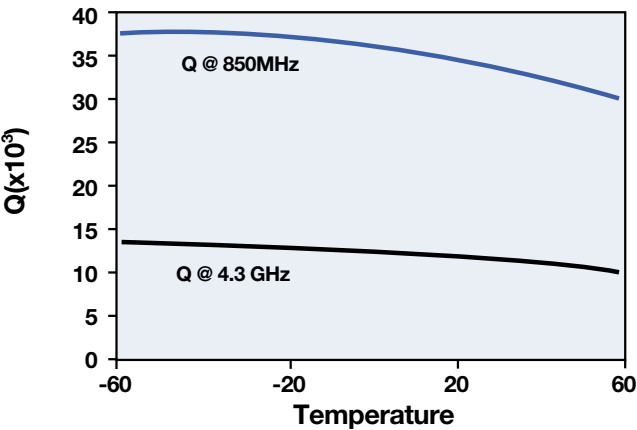## Typical Q vs Frequency
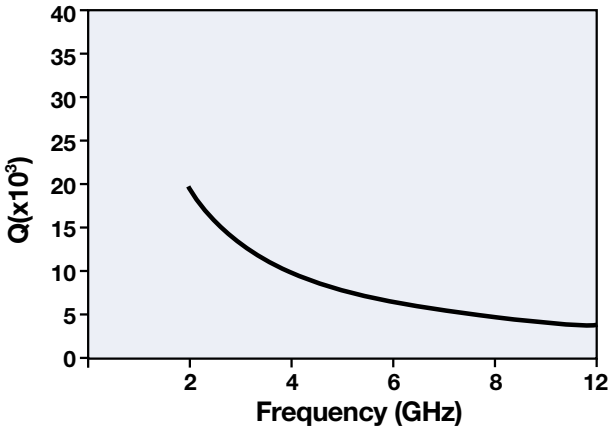
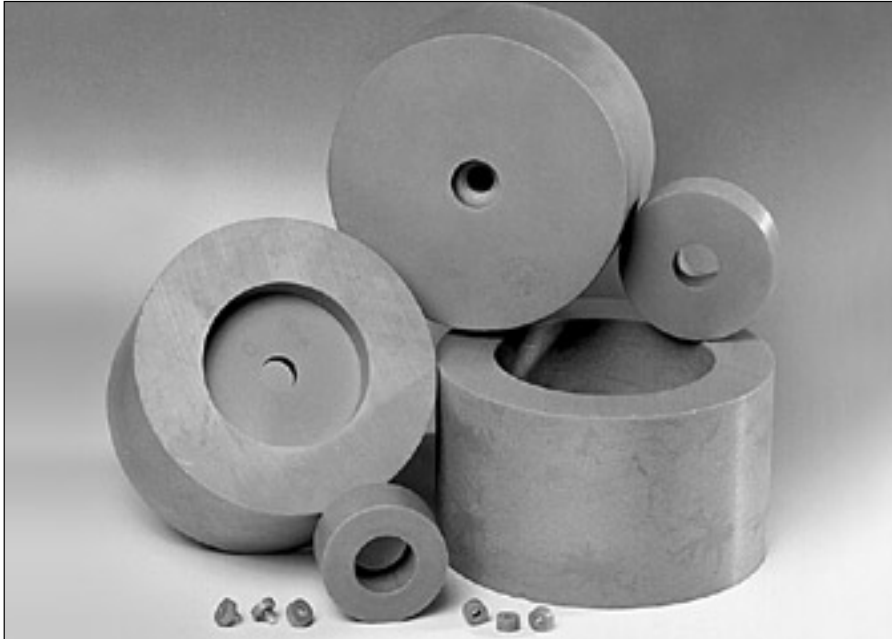## Typical (ε_r) vs Frequency

Q vs Temperature (Typical)

8300 Series
Temperature Stable Resonators

Features
- High ε'
- High Q
- linear τ_f
- Frequency stability vs temperature

Benefits
- Reduced size & weight
- Low loss
- Close channel spacing
- Ease of temperature compensation

Applications
- AMPS/GSM/PCS/DBS/TVRO
- Dielectric resonator oscillators
- Microwave filters and combiners

Introduction

8300 is Trans-Tech's standard material for PCS/PCN/DCS/GSM application, combining good Q with reasonable cost. A wide range of temperature coefficients is available.

Material Characteristics

Dielectric Constant 35.0-36.5
Temperature Coefficient of Resonant Frequency
   (τf) (ppm/°C) . . . .-3 to +9
Q (1/tan δ) min . . . . .9,500 at 4.3GHz
   . . . . .and 28,000 at 850 MHz
Insulation Resistance (ohm cm)
  (volume resistivity) @ 25°C . . . .~10^{13}
Thermal Expansion (ppm/°C) (20-200°C) 10
Thermal Conductivity (cal/cm sec°C) @ 25°C 0.0045
Specific Heat (cal/g °C) 0.15
Density (g/cc) . . . .>4.65
Water Absorption . . . .<0.01
Composition . . . . .Titanate Based
Color . . . . Rust

Size Recommendations

Common sizes accommodate frequencies from 0.8 to 13.5 GHz. Trans-Tech's market leadership in this area has given us experience to guide designers toward the best mechanical configuration for optional performance in customer cavities.

Temperature Characteristics

Series	Type	Dielectric Constant	Temperature Coefficient of f_o (τ_f) $\pm$ 2	Q at 4.3 GHZ
D/C83	74	36.5 $\pm$ 1	+9 ppm/°C	>9,500
D/C83	73	36.0 $\pm$ 1	+6 ppm/°C	>9,500
D/C83	72	35.7 $\pm$ 1	+3 ppm/°C	>9,500
D/C83	71	35.5 $\pm$ 1	0 ppm/°C	>9,500
D/C83	70	35.0 $\pm$ 1	-3 ppm/°C	>9,500

Note: Contact factory for custom τ_f and tolerances.
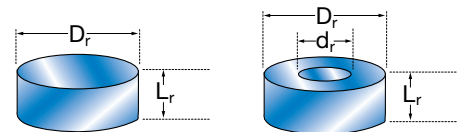
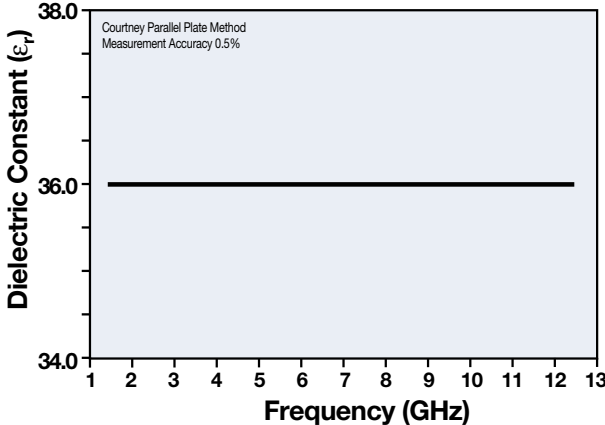|	Disk	Cylinder
	Diameter Range	
D_r	0.975 - 0.160	1.400 - .245
L_r	35% to 45% of D_r	35% to 45% of D_r
d_r	N/A	0.162 - 0.083
	Frequency Range	
	2080 to 13800 MHz	1450 to 9010 MHz

Note: Components will be custom manufactured. Consult Trans-Tech's Applications Engineering for advice on supports, tuning, and resonator configurations. Frequency accuracy to 0.5% of a customer provided correlation sample is standard.

8300 Series
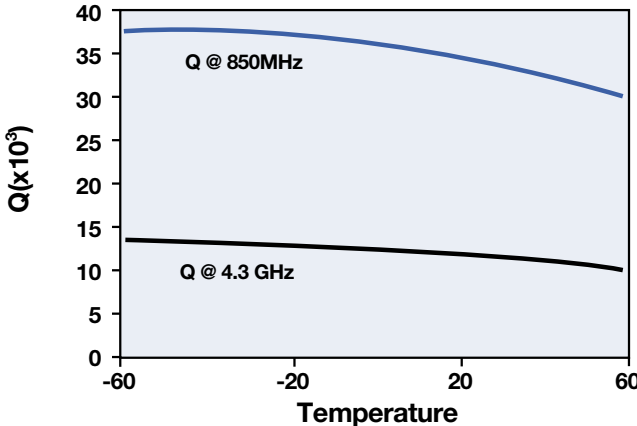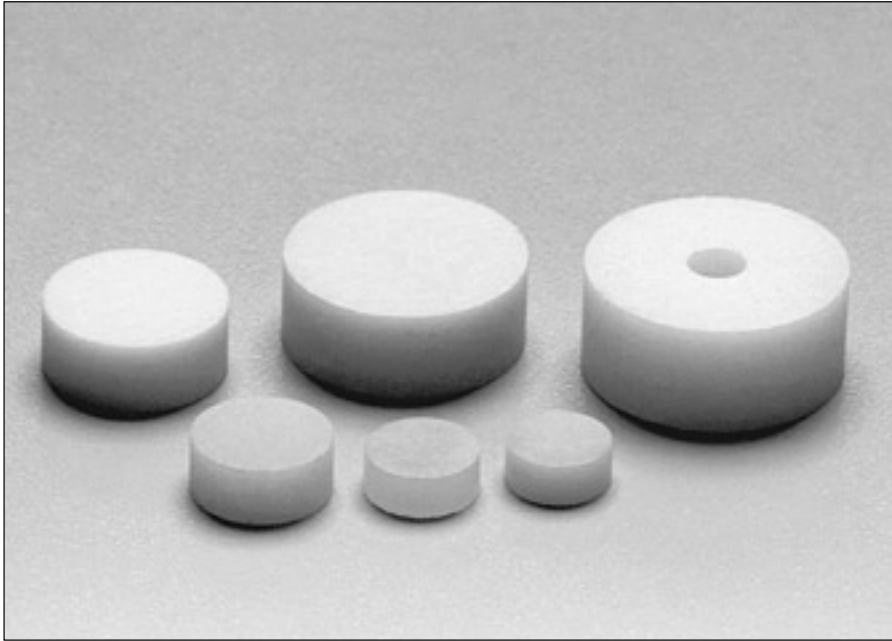# Temperature Stable Resonator
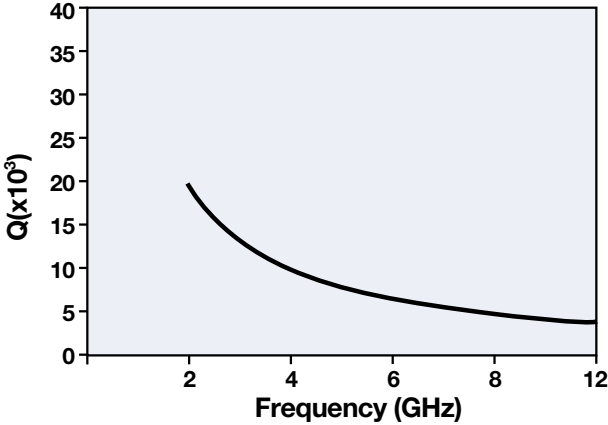
Typical Q vs Frequency

Typical (eᵣ) vs Frequency

Courtney Parallel Plate Method
Measurement Accuracy 0.5%

Q vs Temperature (Typical)

Q @ 850MHz

Q @ 4.3 GHz

8700 Series
Temperature Stable Resonators

Features
- High ε_r
- Q>10,000
- Wide range of τ_f
- Frequency stability vs temperature

Benefits
- Small size
- Reduced Weight
- High stability DRO design
- Ease of compensation for temperature drift
- Repeatability of design
- Negligible aging effects

Applications
- Microwave filters
- LMDS
- High stability DROs
- Satellite communications
- Telemetry
- Automobile Collision Avoidance

Introduction

The 8700 series is designed for use from 6 GHz to 40 GHz and features excellent loss characteristics. This series offers a wide selection of temperature coefficients of resonant frequency for easier circuit compensation and a Q greater than 10,000 at 10 GHz for high stability DRO designs up to millimeter wave frequencies.

Material Characteristics

Dielectric Constant 29.0- 30.7
Temperature Coefficient of Resonant Frequency
   (τ_f) (ppm/°C) . . . . -2 to +4
Q (1/tanδ) min . . . . >10,000 at 10.0 GHz
Insulation Resistance (ohm cm) . . . . >-10^{14}
Thermal Expansion
 (ppm/°C) (20-200 °C) 10
Thermal Conductivity
 (cal/cm°C sec) at 25°C 0.006
Specific Heat (cal/g °C) 0.07
Density (g/cc) . . . . >7.6
Water Absorption (%) . . . . <.01
Vicker Hardness No. (kg/mm) 700
Flexural Strength (psi) 10,000
Composition . . . . Ba, Zn, Ta-oxide (perovskite)
Color . . . . Yellow

Temperature Characteristics

Series	Type	Dielectric Constant	Temperature Coefficient of f_o (τ_f)±2	Q at 10.0 GHz
D/C 87	35	30.7 ± 1	±4 ppm/°C	>10,000
D/C 87	34	30.4 ± 1	±2 ppm/°C	>10,000
D/C 87	33	30.0 ± 1	0 ppm/°C	>10,000
D/C 87	32	29.0 ± 1	- 2 ppm/°C	>10,000

Note: Contact factory for custom τ_f and tolerances.
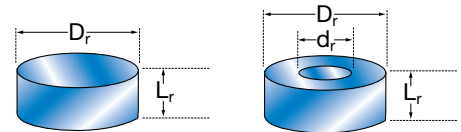
	Disk	Cylinder
	Diameter Range	
D_r	0.405 - 0.076	0.405 - 0.245
L_r	35% to 45% of D_r	35% to 45% of D_r
d_r	N/A	.083
	Frequency Range	
	5550 to 32150	5550 to 9870

8700 Series
Temperature Stable Resonator

Typical Q vs Frequency

Typical (ε_r) vs Frequency

Courtney Parallel Plate Method
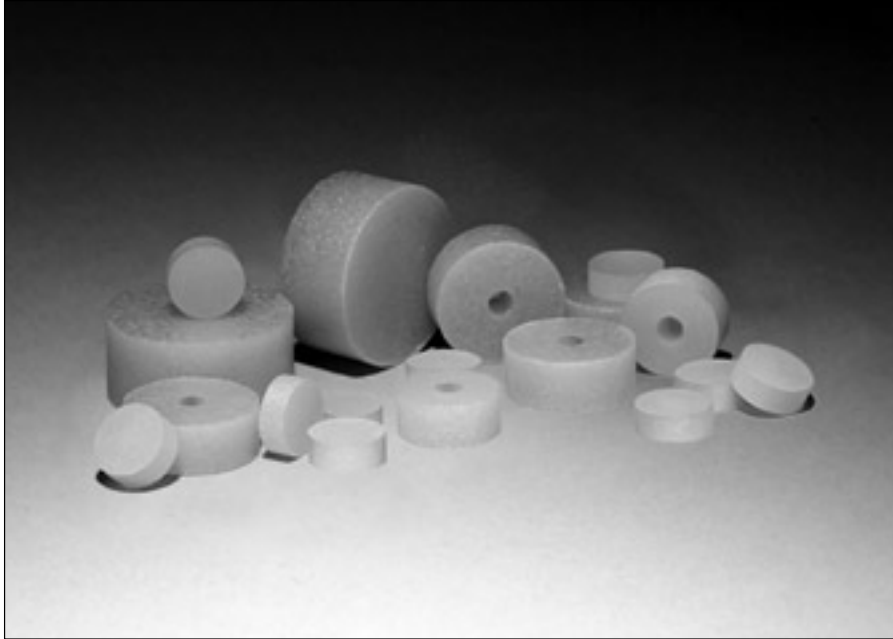Measurement Accuracy 0.5%
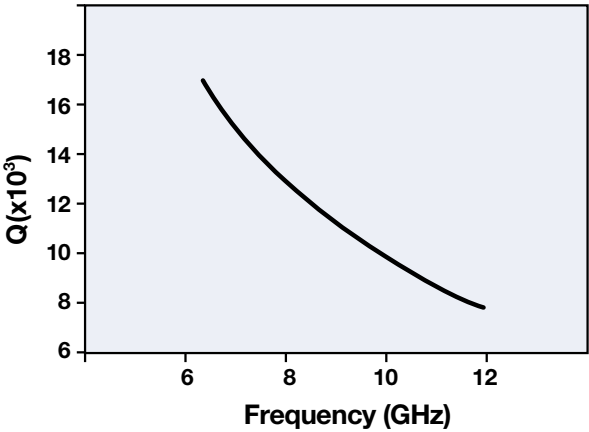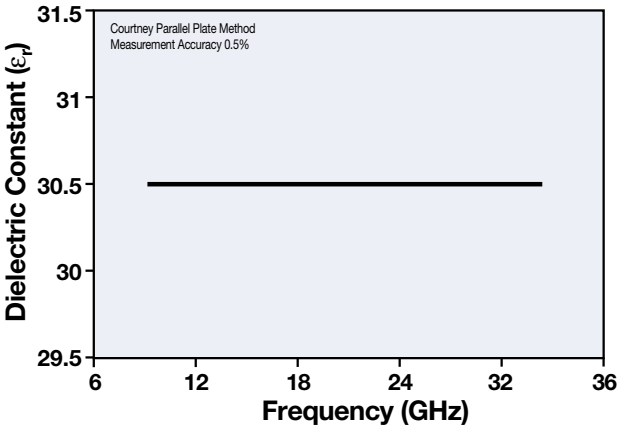
Typical Q vs Temperature @ 10 GHz
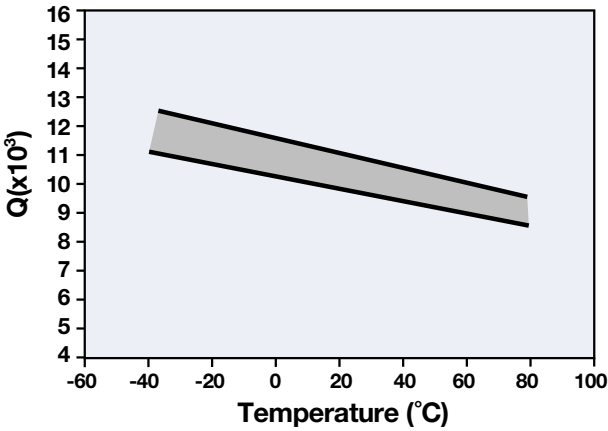
3500 Series
Temperature Stable Dielectric Resonators

Features
■ High Q (Qf >70,000)
■ Linear τ_f
■ Low cost
■ Wide τ_f range
■ Mid range E'

Benefits
■ Potential size reduction
■ Temperature stability
■ Low loss
■ Applications up to 13.8 GHz

Applications
■ Multi-pole filters
■ DRO's
■ Fixed & Autotuned combiners

Introduction

The 3500 ceramic material is intended primarily for osillators and multi-pole filters within the 1500 MHz - 13,800 MHz frequency range. This material typically yields an unloaded Q of 35,000 at 2 GHz.

Material Characteristics

Dielectric Constant . . . . 33.5 - 35.5
Temperature Coefficient of Resonant Frequency
   (τ_f) (ppm/°C) (25 to 60°C) . . . .-3 to +6
Q(1/tan δ) min . . . .>35,000 at 2 GHz
Thermal Expansion
   (ppm/°C) (20-200°C) 10
Thermal Conductivity
   (cal/cm-sec °C) at 25°C . . . .~0.006
Non-Linearity Coefficient (τ'_f) (ppm/°C^2) . . . .<0.01
Specific Heat (cal/g°C) . . . .~.07
Density (g/cc) . . . .>6.4
Water Absorption (%) . . . .<.01

Temperature Characteristics

Series	Type	Dielectric Constant	Temperature Coefficient of f_o (τ_f)$\pm$$^1/_2$	Q at 4.3 GHZ
D/C35	16	35.5	+6	>35,000
D/C35	13	34.75	+3	>35,000
D/C35	00	34.5	0	>35,000
D/C35	03	33.5	-3	>35,000

Note: Contact factory for custom τ_f and other tolerances.

3500 Series
Temperature Stable Resonator

Typical Q vs Frequency

Typical (ε_r) vs Frequency

Courtney Parallel Plate Method
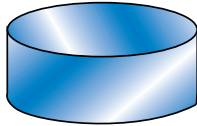Measurement Accuracy 0.5%

Typical Q vs Temperature @ 2 GHz

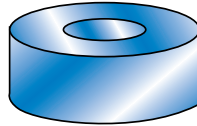# Dielectric & Alumina Supports

Dielectric Supports

Dielectric supports can be used with all disc or cylinder type dielectric resonators to improve coupling and temperature stability. Contact Trans-Tech for other support configurations.

Disk Type **Cylinder Type**

For disk type support, use Ds & Ls dimension only.

$D_s(\pm.005)$	$d_s(\pm.004)$	$L_s(\pm.001)$		Available Mat'ls
0.472	0.158	0.040-0.410	Increments of 0.010	D4, D6
0.394	0.158	0.040-0.315		D4, D6
0.315	0.158	0.040-0.150		D4, D6
0.236	0.118	0.050-0.100		D4, D6
0.138	0.079	0.020-0.100		D4, D6
0.120	0.079	0.020-0.090		D4, D6

$D_s(\pm.002)$	$d_s(\pm.004)$	$L_s(\pm.002)$		Available Mat'ls
0.120	-	0.020-0.100	Incr. of 0.005	Alumina
0.142	0.075	0.039		Alumina
0.170	0.098	0.059		Alumina
0.317(±.005)	0.125	0.080		Alumina

Alumina Supports for High Frequency Applications

For high frequency application (above 6 GHz) we offer a special grade of alumina with the following properties.

Material Characteristics

Composition . . . . Alumina
Dielectric Constant 7.6
Dielectric Loss . . . . <.0006
Volume Resistivity (ohm cm) at 20°C . . . . 2×10^{10}
Thermal Conductivity
 (cal/cm°C sec) at 25°C 0.042
Water Absorption . . . . <.04

Alumina Supports for Cellular and PCS Applications

For cellular and PCS frequencies we offer a different grade of alumina, with the following properties. Contact factory for available sizes.

Material Characteristics

Composition . . . . Alumina
Dielectric Constant 9.5
Dielectric Loss . . . . <.001
Temperature Coefficient of (τ_f) (ppm/°C) 114
Volume Resistivity (ohm cm) at 20°C . . . . 10^{16}
Coefficient of Thermal Expansion
 (ppm/°C) (25-200°C) 6.5
Thermal Conductivity
 (cal/cm°C sec) at 25°C 0.08
Water Absorption . . . . <.01

D4 and D6 Supports for High Frequency Applications

Ordering Information

Disk Type *Example:* SPT-138-D4-025D

SPT	138	D4	025	D

- Disk Style
- $x10^{-3} = L_s$ (Thickness)
- Material Type
- $x10^{-3} = D_r$ (OD)
- Support

Material Characteristics (D4)

Composition . . . . .Cordierite (Mg, Al, Silicate)
Dielectric Constant 4.5
Dielectric Loss . . . .<.0002
Temperature Coefficient of (τ_f) (ppm/°C) 100
Volume Resistivity (ohm cm) at 20°C . . . . 10^{14}
Coefficient of Thermal Expansion
 (ppm/°C) (25-200°C) 2.4
Thermal Conductivity
 (cal/cm°C sec) at 25°C 0.10
Water Absorption . . . .<.01

Cylinder Type *Example:* SPT-120-D6-060-C

SPT	120	D6	060	C

- Cylinder
- $x10^{-3} = L_s$ (Thickness)
- Material Type
- $x10^{-3} = D_r$ (OD)
- Support

Material Characteristics (D6)

Composition . . . . Forsterite (Mg, Silicate)
Dielectric Constant 6.3
Dielectric Loss . . . . <.0002
Temperature Coefficient of (τ_f) (ppm/°C) 107
Volume Resistivity (ohm cm) at 20°C . . . . 10^{14}
Coefficient of Thermal Expansion
 (ppm/°C) (25-200°C) 2.4
Thermal Conductivity
 (cal/cm°C sec) at 25°C 009
Water Absorption (%) . . . . <0.6

Properties, Test Methods & Mounting

Basic Dielectric Resonator (DR) Material Properties

The most important material properties for a DR are it's dielectric constant (ε_r), quality factor (Qu), and temperature coefficient of resonant frequency (τ_f).

Dielectric Constant (ε_r)

The usual reason for choosing a DR as a resonating element is the size reduction afforded by the high ε_r of modern ceramics. But dielectric *constant* is a misnomer, not only does ε_r vary slightly for different temperature coefficient blends within the same material family, but lot-to-lot ceramic process variations cause ε_r to swing typically ±1 unit between lots. *Within* a given lot, the variation is much smaller. For example, our catalog lists the ε_r of material D8371 as 35.5 ± 1. Trans-Tech offers customer service of proper resonator sizing and specifying for production. Please see comments below regarding sizing. We measure ε_r accurately using a Courtney fixture, as described later. Trans-Tech measures the ε_r of the ceramic lot, not of the individually-shaped DR's. Unless stipulated otherwise, we choose a size for the test sample which will resonate close in frequency to where the material is Qu-specified.

Quality Factor (Qu)

The measure of the DR's ability to store microwave energy with minimal signal loss is its Qu. As discussed below, every DR application is unique, and since the RF fields of the most commonly-used $TE_{01\delta}$ mode do not end at the boundaries of the ceramic, metal wall losses will lower the Qu of the shielded DR.

It's worth emphasizing that measured Qu is both mode and temperature dependent, and the wary designer will qualify a potential ceramic supplier's Qu-claims with regard to measurement technique, temperature, and mode of operation. Higher-order modes and superconducting temperatures can make "Qu-factors" look phenomenal, but seldom represent the user's application. Bear in mind that these figures are ideal, and typically apply for resonators which are isolated from conducting surfaces.

We characterize and specify Qu with the DR essentially "isolated" in an enclosure several times the size of the DR, described later. Our Qu-specs apply for the $TE_{01\delta}$ mode, measured at laboratory ambient temperature. As in the case of ε_r measurement,

we choose a test sample size which will resonate near the frequency where the material is Qu-specified. It's typical for the microwave integrated circuit (MIC) environment, with thin substrate and nearby metallic enclosure, to reduce Qu to a fraction of the catalog advertised value. Ultimately, Qu can and should be measured in the user's MIC environment (see references, A.P.S. Khanna's January 1984 article). Please note that Qu can be degraded by inadvertent marking with graphite pencil!

Temperature Coefficient (τ_f)

The time and care required to thermally stabilize the sample, as well as the test fixture, makes temperature coefficient a time-consuming parameter to measure. An "isolated" measurement (see above) is necessary to discern the ceramic properties from other influences. Unless otherwise stipulated by our customer, we test a standard-size lot sample in the $TE_{01\delta}$ mode, not parts which have been sized to Fo for circuit application. In general, the temperature coefficient measured by the customer, *in-circuit*, will be different from our data. Proper record-keeping insures a stable product for the DR user. See the example under Temperature Compensation, which follows later in this section. We offer a standard *tolerance* on temperature coefficient of ± 2 ppm/°C. For example, we offer D8371 material with τ_f = 0 ppm/°C ± 2 ppm/°C. Tighter τ_f tolerances are available on request, but the practical reproducible measurement accuracy limit is about ± 0.5 ppm/°C. Tighter τ_f tolerances drive cost, so do not overspecify this parameter.

Test Methods

Dielectric Constant Measurement

When the DR is bounded by metallic walls at its two flat faces, the dielectric constant can be determined accurately from the DR dimensions and the resonant frequency as measured on a network analyzer. The fixture, shown below is called a Courtney holder and is described in the references.

1

Courtney Holder Fixture for
Dielectric Constant Measurement

Q-Factor Measurement

Q- factor, or unloaded Qu, is measured in a test cavity whose dimensions are at least three times the size of the DR, to simulate an "isolated" but shielded resonator. Low-loss supports, such as quartz blocks or alumina wafers, suspend the DR test specimen in the middle of the cavity away from the influence of the metallic walls. We arrange two RF probes, connected to a network analyzer, to couple the microwave energy to and from the DR. The degree of coupling is adjusted such that the transmission loss is on the order of -40 dB. From the measured 3 dB bandwidth (BW), loss (IL), and center frequency (Fo), we determine Qu from the relationship.

$$Q_u = \frac{\dfrac{F_o}{BW}}{1 - 10^{\left(\frac{IL}{20}\right)}}$$

The test is performed at laboratory ambient conditions, and the resonance measured is the $TE_{01\delta}$ mode.

Temperature Coefficient of Resonant Frequency (τ_f) Measurement

Tf is measured in a simulated "isolated" DR condition, similar to that described for Q-factor above except that the $TE_{01\delta}$ mode is observed in a reflection mode, measured with a network analyzer. The entire test cavity and DR specimen is placed in a temperature chamber, and the frequency of the resonance is measured at 25°C and at 60°C. Then τ_f is determined from

$$\tau_f = \frac{\Delta F\ (Hz)}{F_o\ (MHz)} \times \frac{1}{\Delta T} \quad ppm/°C$$

where

ΔF	=	(resonant frequency at 60°C) - (resonant frequency at 25°C) in Hz
F_o	=	resonant frequency at 25°C in MHz
ΔT	=	60°C - 25°C = 35°C

Dielectric Resonator (DR) Frequency ($TE_{01\delta}$ mode)

The frequency of an *isolated* dielectric resonator in the $TE_{01\delta}$ mode can be estimated to about 6% with a scientific calculator and the following formula:

$$F_o\ (GHz) = \frac{8.553}{\sqrt{\varepsilon_r}\left(\frac{\pi}{4}D_r^2 L_r\right)^{1/3}}$$

where

D_r	=	resonator diameter, in inches
L_r	=	resonator length, in inches
ε_r	=	resonator dielectric constant

Although this expression lacks high accuracy, especially when the DR is in close proximity to metal boundaries, it can still be used to estimate the sensitivity of frequency to D_r, L_r, and ε_r by differentiating and approximating:

$$\frac{\Delta F_o}{\Delta D_r} = \frac{-2 * F_o}{3 * D_r}$$

$$\frac{\Delta F_o}{\Delta L_r} = \frac{-F_o}{3 * L_r}$$

$$\frac{\Delta F_o}{\Delta \varepsilon_r} = \frac{-F_o}{2 * \varepsilon_r}$$

For instance, using Trans-Tech's 8371 material for a 10 GHz DR, the following estimates can be found:

D_r = .212"	$\Delta D_r = \pm$ .001"	$DF_o = \pm$ 31 MHz
L_r = .090"	$\Delta L_r = \pm$ .001"	$\Delta F_o = \pm$ 37 MHz
ε_r = 35.5	$\Delta \varepsilon_r = \pm$ 1	$\Delta F_o = \pm$ 141 MHz

This demonstrates why ordering a DR with just catalog dimensions can result in large variances in F_o. Trans-Tech's catalog sizes are intended as guidance for *beginning* a DR design, to approximate the desired frequency. See Resonator F_o Sizing, on the following page, for refinement.

The sensitivity formulas above can also be used to estimate the change, for example in height, required to modify the frequency of a DR. For example, if experiment shows that a 10 GHz DR's frequency must be increased that F_o changes by + 31 MHz per + .001" change in height. The DR needs to be raised +500 MHz, so a simple ratio will give the change as

$$\frac{.001}{-31} = \frac{\Delta L_{NEW}}{+500}$$

or ΔL_{NEW} = -.016." The height of the DR should be reduced to .074" to raise F_o to 10.5 GHz.

Ordering Dielectric Resonators to Frequency

Don't order production DR's by size alone. The tolerances in dielectric constant and dimensions will result in frequency variations that are unacceptable for most applications. Avoid trying to control frequency by simply imposing tight dimensions, or restricting the range of dielectric constant. This only drives yield down and cost up. Rather, specify a frequency-tuned part, one in which Trans-Tech adjusts the thickness or diameter to achieve the desired frequency and tolerance.

Ordering a DR simply by dimensions and material won=t guarantee correct performance. It is not difficult to estimate DR dimensions for a target frequency when the enclosure and mounting is defined, but the choice of dimensions is not unique. Please call our Application Engineers for assistance in choosing the best material, size and support. We can often cut weeks from your prototype development by suggesting sizes and materials already on hand, and even tailor inventoried DR=s to your prototype needs.

Years of experience sizing resonators has shown that every DR application is unique, and that the best way for a designer to insure product repeatability is to follow a few basic steps:

1. Get the DR prototype circuit on frequency, or nearly so, with initial samples from the catalog listings. DR frequency can be raised slightly by sanding the height (L_r) with fine emery paper.

2. Make a note of
   a) the in-circuit frequency;
   b) the desired frequency;
   c) the Trans-Tech QC number of the prototype sample.

3. Send the prototype DR with the information in (2.) above to Trans-Tech. We suggest that you assign a part number of your choosing to each prototype DR for correspondence and record-keeping. We will retain this F_o correlation sample DR, and use it to fill next-iteration DR orders, with F_o tuned to within 0.5% of your desired frequency. We call the differ-

ence between a) and b) the offset, and it's best to stipulate this offset in terms of MHz desired above or below the correlation sample. A typical specification might read:

"DR Frequency shall be that of correlation sample (your part number assigned to the sample) plus 120 MHz, with a tolerance of 0.5%."

When possible, it's preferable from a manufacturing standpoint to adjust F_o by altering the height, L_r, rather than the diameter. When specifying a DR on a formal drawing, allow Trans-Tech this freedom by stating that the height L_r is nominal, and that L_r is to be adjusted to give F_o to the frequency of the correlation sample plus offset, if any. Consult the catalog pages for typical diameter (D_r) tolerances.

Temperature Compensation

The unique nature of each DR circuit may necessitate adjustment for temperature-induced frequency drift. In an MIC environment, the expansion of the enclosure and tuning mechanism will typically increase the air gap above the resonator, lowering F_o as temperature increases. The change in F_o, in this case a negative $\Delta F_o/\Delta T$, can be compensated somewhat with a more positive Tf of the ceramic DR. It's important to know the Tf of the sample which was circuit-tested, so that this correction can be made. This figure is available from our records if the *Trans-Tech QC number*, available from test data shipped with the sample, is specified. It's best to determine the DR size for frequency (F_o) first, particularly in an MIC application, because the proximity of the tuning screw can profoundly effect temperature drift. The t_f is expressed in ppm/°C. In this context, the meaning is 1 Hz change for each MHz of operating frequency, for a given temperature range.

$$\tau_f = \frac{\Delta F\ (Hz)}{F_o\ (MHz)} \times \frac{1}{\Delta T}$$

Example:
An oscillator running at 10,750 MHz (10.750 GHz) decreases in frequency by a total of 1.5 MHz over a -20°C to +70°C temperature range. The temperature coefficient of the entire oscillator circuit, τ_c, is

$$\tau_c = \frac{1.5 \times 10^6\ Hz}{10750\ MHz} \times \frac{1}{(70°C - -20°C)}$$

$$= -1.55\ ppm/°C$$

This oscillator could be compensated for near-zero temperature drift by increasing the τ_f of the dielectric resonator by +2 ppm/°C.

Mounting

Filter Applications

The mounting of DR's in filter applications is notoriously designer-unique and is usually proprietary. Here, in-circuit Q is paramount and the DR is often supported with at least one DR thickness (L_r) above and below the DR, with a low-loss material having substantially lower dielectric constant than the DR's ε_r. High-purity Alumina is a good choice, and the less mass the support has, the less field energy will be stored *in the support*

DRO Applications

MIC environments have to trade off adequate coupling to the microstrip line vs. DR height above the metal floor. The DR is sometimes placed directly on the substrate without a support for cost reduction, but F_o drift vs. temperature can be prohibitive. The large expansion coefficient of most soft substrates will effectively "lift" the DR as temperature increases, lowering frequency. Even high-volume applications such as satellite low-noise block converters (LNB's) will use a stable ceramic support between the DR and the metal floor. The support might be 2/3 the resonator diameter. As an example, for a good trade-off between microstrip coupling and high loaded circuit Q, a 10 GHz DR will be spaced 0.040" to 0.090" (0.060" nominal) from the floor with a .120" diameter support having a dielectric constant $\varepsilon_s = 6$. See Trans-Tech application notes for tips to achieve good DRO phase noise performance.

Resonator Tuning

Tuning a dielectric resonator means adjusting its resonant frequency by mechanical means. Several techniques can be used to achieve this:

　☐ changing the thickness of the dielectric resonator
as
　☐ previously discussed
　　perturbing the fringing fields outside the dielectric
　　resonator with screws, tuning stubs, or
　　dielectric material

For example, the tuning of TE modes is easily achieved by metallic or dielectric tuning stubs placed perpendicular to the dielectric resonator's top surface. Metal tuning stubs (a) approaching the dielectric resonator will pull the frequency up and dielectric tuning stubs (b) will push the frequency down.
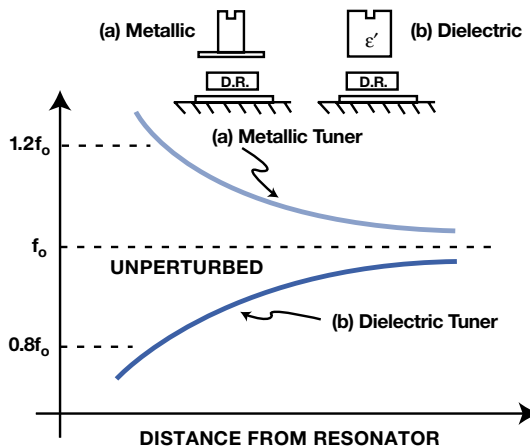
Approximately 20% of f_o tuning can be achieved by these methods. It is, however, good practice to restrict this amount to below five percent to minimize degradation of both temperature coefficient and unloaded Q.

References

General/Miscellaneous References

Courtney, W.E., "Analysis and evaluation of a method of measuring the complex permittivity and permeability of microwave insulators," IEEE Trans. Microwave Theory Tech., Vol. MTT-18, pp. 476-485, August 1970. [description of the Courtney test fixture for Er measurement]

T. Higashi and T. Makino, "Resonant frequency stability of the dielectric resonator on a dielectric substrate," IEEE Trans. Microwave Theory Tech., Vol. MTT-29, pp. 1048-1052, October 1981. [approximate formulas, temperature stability on substrate]

Kajfez, D. and Guillon, P., "Dielectric Resonators," ARTECH House 1986, ISBN 0-89006-201-3. [theory, applications, and computer programs]

Kajfez, D., "PC program evaluates higher-order modes in shielded dielectric resonators," Microwave Journal, May 1988, pp. 345-355. [introduction to FOAM program]

R.K. Mongia, "Easy resonant frequency computations for ring resonators," Microwave Journal, November 1992, pp. 105-108. [effect of center axial hole on frequency]

N. Klein et al, "Properties and applications of HTS-shielded dielectric resonators: a state-of the-art report," IEEE Trans. Microwave Theory Tech., Vol. MTT-44, No. 7, July 1996, pp.1369-1373. [results of superconducting experiments]

Coupling References

R. Boneti, A. Atia, "Analysis of microstrip circuits coupled to dielectric resonators," IEEE Trans. Microwave Theory Tech., Vol. MTT-29, No. 12, December 1981, pp. 1333-1337. [single curved microstrip line]

J. Brand and J. Ronnau, "Practical determination of dielectric resonator coupling coefficients," Microwave Journal, November 1986, pp. 141-144. [Empirical image technique for finding coupling coefficients]

P. Champagne, "Better coupling model of DR to microstrip insures repeatability," Microwaves & RF, September 1987, pp. 113-118. [coupling to single line]

Q-Measurement References

A. Podcameni et al, "Unloaded quality factor measurement for MIC dielectric resonator applications," Electronic Letters, 3rd September 1981, Vol. 17, No. 18, pp. 656-657. [network analyzer measurement of DR's coupled to 50-ohm microstrip]

A.P.S. Khanna, "Q Measurement of microstrip-coupled dielectric resonators," Microwaves & RF, January 1984, pp. 81-86. [equivalent circuit, network analyzer measurement of DR's coupled to 50-ohm microstrip]

DRO References

J. Walworth, "Theory of operation of the DRO," RF Design, January 1985, pp. 26-31. [coupling to one or two lines, equivalent circuits, empirical determination of coupling]

K. Agarwal, "Applications of GaAs heterojunction bipolar transistors in microwave dielectric resonator oscillators," Microwave Journal, November 1986, pp. 177-182. [phase noise comparison]

U. Rhode, "Designing a low noise oscillator using CAD tools," Microwave Journal, December 1986, pp. 140-144. [Noise reduction by locking 13 GHz DRO. Example of author's CAD program].

R. Jaques, "Paving the way for stabilized DR oscillators," Microwaves & RF, September 1987, pp. 103-108. [temperature drift analysis]

A. Murphy and P. Murphy, "Computer program aids dielectric resonator feedback oscillator design," Microwave Journal, September 1988, pp.131-148. [Fortran, feedback configuration]

A.P.S. Khanna, "A highly-stable 36 GHz GaAs FET DRO with phase-lock capability," Microwave Journal, July 1989, pp. 117-122.

A.P.S. Khanna, "Understand DRO design methods and operation," Microwaves & RF, April 1992 pp. 120 - 124.

A.P.S. Khanna, "Picking devices for optimum DRO performance," Microwaves & RF, May 1992 pp. 179 - 182.

A.P.S. Khanna, "Evaluate DRO noise and tuning characteristics," Microwaves & RF, June 1992 pp. 99 - 108.

H. Ashoka, "Directly-modulated DRO drives S-band video links," Microwaves & RF, June 1992 pp. 89 - 90.

A.P.S. Khanna, "Design a wide range of quiet DRO circuits," Microwaves & RF, July 1992 pp. 95 - 98.

J. Floch, "Technique allows simple design of microwave DROs," Microwaves & RF, March 1995, pp. 107-112. [Series feedback example near 10 GHz].

Filter References

K. Leong and J. Mazierska, Precise measurements of the Q factor of dielectric resonators in the transmission mode - accounting for noise, crosstalk, delay of uncalibrated lines, couplin gloss, and coupling reactance,@ IEEE Trans. Microwave Theory Tech., vol. 50, pp. 2115 - 2127, September 2002.

O. Bernard, "Simulate and build a Ku-band DRO," (Part 1) Microwaves and RF, May 2000.

O. Bernard, "Model and build a Ku-band DRO," (Part 2) Microwaves and RF, June 2000.

S. Cohn, "Microwave bandpass filters containing high-Q dielectric resonators," IEEE Trans. Microwave Theory Tech., Vol. MTT-16, No. 4, April 1968, pp. 218-227. [experimental coupling coefficients and simplified formula for DR's in waveguide]

A. Podcameni et al, "Design of microwave oscillators and filters using transmission-mode dielectric resonators coupled to microstrip lines," IEEE Trans. Microwave Theory Tech., Vol. MTT-33, No. 12, December 1985, pp. 1329-1332. [equivalent circuit for transmission-mode, coupling to two lines]

Microwave Dielectrics
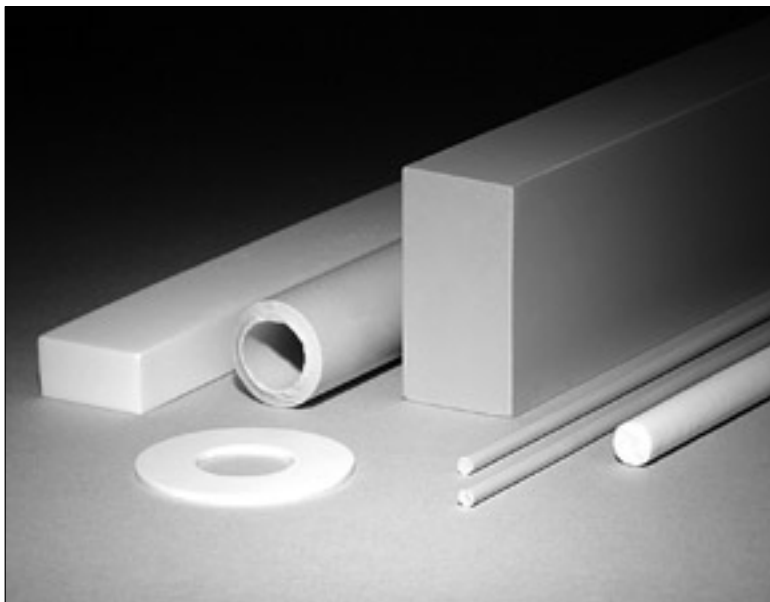
Bulk Microwave Dielectrics

Trans-Tech offers a broad range of ceramic materials which are not characterized for resonator applications, but for bulk, miscellaneous shapes, or substrates. Typical applications would be patch antenna substrates, matching structures for circulators and isolators, and miscellaneous support structures. Since such applications are non-resonant, temperature coefficient of resonant frequency does not apply. Rather, we list the temperature-dependent coefficients of dielectric constant and linear expansion. The Magnesium Aluminum Titanate (SMAT) and Magnesium Calcium Titanate (MCT) series are notable easier to machine than most microwave ceramics, and may be more suitable for appliations requiring precision machining. D-4, or Corderite, is a very hard ceramic noted for its low temperature coefficient of expansion which approaches the metal alloy Invar. It is not suitable for substrates. It is occasionally used for dielectric resonator supports due to its low dielectric constant and/or low thermal expansion rate.

Contact the factory for custom sizes and shapes.

NOTE: Temperature Stable Dielectrics found in Temperature Stable Materials catalog.

COMPOSITION AND TYPE NUMBER	DIELECTRIC CONSTANT (ε')	DIELECTRIC LOSS TANGENT ($\varepsilon'/\varepsilon''$)	TEMPERATURE COEFFICIENT DIELECTRIC CONSTANT ($°C^{-1}$)	TEMPERATURE COEFFICIENT OF THERMAL EXPANSION ($°C^{-1}$)	THERMAL CONDUCTIVITY (cal/cm²/cm/sec/°C)	DENSITY (g/cm³)	WATER ABSORPTION %
			(Nominal Value)	(Nominal Value)	(Nominal Value)	(Nominal Value)	(Nominal Value)
BASIC DIELECTRICS							
D-4 Cordierite	4.5 ± 0.2 @ 9.4 GHz	< 0.0002	+55 x 10^{-6}	2.0 x 10^{-6}	0.007	2.45	–
DS-6 Forsterite	6.3 ± 0.3 @ 9.4 GHz	< 0.0002	+107 x 10^{-6}	10.0 x 10^{-6}	0.009	2.89	0.6
D-15 Mg-Ti	15.0 ± 0.5 @ 9.4 GHz	< 0.0002	+98 x 10^{-6}	7.50 x 10^{-6}	0.000	3.50	–
D-16 Mg-Ti	16.0 ± 0.5 @ 9.4 GHz	< 0.0002	+98 x 10^{-6}	7.50 x 10^{-6}	0.010	3.60	0.0
D-38 Ba-Ti	37.0 ± 5% @ 6.0 GHz	< 0.0005	-25 x 10^{-6}	9.40 x 10^{-6}	0.010	4.40	0.3
D-50 Ba-Ti	50.0 ± 5% @ 6.0 GHz	< 0.0005	-250 x 10^{-6}	7.50 x 10^{-6}	0.010	4.35	–
D-100 Titania	100.0 ± 5% @ 6.0 GHz	< 0.0010	-575 x 10^{-6}	7.50 x 10^{-6}	0.010	3.90	0.1
MAGNESIUM ALUMINUM TITINATE							
SMAT-9	9.0 ± 0.3 @ 9.4 GHz	< .00015	+100 x 10^{-6}	7.50 x 10^{-6}	0.025	3.46	0.1
SMAT-9.5	9.5 ± 0.3 @ 9.4 GHz	< .00015	+100 x 10^{-6}	7.50 x 10^{-6}	0.025	3.46	0.1
SMAT-10	10.0 ± 0.5 @ 9.4 GHz	< .00015	+100 x 10^{-6}	7.50 x 10^{-6}	0.025	3.46	0.1
SMAT-11	11.0 ± 0.5 @ 9.4 GHz	< .00015	+100 x 10^{-6}	7.50 x 10^{-6}	0.025	3.45	0.1
SMAT-12	12.0 ± 0.5 @ 9.4 GHz	< .00015	+100 x 10^{-6}	7.50 x 10^{-6}	0.025	3.45	0.1
SMAT-13	13.0 ± 0.5 @ 9.4 GHz	< .00015	+100 x 10^{-6}	7.50 x 10^{-6}	0.025	3.44	0.1
SMAT-14	14.0 ± 0.5 @ 9.4 GHz	< .00015	+100 x 10^{-6}	7.50 x 10^{-6}	0.025	3.44	0.1
MAGNESIUM CALCIUM TITINATE							
MCT-18	18.0 ± 3% @ 9.4 GHz	< .0015	-70 x 10^{-6}	8.40 x 10^{-6}	0.010	3.47	0.1
MCT-20	20.0 ± 5% @ 9.4 GHz	< .0015	-130 x 10^{-6}	8.60 x 10^{-6}	0.010	3.50	0.1
MCT-25	25.0 ± 5% @ 9.4 GHz	< .0015	-245 x 10^{-6}	8.90 x 10^{-6}	0.010	3.54	0.1
MCT-30	30.0 ± 5% @ 9.4 GHz	< .0015	-370 x 10^{-6}	9.20 x 10^{-6}	0.010	3.59	0.1
MCT-40	40.0 ± 5% @ 6.0 GHz	< .0015	-580 x 10^{-6}	9.50 x 10^{-6}	0.010	3.62	0.1
MCT-50	50.0 ± 5% @ 6.0 GHz	< .0015	-730 x 10^{-6}	9.70 x 10^{-6}	0.010	3.65	0.1
MCT-55	55.0 ± 5% @ 6.0 GHz	< .0015	-800 x 10^{-6}	9.80 x 10^{-6}	0.010	3.68	0.1
MCT-70	70.0 ± 5% @ 6.0 GHz	< .0015	-960 x 10^{-6}	10.0 x 10^{-6}	0.010	3.70	0.1
MCT-85	85.0 ± 5% @ 6.0 GHz	< .0015	-1070 x 10^{-6}	10.1 x 10^{-6}	0.010	3.75	0.1
MCT-100	100.0 ± 5% @ 6.0 GHz	< .0015	-1120 x 10^{-6}	10.3 x 10^{-6}	0.010	3.78	0.1
MCT-115	125.0 ± 5% @ 6.0 GHz	< .0015	-1160 x 10^{-6}	10.4 x 10^{-6}	0.010	3.80	0.1
MCT-125	125.0 ± 5% @ 6.0 GHz	< .0015	-1180 x 10^{-6}	10.5 x 10^{-6}	0.010	3.83	0.1
MCT-140	140.0 ± 10% @ 6.0 GHz	< .0015	-1200 x 10^{-6}	10.7 x 10^{-6}	0.010	3.85	0.1

NOTE: Bars and Rods are Available for All Material Types

An Overview of Coaxial Resonators &
Inductors for Use in RF Filter &
VCO Applications.

Introduction & Applications
for Coaxial Resonators & Inductors (300 MHz - 6.0 GHz)
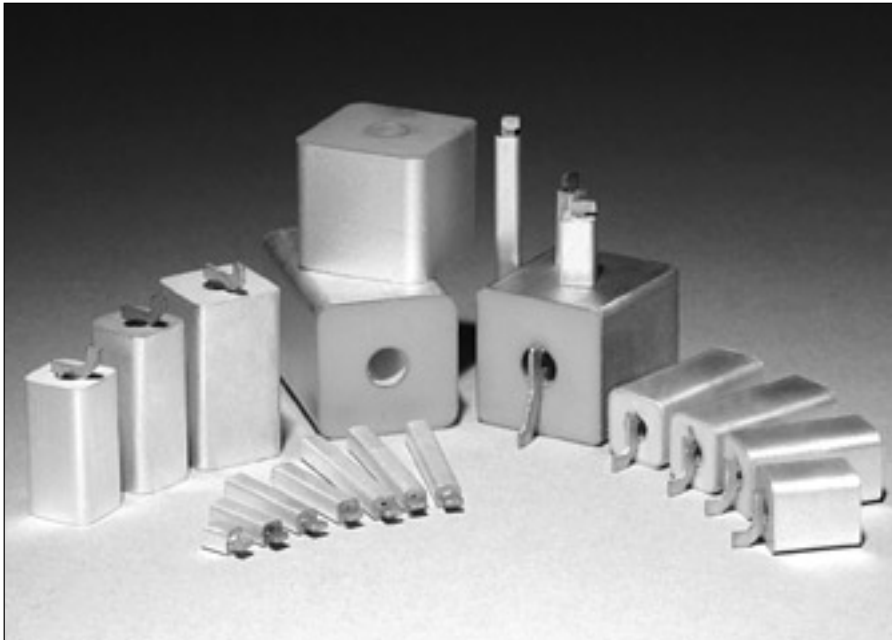
Features
■ Frequency tuned to 0.5% and 1%
■ High dielectric constant
■ Rugged construction
■ Low loss silver
■ Act as parallel resonant circuit or
  a high quality inductor

Benefits
■ Circuit miniaturization
■ Eliminate microphonics
■ Repeatability of design
■ Negligible aging effects
■ Excellent solderability
■ Improved circuit Q
■ High resonant impedance
■ Automation compatible

Introduction

Trans-Tech offers ceramic coaxial line elements in seven sizes and four dielectric constants to span applications from 300 MHz to 6 GHz. The VHF/UHF frequency bands are traditionally awkward for realizing discrete inductors and capacitors. Metallized ceramics provide an attractive alternative, since the wireless communication market now forces a continuous trade-off between performance and miniaturization.

Trans-Tech's ceramic solution offers advantages of high Q, reduced size, better shielding, and temperature performance superior to that obtainable from conventional L-C circuits or microstrip construction.

Two types of coaxial resonators are offered by Trans-Tech, a quarter-wave short (λ/4) and a half-wave open (λ/2). The quarter-wave has thick-film silver applied to one end. The half-wave has both ends un-metallized.

Trans-Tech's four dielectric materials are briefly summarized in **Figure 2.1** along with their recommended frequencies of use. The Material Properties Chart **(Figure 2.2)** can be used to determine the optimum material necessary for an application.

Typical Applications

■ Low Phase Noise VCO's
■ DRO/VCO Oscillators
■ Narrow band filters
■ Nationwide pagers
■ Duplexers
■ Global positioning systems
■ UHF tuned potential amplifiers
■ Wireless communications
■ Tuned Oscillators

Material Selection Chart

Frequency (GHz)

| 0 | .5 | 1.0 | 1.5 | 2.0 | 2.5 | 3.0 | 3.5 | 4.0 | 4.5 | 5.0 | 5.5 | 6.0 |
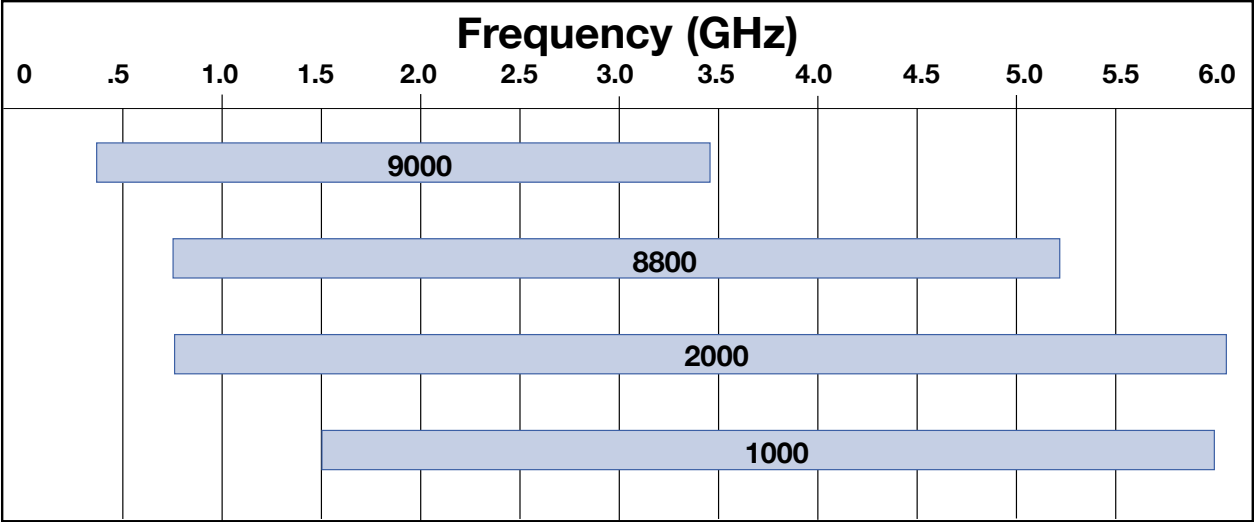
- 9000
- 8800
- 2000
- 1000

Figure 2.1 - *Frequency Chart of Coaxial Resonator Applications*

Material Properties

	Material Type			
	1000	2000	8800	9000
Dielectric Constant	10.5 ± 0.5	20.6 ± 1.0	39 ± 1.5	90 ± 3
Temperature Coefficient of Resonant Frequency τ_f (ppm°C)	0 ±10	0 ±10	+4 ± 2	0 ± 10

Figure 2.2 - *Material Properties*

Properties given for the ceramic materials used to produce the coaxial line elements are measured for internal quality control purposes. The electrical quality factor (Q) of the coaxial line elements is determined primarily by the metallization. Typical properties of the coaxial line elements are listed on pages 2-39 and 2-40.

SM – Sub-Miniature
Profile
(2mm)

MP –Miniature
Profile
(3mm)

LP – Low Profile
(4mm)

LS – Large Diameter
(4mm)

SP – Standard Profile
(6mm)

EP – Enhanced Q
(8mm)

HP – High Profile
(12mm)
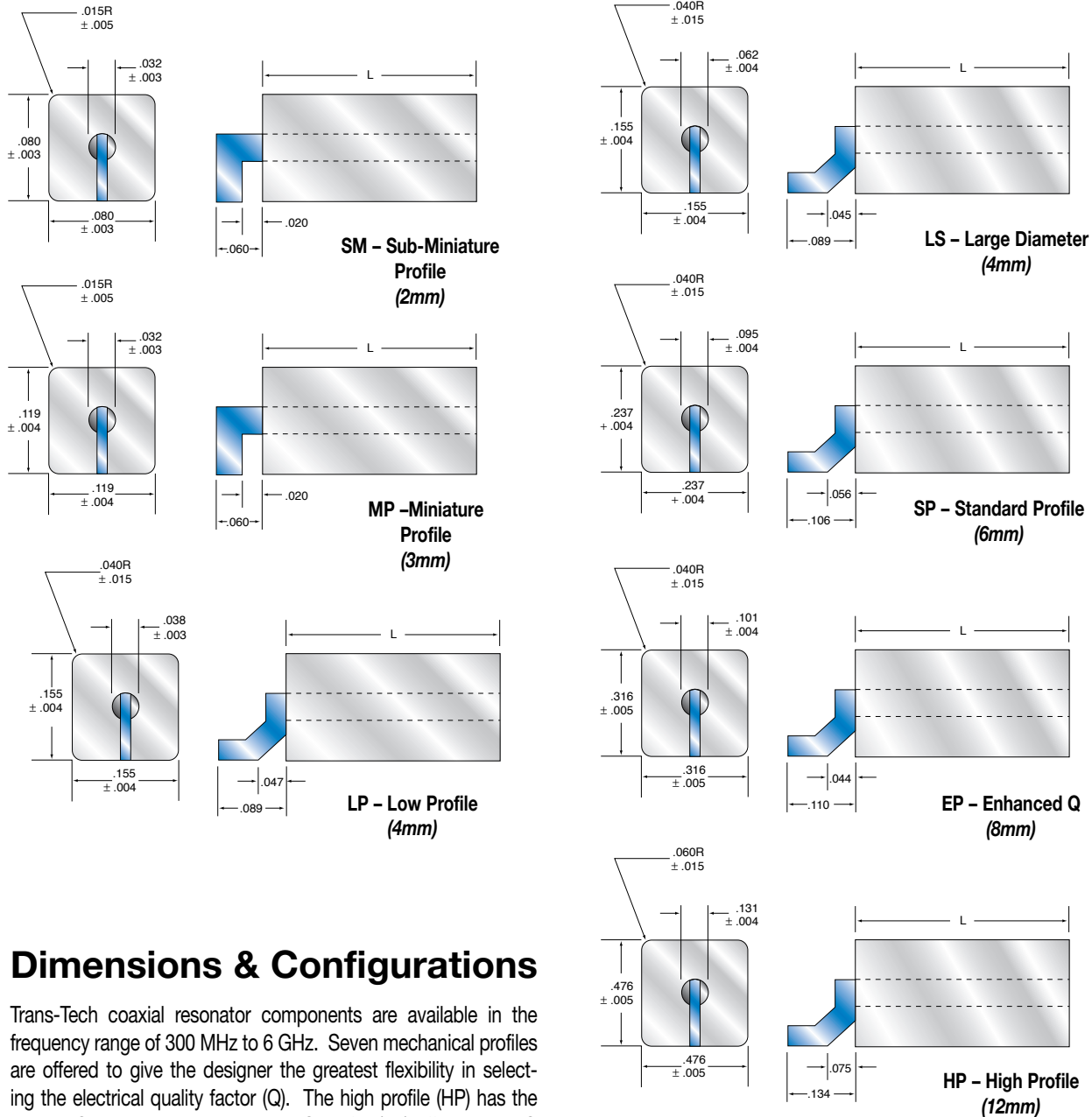
Dimensions & Configurations

Trans-Tech coaxial resonator components are available in the frequency range of 300 MHz to 6 GHz. Seven mechanical profiles are offered to give the designer the greatest flexibility in selecting the electrical quality factor (Q). The high profile (HP) has the highest Q and size. The enhanced Q profile (EP) offers a high Q and wide frequency offering. The standard profile (SP) offers a compromise of electrical Q and size, and should be considered the component of choice for most applications.

Trans-Tech offers four smaller profiles for occasions when available space is restricted. The low profile (LP), large profile (LS), miniature profile (MP), and sub-miniature profile (SM) provide the designer with a trade-off between electrical Q and compact size. Trans-Tech's low profile (LP) and large profile (LS) both have the same outer physical dimensions. They differ in the dimension of the inner diameter, which allows for different characteristic impedances, and increases the options available to designers. Overall comparisons can be determined from the given Q curves or by utilizing Trans-Tech's COAX Program.

These components are available in square configurations with dimensions shown in **Figure 2.3**.

Frequency Specifications

The various profiles, materials and types available for the Trans-Tech coaxial TEM mode resonators are summarized in the *Selection Charts* below and on page 2-37. You have a choice of two types, four materials and seven profiles. This range of component variables should meet most circuit design requirements. While the component is manufactured to frequency, a formula is given so that the approximate length can

be determined. The selected resonant frequency is available with two standard frequency tolerances of ± 0.5% and ± 1.0%. The minimum tolerance is ± 2MHz. Please note that the ordered value of f_O will be set according to our measurement procedure (see page 2-42). The f_O in your circuit may vary due to stray reactance. This offset can be corrected by changing the ordered value of f_O.

Recommended Frequencies 1000 Series

$\varepsilon r = 10.5 +/- .5$ $Tf = 0 +/- 10$

Type	Profile	Recommended Range f_o (MHz)	Nominal Length (inches) +/- 0.030in.	Nominal Length Range (inches)	Characteristic Impedance (Ω)
$\lambda/4$ Quarter Wave length	HP	1150 to 1800		0.506 to 0.792	25.3
	EP	1150 to 2500		0.364 to 0.792	22.5
	SP	1150 to 3100		0.294 to 0.792	18.3
	LS	1150 to 4600	$L = 911 / f_o (MHz)$	0.198 to 0.792	18.4
	LP	1150 to 4100		0.222 to 0.792	27.4
	MP	1150 to 5100		0.179 to 0.792	25.7
	SM	1150 to 5100		0.179 to 0.792	18.4
$\lambda/2$ Half Wave length	HP	2300 to 3400		0.536 to 0.792	25.3
	EP	2300 to 5000		0.364 to 0.792	22.5
	SP	2300 to 6000		0.304 to 0.792	18.3
	LS	2300 to 6000	$L = 1821 / f_o (MHz)$	0.304 to 0.792	18.4
	LP	2300 to 6000		0.304 to 0.792	27.4
	MP	2300 to 6000		0.304 to 0.792	25.7
	SM	2300 to 6000		0.304 to 0.792	18.4

1000 Series Selection Chart

Recommended Frequencies 2000 Series

$\varepsilon r = 20.6 +/- 1$ $Tf = 0 +/- 10$

Type	Profile	Recommended Range f_o (MHz)	Nominal Length (inches) +/- 0.030in.	Nominal Length Range (inches)	Characteristic Impedance (Ω)
$\lambda/4$ Quarter Wave length	HP	800 to 1200		0.542 to 0.813	18.1
	EP	800 to 1700		0.382 to 0.813	16.1
	SP	800 to 2200		0.296 to 0.813	13.1
	LS	800 to 3200	$L = 650 / f_o (MHz)$	0.203 to 0.813	13.1
	LP	800 to 2900		0.224 to 0.813	19.6
	MP	800 to 3600		0.181 to 0.813	18.4
	SM	800 to 3600		0.181 to 0.813	13.1
$\lambda/2$ Half Wave length	HP	1600 to 2500		0.520 to 0.813	18.1
	EP	1600 to 3500		0.372 to 0.813	16.1
	SP	1600 to 4500		0.289 to 0.813	13.1
	LS	1600 to 6000	$L = 1300 / f_o (MHz)$	0.217 to 0.813	13.1
	LP	1600 to 6000		0.217 to 0.813	19.6
	MP	1600 to 6000		0.217 to 0.813	18.4
	SM	1600 to 6000		0.217 to 0.813	13.1

2000 Series Selection Chart

Recommended Frequencies 8800 Series

$\epsilon r = 39 +/- 1.5$ $Tf = 4 +/- 2$

Type	Profile	Recommended Range f_0 (MHz)	Nominal Length (inches) +/- 0.030	Nominal Length Range (inches)	Characteristic Impedance (Ω)
$\lambda/4$ Quarter Wave length	HP	600 to 900		0.525 to 0.787	13.1
	EP	600 to 1200		0.394 to 0.787	11.7
	SP	600 to 1600		0.295 to 0.787	9.5
	LS	600 to 2300	$L = 472 / f_0$ (MHZ)	0.205 to 0.787	9.5
	LP	600 to 2100		0.225 to 0.787	14.2
	MP	600 to 2600		0.182 to 0.787	13.3
	SM	600 to 2600		0.182 to 0.787	9.5
$\lambda/2$ Half Wave length	HP	1200 to 1900		0.497 to 0.787	13.1
	EP	1200 to 2500		0.378 to 0.787	11.7
	SP	1200 to 3200		0.295 to 0.787	9.5
	LS	1200 to 4700	$L = 945 / f_0$ (MHZ)	0.201 to 0.787	9.5
	LP	1200 to 4300		0.220 to 0.787	14.2
	MP	1200 to 5200		0.182 to 0.787	13.3
	SM	1200 to 5200		0.182 to 0.787	9.5

8800 Series Selection Chart

Recommended Frequencies 9000 Series

$\epsilon r = 90 +/- 3$ $Tf = 0 +/- 10$

Type	Profile	Recommended Range f_0 (MHz)	Nominal Length (inches) +/- 0.030	Nominal Length Range (inches)	Characteristic Impedance (Ω)
$\lambda/4$ Quarter Wave length	HP	400 to 600		0.518 to 0.778	8.6
	EP	300 to 800		0.389 to 1.037	7.7
	SP	300 to 1000		0.311 to 1.037	6.3
	LS	300 to 1500	$L = 311 / f_0$ (MHZ)	0.207 to 1.037	6.3
	LP	300 to 1400		0.222 to 1.037	9.4
	MP	400 to 1700		0.183 to 0.778	8.8
	SM	400 to 1700		0.183 to 0.778	6.3
$\lambda/2$ Half Wave length	HP	800 to 1200		0.518 to 0.778	8.6
	EP	800 to 1700		0.366 to 0.778	7.7
	SP	800 to 2100		0.296 to 0.778	6.3
	LS	800 to 3100	$L = 622 / f_0$ (MHZ)	0.201 to 0.778	6.3
	LP	800 to 2800		0.222 to 0.778	9.4
	MP	800 to 3400		0.183 to 0.778	8.8
	SM	800 to 3400		0.183 to 0.778	6.3

9000 Series Selection Chart

Coaxial Resonator Order Information

An Order Example:

| SR | 8800 | SP | Q | 1300 | B | Y |

Tab: Y = Yes   N = No

Frequency Tolerance: B = +1.0%   A = .5%

Resonant Frequency: state in MHz

Type: Q for $\lambda/4$ H for $\lambda/2$

Profile: HP, EP, SP, LP, LS, MP, SM

Material: 8800, 9000, 1000, 2000

Product Code: SR - square coaxial resonator

Specifications

Quality Factor (Q) Specification - 1000 & 2000

The quality factors for various resonator profiles are shown in **Figure 2.4a and 2.4b**. The resonators are grouped by wavelength type (λ/4 & λ/2), material (1000 & 2000), and profile (HP, EQ, SP, LS, MP, SM). The listed Q value on each curve is the value guaranteed for the lowest operating frequency of each component type. The Q increases approximately as the square-root of increasing frequency. Typical Q's are 10% to 15% higher.

1000 Series Q Curves

D1000 Quarter-Wave Q Curves   D1000 Half-Wave Q Curves
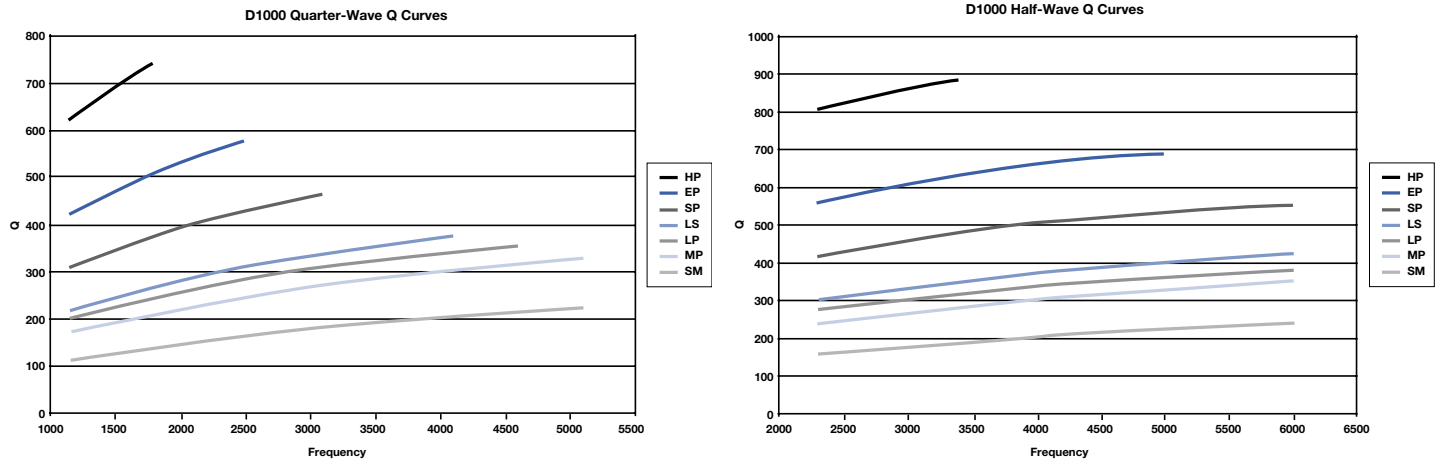
Figure 2.4a

2000 Series Q Curves

D2000 Quarter Wave Q Curves   D2000 Half-Wave Q Curves
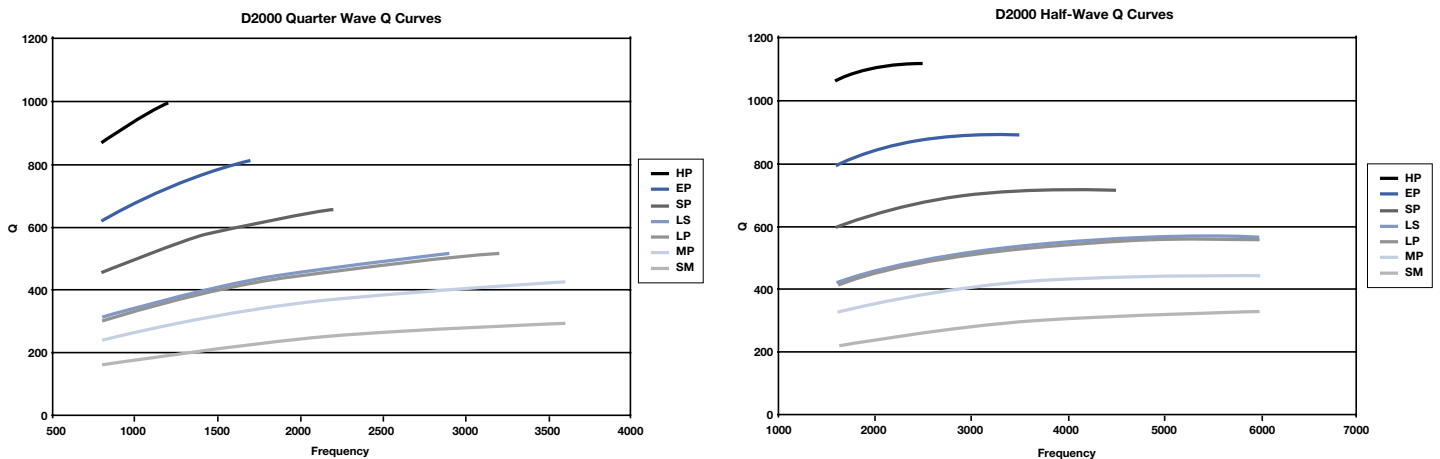
Figure 2.4b

Quality Factor (Q) Specification - 8800 & 9000

The specified quality factors of the various resonator components offered are shown in **Figure 2.4c and 2.4d**. the resonators are grouped by wavelength type ($\lambda/4$ & $\lambda/2$), material (8800 & 9000), and profile (HP, EP, SP, LP, LS, MP, SM). The listed Q value on each curve is the minimum value for the lowest operating frequency of each component type. The Q increases approximately as the square-root of increasing frequency. Typical Q's are 10% to 15% higher.

8800 Series Q Curves
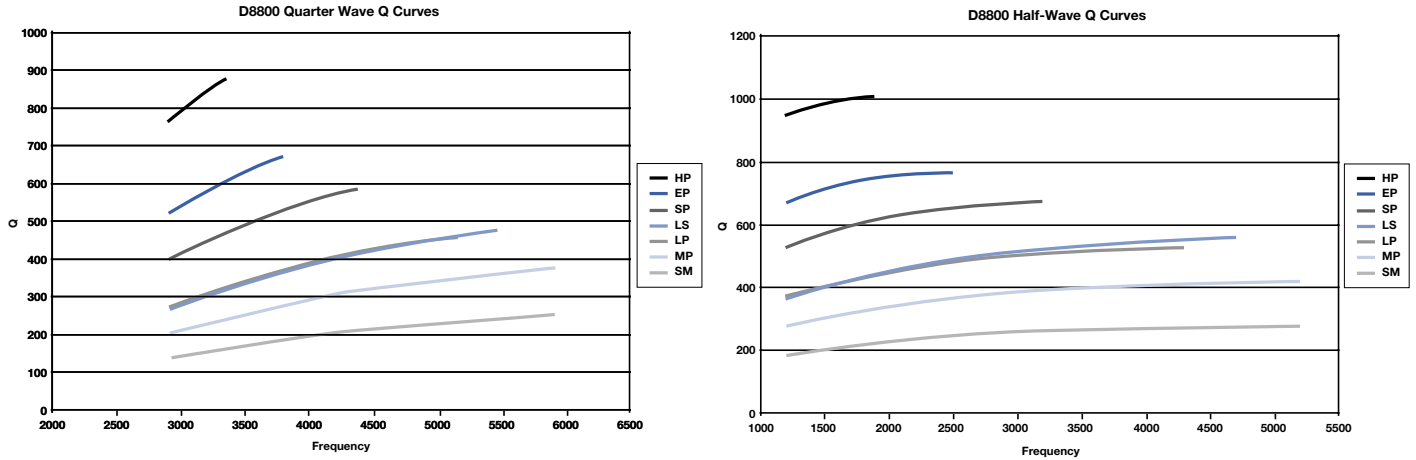
Figure 2.4c

9000 Series Q Curves

Figure 2.4d

2
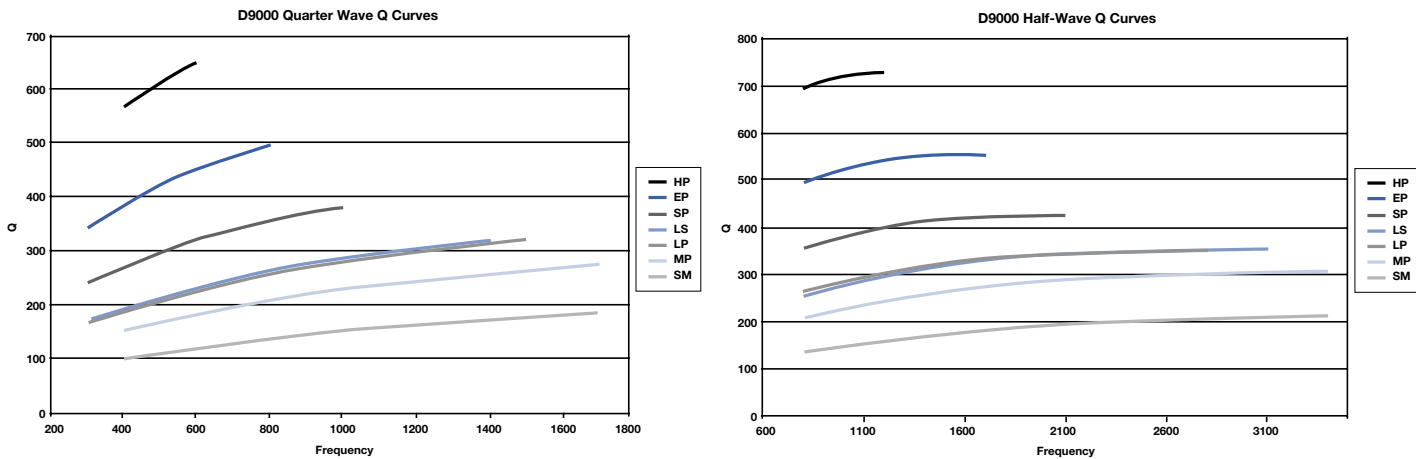
Coaxial Inductor

Trans-Tech's coaxial inductors are most frequently used in the resonant circuit of voltage-controlled oscillators (VCO's), where a varactor provides the tuning capability. The designer is usually confronted with trade-offs between high Q for best phase noise and component size vs circuit board real estate. An algorithm for selecting the correct Trans-Tech part follows. In addition Trans-Tech's COAX Program can provide valuable assistance for determining the correct Trans-Tech part. Application notes and references are included that give example circuits, basic principles, and some helpful hints.

While there is no physical distinction between a coaxial resonator and a coaxial inductor, the selection of an inductor for a VCO begins by first knowing (from analysis or experiment) the equivalent inductance that the active circuit, including the varactor, must see. In general, the VCO active circuit loads the 'resonator,' lowering the resonator's self-resonant frequency (SRF). The situation is analogous to externally capacitively loading a discrete parallel resonant L-C circuit.

While there is an approximate equivalent L-C circuit for the coaxial resonator close to resonance, this model has limited application. The coaxial resonators and inductors are more accurately modeled as a transmission line. Our included application notes and references delve further into this topic.

Values of inductance that can be achieved depend upon the separation between the VCO frequency and the SRF of the coaxial line element. Values less than 1 nH are not practical since the metal connection tab itself has an equivalent inductance of this order. In our experience, equivalent inductances in the range of 3-20 nH have been popular among designers of VCO's for wireless equipment.

Call for availability, utilize the Inductor Selection Guide, use the COAX Program, or refer to the included application notes for assistance with ordering the correct part.
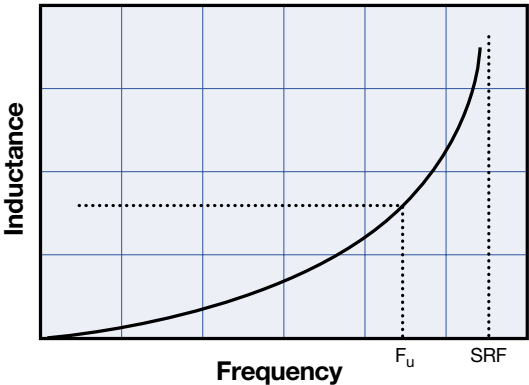
Frequency of Use vs. Inductance

Coaxial Inductor Order Information
An Order Example:

SI	8800	LP	Q	0450	Y	6.3

Inductance: (see Figure 8) avail. in .01 nH increments

Tab: Y = Yes   N = No

Frequency of Use (F_u): (see Figure 8 for definition)

Type: Q for $\lambda/4$ standard

Profile: HP, EP, SP, LP, LS, MP, SM

Material 1000, 2000, 8800, 9000

Product Code: SI - square coaxial inductor

Coax Line Properties vs. Profile and Material

Profile	1000	2000	8800	9000	Tab Inductors
HP	25.3Ω	18.1Ω	13.1Ω	8.6Ω	1.8nH
EP	22.5Ω	16.1Ω	11.7Ω	7.7Ω	1.0nH
SP	18.3Ω	13.1Ω	9.5Ω	6.3Ω	1.0nH
LS	18.4Ω	13.1Ω	9.5Ω	6.3Ω	0.9nH
LP	27.4Ω	19.6Ω	14.2Ω	9.4Ω	1.0nH
SP	25.7Ω	18.4Ω	13.3Ω	8.8Ω	0.6nH
SM	18.4Ω	13.1Ω	9.5Ω	6.3Ω	0.6nH

Wavelength (λ_g) in Dielectric

Material	ε_r	Wavelength Formula for λ_g (inches)
1000	10.5 ± 0.5	3642 / f_o
2000	20.6 ± 1	2601 / f_o
8800	39 ± 1.5	1890 / f_o
9000	90 ± 3	1244 / f_o

Figure 2.5

Inductor Selection Guide

1) Select one of Trans-Tech's four dielectric materials.

2) Determine the VCO's operating frequency (f_{vco}).

3) Determine the desired inductance or circuit impedance (Z_{in}). Note: Convert inductances to impedances by using:
$$Z_{in} = 2 * \pi * f_{vco} * L_{in} \text{ ohms}$$

4) Calculate the effect of the tab. Tab inductances are given in Figure 9. Use the formula $(Z_{in} = 2 * \pi * f_{vco} * L_{tab} \text{ ohms})$ to convert the tab inductances to impedances.

5) Determine the input impedance by subtracting off the effect of the tab using: $Z_{input} = Z_{in} - Z_{tab}$

6) Calculate the wavelength (λ_g) of the part in the dielectric (see **Figure 2.5** for appropriate formula).

7) Determine the characteristic impedance (Z_0) of the part (see **Figure 2.6**)

8) Calculate the physical length of the art using the formula: $1 = (\lambda_g / 2 * \pi) \tan^{-1} (Z_{input} / Z_0)$ inches

9) Determine the SRF of this part using:
$$SRF = (\lambda_g * f_{vco}) / (4 * 1) \text{ MHz}$$

10) Check the Recommended Frequency Chart for the appropriate material to ensure a valid part.

Measurement Description of Q, fo , and L

Evaluation of Q (quality factor) and f_o (resonant frequency) of coaxial components is made with a one-port reflection measurement on a network analyzer. The probe is moved into the inner diameter (ID) of the device until the input resistance of the device matches the terminal resistance of the network analyzer. This is indicated by a 50 Ω circle on the Smith Chart display and is known as "critical" coupling. The point on this circle where the response is purely resistive (capacitance reactance equals inductive reactance) is the point of resonance and will be defined by a complex impedance of Z = 50 + j ohms. The Q is computed by observing the frequency span between VSWR-2.616 (Z = 50 ± j50 ohms) on either side of f_0. The Q is defined as $f_o/\Delta f$.

The inductance parameter (L) is measured with an APC-7mm connector mounted flush with a conducting plane and a full one-port calibration (open, short, broadband 50 Ω load) is performed. The inductor is then clamped into place with the tab touching the inner conductor and the metallized body touching the grounding plane. The inductance (L) is measured at the frequency of use. The impedance vector on the Smith Chart of an ANA gives the necessary information where Z=R + jwL.

Characteristic Impedance

As shown in **Figure 2.6**, the characteristic impedance (Z_0) of the coaxial TEM mode components is a function of the profile dimensions and the dielectric constant of the material. Z_0 is reduced over its air line value by the square root of the dielectric constant of the material. At one-eighth wavelength, the short-circuit line exhibits an inductive reactance while the open-circuit line exhibits a capacitive reactance equal in magnitude to Z_0.

$$Z_o = \text{character impedance} = \frac{60}{\sqrt{\varepsilon_R}} \ln\left(1.079\, \frac{W}{d}\right)$$

where:

w	=	width of resonator
d	=	diameter of inner conductor
ε_r	=	dielectric constant

Profile	1000	2000	8800	9000
HP	25.3 Ω	18.1 Ω	13.1 Ω	8.6 Ω
EP	22.5 Ω	16.1 Ω	11.7 Ω	7.7 Ω
SP	18.3 Ω	13.1 Ω	9.5 Ω	6.3 Ω
LS	18.4 Ω	13.1 Ω	9.5 Ω	6.3 Ω
LP	27.4 Ω	19.6 Ω	14.2 Ω	9.4 Ω
MP	25.7 Ω	18.4 Ω	13.3 Ω	8.8 Ω
SM	18.4 Ω	13.1 Ω	9.5 Ω	6.3 Ω

Figure 2.6

2

Soldering Conditions

Trans-Tech's coaxial components are compatible with standard surface mount re-flow and wave soldering methods. The HP profile components may require mechanical support mounting because of the larger size. Consult the factory for details.

Use silver-bearing solder such as SN62 (62Sn-36Pb-2Ag). Trans-Tech tabs are pretinned to improve solderability. Additional attaching methods include hot air gun, infrared source, soldering iron, hot plate, vapor phase and others. The coaxial component body is a ceramic and subject to thermal shock if heated or cooled too rapidly. **Figure 2.7** is the recommended soldering profile, not to exceed 230°C for a duration of about 10 seconds. Repeatable results can be best achieved with air cooling only, not quenching.

Figure 2.8 indicates the maximum tolerance of the component planarity with respect to the datum plane.

Equation (1) Input Impedance f_o

$$Z_{input} = f Z_o \tan\left(\frac{2\pi f_o}{4\ SRF}\right)$$

where: f_o = use frequency

Equation (2) Resonant Frequency

$$\iota = \frac{c}{4\ SRF\sqrt{\varepsilon_r}}$$

where: c = speed of light ε_r =   39   8800 material
                                        90   9000 material
                                      10.5   1000 material
                                      20.6   2000 material
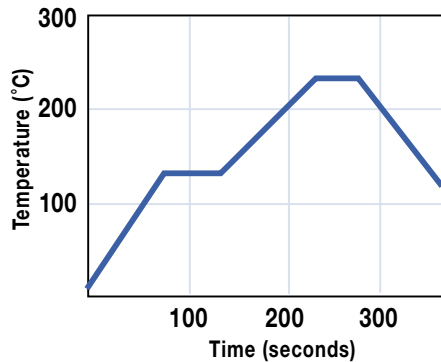
Figure 2.7 - *Soldering Profile*
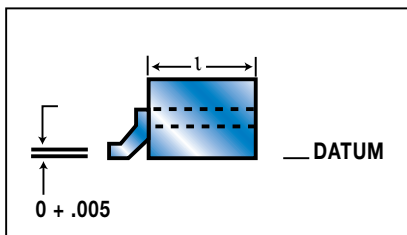
Figure 2.8 - *Surface Mount Tolerance for Components with Tabs*

Packaging

Tape and reel packaging is available. Consult the factory for details.

Notes: 1. Dimension "L" is length which depends on frequency.
Key: ▨ = Solder over metallic mounting pad
        ▪ = Solder mask over metallic mounting pad
        ☐ = Exposed metallic mounting pad

2MM (5M) Coaxial Resonator Footpad Dimensions

3MM (MP) Coaxial Resonator Footpad Dimensions

4MM (LP/LS) Coaxial Resonator Footpad Dimensions

CERAMIC FILTERS

3
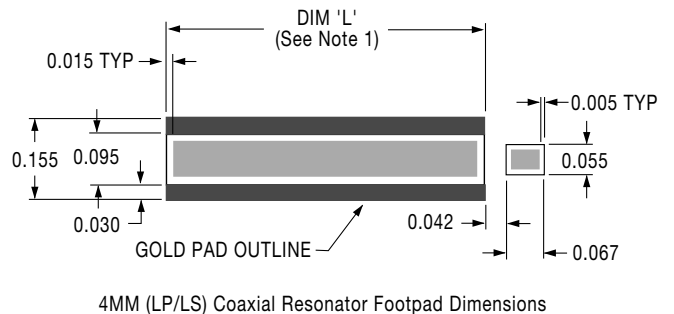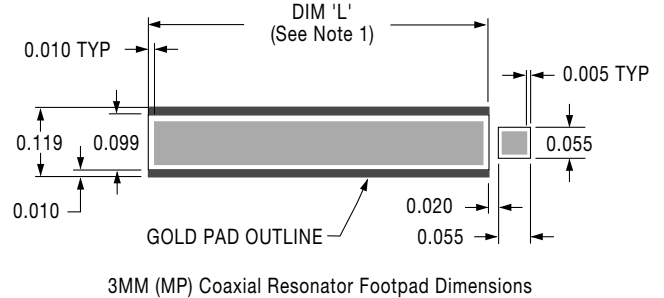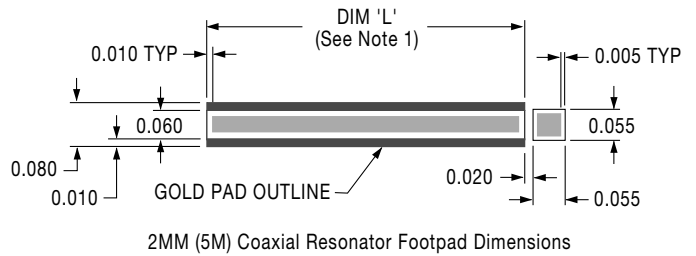
An Overview of Ceramic Bandpass Filters and Diplexers

Introduction & Applications
for Ceramic Bandpass Filters

Introduction

Trans-Tech Inc. is a world class supplier of high performance ceram-ic band-pass filters. Specializing in band-pass, Notch and Diplex-ing applications, Trans-Tech can cover a frequency range from 300 Mhz to 6000 Mhz with surface mount or connectorized devices. Utilizing state of the art assembly automation, Trans-Tech provides cost effective solutions meeting high performance specifications.

Tran-Tech's surface mount PCB configured filters are designed to comply with "Green" manufacturing initiatives eliminat-ing heavy metal elements. This configuration is designed to comply with pending European regulations regarding the elimination of lead in electronic assemblies. Custom assem-blies can be obtained with Flat Pack style SMT devices, Through-hole or Sn/Pb coated PCB surface mount designs.

Trans-Tech's assembly methodology offers a wide array of designs, from 2mm x 2 pole – 8mm x 10 pole band-pass filters and Diplex-ors, to advanced Band Stop (Notch) designs and High-pass or Low-pass Filters. Typical applications and ranges of products are listed on pages 3-50, 3-51 and 3-52. Detailed specifications, both mechanical and electrical, are maintained for many popular designs on our website, or by contacting the factory.

The nature of applications utilizing a band pass filter, duplexor or notch filter, necessitates the close interaction of the cus-tomer and Trans-Tech application engineering. Our application engineers, employ the latest in simulation and circuit analysis software, with accurately defined design rules, to provide rapid turnaround on new filter designs. With our experience and-design aids, Trans-Tech can provide the necessary support for your application from prototype through production. In addi-tion to the personal attention, Trans-Tech offers a computer-aided design tool, CRaFT, to assist engineers designing filters. Please refer to the CRaFT section of this catalog, or download the latest version from our website at www.trans-techinc.com.

The strength of Trans-Tech's designs, begin with our ability to produce our own Coaxial Resonators from Proprietary ceramic formulations. These resonators provide a High Q element that allows us to maintain our low filter insertion loss values. With numerous design package styles, Trans-Tech offers aggres-sive leadtimes on both prototype and volume applications.

Standard Filter Selection Guide

Trans-Tech has a wide range of standard filters as well as the capability to rapidly create new custom designs. **Figure 3.1** illustrates our general capability for filters. If a desired requirement falls within the listed categories, Trans-Tech can easily offer a suitable design. Beyond this general list Trans-Tech has a staff of experienced filter designers who can provide new custom and more technologically difficult filters. In addition, the craft program functions as useful tool when analyzing filter requirements. Trans-Tech welcomes the chance to review specifications and determine a design solution.

Standard Capabilities*

Center Frequency	300 MHz to 6GHz
Standard Filter Type	Ceramic Bandpass, Duplexor, Notch, LPF
Number of Poles	2-10
Resonator Sizes	2,3,4,6,8 and 12
Bandwidth	1.0%-10% (May vary depending on resonator size, F_o & ε_r)
Insertion Loss	1 to 4 dB typical by design
Attenuation	Varies by # of poles
Impedance	50 or 75 ohms
VSWR	2.0:1 maximum
Operating Temperature Range	-40 to +85 Degrees C
Mechanical Packaging Options	PCB Surface Mount, Thru-hole, & Flat Pack Surface Mount
Power Handling (continuous)	1 watt typical

Figure 3.1

* Contact Trans-Tech Application Engineering for assistance for any other requirement.

Standard Filters / Duplexors

This list contains Trans-Tech's most popular filter and diplexor designs. A variety of footprints and configurations is available for application specific needs. Please contact the factory with your specifications or for more information on any of these designs.

Trans-Tech maintains a list of over 700 active filters and diplexors. We welcome every opportunity to assist in the selec-tion or creation of a filter or diplexor that will meet your specifications.

CATV (400 - 550 Mhz / 1000 - 1100 Mhz)						
Part #	Filter Type	Size/Poles	Center Frequency (Mhz)	Bandwidth (Mhz)	Insertion Loss (dB)	Package
TT6P3-0427.5T-0125	Bandpass	6mm/3pole	427.5	1	2.5	Through-hole
TT6P3-0439T-0150	Bandpass	6mm/3pole	439	1	5.0	Through-hole
TT6P3-0445T-0145	Bandpass	6mm/3pole	445	1	4.5	Through-hole
TT6P3-0451T-0150	Bandpass	6mm/3pole	451	1	5.0	Through-hole
TT6P3-0495.25T-0145	Bandpass	6mm/3pole	495.25	1	4.5	Through-hole
TT6P3-0527.25T-0145	Bandpass	6mm/3pole	527.25	1	4.5	Through-hole
TT6P3-0547.25T-0145	Bandpass	6mm/3pole	547.25	1	4.5	Through-hole
TT4P3-1000P0-2525	Bandpass	4mm/3pole	1000	25	2.5	PCB SMT
TT6P4-1090P0-1050	Bandpass	6mm/4pole	1090	10	5.0	PCB SMT
WCS (746 - 794 Mhz / 2305 - 2360 Mhz / 3650 - 3700 Mhz / 4940 - 4990 Mhz)						
Part #	Filter Type	Size/Poles	Center Frequency (Mhz)	Bandwidth (Mhz)	Insertion Loss (dB)	Package
TT2P6-0757P0-7540	Bandpass	2mm/6pole	757	75	4.0	PCB SMT
TT6P6-0785P6-3022	Bandpass	6mm/6pole	785	30	2.2	PCB SMT
TT6P5-0794P3-2430	Bandpass	6mm/5pole	794	24	3.0	PCB SMT
TT4P2-2332.5P2-2730	Bandpass	4mm/2pole	2332.5	27	3.0	PCB SMT
TT6P5-2312P1-7032	Bandpass	6mm/5pole	2312	70	3.2	PCB SMT
TT6P5-2340P1-12032	Bandpass	6mm/5pole	2340	120	3.2	PCB SMT
TT6P4-3650P1-50014	Bandpass	6mm/4pole	3650	500	1.4	PCB SMT
TT6P3-3675P0-5020	Bandpass	6mm/3pole	3675	50	2.0	PCB SMT
TT4P4-T2382-R2518	Diplexor	4mm/4pole	T2382/R2518			PCB SMT
TT6P7-T0712-R0757	Diplexor	6mm/4x3pole	T712/R757			PCB SMT
MDS (2110 - 2160 Mhz / 2500 - 2690 Mhz)						
Part #	Filter Type	Size/Poles	Center Frequency (Mhz)	Bandwidth (Mhz)	Insertion Loss (dB)	Package
TT3P2-2110P0-2426	Bandpass	3mm/2pole	2110	24	2.6	PCB SMT
TT4P3-2120P2-6020	Bandpass	4mm/3pole	2120	60	2.0	PCB SMT
TT3P4-2140P1-10030	Bandpass	3mm/4pole	2140	100	3.0	PCB SMT
TT3P3-2521P0-4220	Bandpass	3mm/3pole	2521	42	2.0	PCB SMT
TT4P4-2593P1-18620	Bandpass	4mm/4pole	2593	186	2.0	PCB SMT
TT4P4-2600P2-20020	Bandpass	4mm/4pole	2600	200	2.0	PCB SMT
TT6P5-2640P1-7032	Bandpass	6mm/5pole	2640	70	3.2	PCB SMT
TT6P6-T2534-R2653	Diplexor	6mm/3x3pole	T2534/R2653			PCB SMT

ISM (900 - 930 Mhz / 2400 - 2484 Mhz / 5650 - 5830 Mhz)						
Part #	Filter Type	Size/Poles	Center Frequency (Mhz)	Bandwidth (Mhz)	Insertion Loss (dB)	Package
TT4P2-0915P2-2620	Bandpass	4mm/2pole	915	26	2.0	PCB SMT
TT4P2-0927F-0230	Bandpass	4mm/2pole	927	2	3.0	Flatpack SMT
TT6P2-0915F-1425	Bandpass	6mm/2pole	915	14	2.5	Flatpack SMT
TT6P3-0927T-0240	Bandpass	6mm/3pole	927	2	4.0	Through-hole
TT6P5-2440P0-4830	Bandpass	6mm/5pole	2440	48	3.0	Through-hole
TT4P3-2400P1-20015	Bandpass	4mm/3pole	2400	200	1.5	PCB SMT
TT6P3-2400P2-0420	Bandpass	6mm/3pole	2400	4	2.0	PCB SMT
TT4P4-5250P0-20017	Bandpass	4mm/4pole	5250	200	1.7	PCB SMT
TT4P4-5300P0-20017	Bandpass	4mm/4pole	5300	200	1.7	PCB SMT
TT4P4-5775P0-10030	Bandpass	4mm/4pole	5775	100	3.0	PCB SMT
TT4P4-5795P0-15017	Bandpass	4mm/4pole	5795	250	1.7	PCB SMT
TT4P8-T5250-T5795	Diplexor	4mm/4x4pole	T5250/R5795			PCB SMT

PCS Data (1910 - 1930 Mhz)						
Part #	Filter Type	Size/Poles	Center Frequency (Mhz)	Bandwidth (Mhz)	Insertion Loss (dB)	Package
TT6P4-1910P3-2140	Bandpass	6mm/4pole	1910	21	4.0	PCB SMT
TT6P4-1930P3-2030	Bandpass	6mm/4pole	1930	20	3.0	PCB SMT

Cellular / PCS / DCS / UMTS (836 - 882 Mhz / 1880 - 1960 Mhz / 2140 - 2360 Mhz)						
Part #	Filter Type	Size/Poles	Center Frequency (Mhz)	Bandwidth (Mhz)	Insertion Loss (dB)	Package
TT3P3-0836.5P0-2526	Bandpass	3mm/3pole	836.5	25	2.6	PCB SMT
TT3P3-0881.5P0-2526	Bandpass	3mm/3pole	881.5	25	2.6	PCB SMT
TT4P3-0863P0-0585	Bandpass	4mm/3pole	863	5	8.5	PCB SMT
TT6P5-881.5P7-2530	Bandpass	6mm/5pole	881.5	25	3.0	PCB SMT
TT4P4-1960P0-6216	Bandpass	4mm/4pole	1960	62	1.6	PCB SMT
TT4P4-1880P0-6216	Bandpass	4mm/4pole	1880	62	1.6	PCB SMT
TT4L4-0836.5P0-2526	Lowpass	4mm/4pole	836.5	25	2.6	PCB SMT
TT8N4-0840P0-0440	Bandstop	8mm/4pole	840	4	4.0	PCB SMT
TT6P3-2140P2-6010	Bandpass	6mm/3pole	2140	60	1.0	PCB SMT
TT6P10-R1950-T2140	Diplexor	6mm/5x5pole	R1950/T2140			PCB SMT

GPS (1227.6 Mhz / 1575.42 Mhz / 1176 Mhz)						
Part #	Filter Type	Size/Poles	Center Frequency (Mhz)	Bandwidth (Mhz)	Insertion Loss (dB)	Package
TT4P2-1176P4-3020	Bandpass	4mm/2pole	1176	30	2.0	PCB SMT
TT3P2-1227P0-2012	Bandpass	3mm/2pole	1227	20	1.2	PCB SMT
TT3P3-1227.6P1-1030	Bandpass	3mm/3pole	1227.6	10	3.0	PCB SMT
TT6P2-1227T-2021	Bandpass	6mm/2pole	1227	20	2.1	Through-hole
TT6P2-1227F-2008	Bandpass	6mm/2pole	1227	20	0.8	Flatpack SMT
TT3P2-1575P1-2012	Bandpass	3mm/2pole	1575	20	1.2	PCB SMT
TT3P3-1575.42P1-1030	Bandpass	3mm/2pole	1575.42	10	3.0	PCB SMT
TT4P4-R1227.6-T1575.42	Diplexor	4mm/2x2pole	R1227.6/T1575.42			PCB SMT
TT4P4-T1575.42-R1227.6	Diplexor	4mm/2x2pole	T1575.42/R1227.6			PCB SMT
TT4P2-1575F-1012	Bandpass	4mm/2pole	1575	10	1.2	Flatpack SMT
TT6P2-1575T-2020	Bandpass	6mm/2pole	1575	20	2.0	Through-hole

3

PMR (700 / 800 / 900 Mhz)						
Part #	Filter Type	Size/Poles	Center Frequency (Mhz)	Bandwidth (Mhz)	Insertion Loss (dB)	Package
TT6P4-0435P0-3019	Bandpass	6mm/4pole	435	30	1.9	PCB SMT
TT6P2-0808T-1946	Bandpass	6mm/2pole	808	19	4.6	Through-hole
TT6P4-0770P0-1240	Bandpass	6mm/4pole	770	12	4.0	PCB SMT
TT6P5-0765P0-11225	Bandpass	6mm/5pole	765	11	2.3	PCB SMT
TT2P6-0575P0-7540	Bandpass	2mm/6pole	575	75	4.0	PCB SMT
TT4P3-0860P3-1820	Bandpass	4mm/3pole	860	18	2.0	PCB SMT
TT6P3-0800P3-1220	Bandpass	6mm/3pole	800	12	2.0	PCB SMT
TT6P3-0730P3-1213	Bandpass	6mm/3pole	730	12	1.3	PCB SMT

WLL / WLAN (3400 - 3700 Mhz)						
Part #	Filter Type	Size/Poles	Center Frequency (Mhz)	Bandwidth (Mhz)	Insertion Loss (dB)	Package
TT4P3-3430P0-60175	Bandpass	4mm/3pole	3430	60	1.8	PCB SMT
TT6P3-3450P2-35016	Bandpass	6mm/3pole	3450	350	1.6	PCB SMT
TT4P3-3462.5P0-2728	Bandpass	4mm/3pole	3462.5	27	2.8	PCB SMT
TT6P3-3470P0-60175	Bandpass	6mm/3pole	3470	60	1.8	PCB SMT
TT4P3-3500P2-10020	Bandpass	4mm/3pole	3500	100	2.0	PCB SMT
TT4P5-3500P1-20020	Bandpass	4mm/5pole	3500	200	2.0	PCB SMT
TT4P3-3520.5P0-4225	Bandpass	4mm/3pole	3520.5	42	2.5	PCB SMT
TT4P5-3550P1-30020	Bandpass	4mm/5pole	3550	300	2.0	PCB SMT
TT6P3-3450P2-35016	Bandpass	6mm/3pole	3450	350	1.6	PCB SMT
TT6P10-T3420-R3520	Diplexor	6mm/5x5pole	T3420/R3520			PCB SMT
TT6P10-T3426-R3550	Diplexor	6mm/5x5pole	T3426/R3550			PCB SMT
TT6P10-T3462-R3562	Diplexor	6mm/5x5pole	T3462/R3562			PCB SMT
TT6P10-T3475-R3575	Diplexor	6mm/5x5pole	T3475/R3575			PCB SMT
TT6P6-T3430-R3530	Diplexor	6mm/3x3pole	T3430/R3530			PCB SMT

Available Packages

Trans-tech offers filters in a number of standard packages. In addition to SMT, Trans-Tech offers a Flat-pack and Thru-Hole configuration. Mechanical drawings are provided for most of our filters. In addition to our standard offering, Trans-Tech has the capability and experience to meet many unique footprint layouts and custom packages.

For each of our 2 to 6 pole packages, Trans-Tech can offer profiles ranging from 2mm to 6mm.

*All dimensions are in inches   ## 2mm SMT

TT2P2—P＿

TT2P3—P＿

TT2P4—P＿

TT2P5—P＿

TT2P6—P＿

SMT Filter Length

	Inches	mm
P1	0.434	11
P2	0.512	13
P3	0.590	15
P4	0.669	17
P5	0.748	19
P6	0.827	21
P7	0.906	23
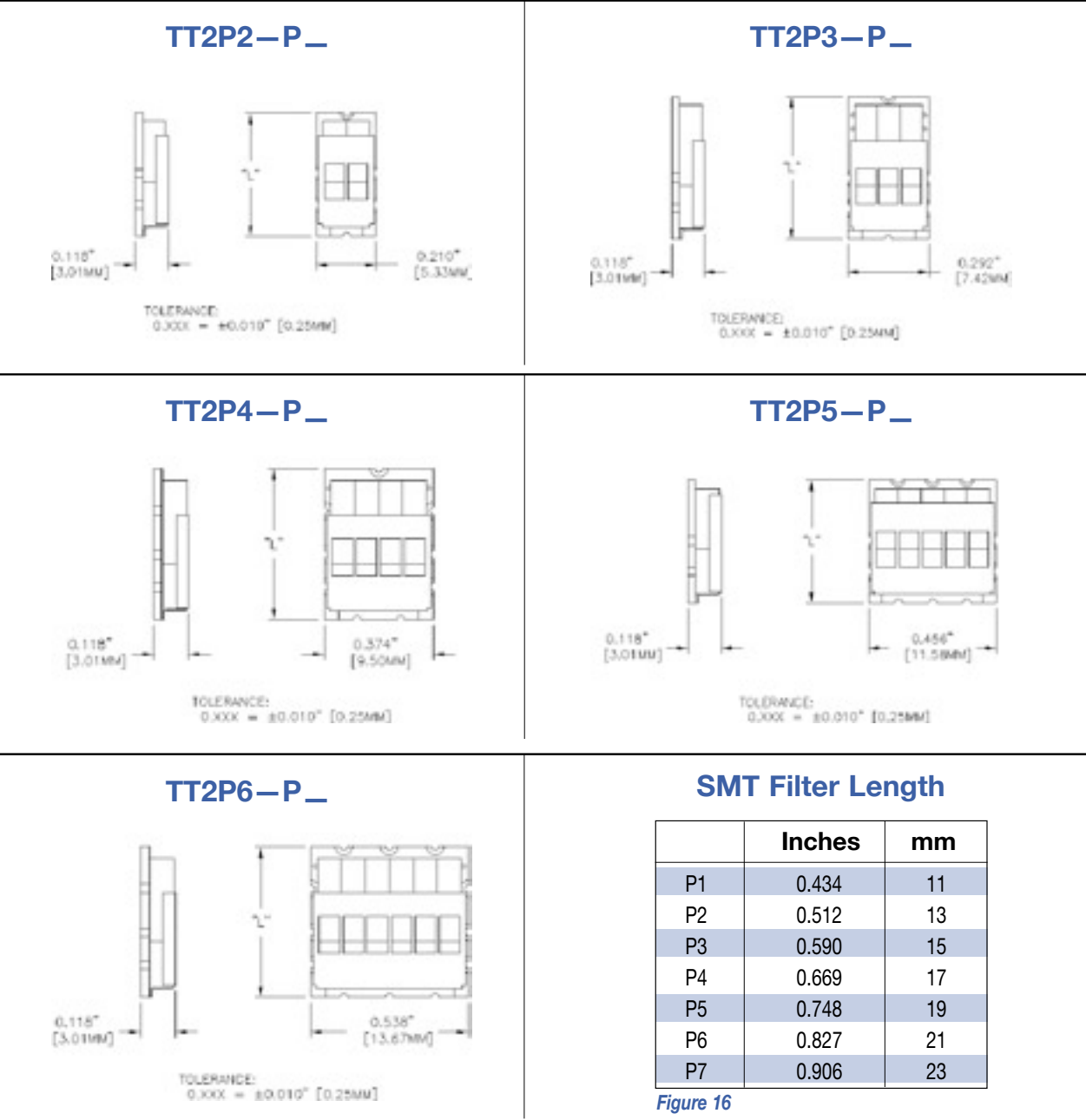
Figure 16

Note: Dimension 'L' will vary in length dependent upon filter's frequency

3mm SMT
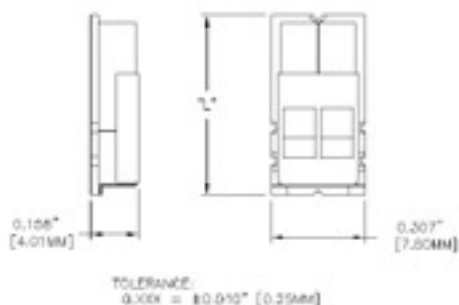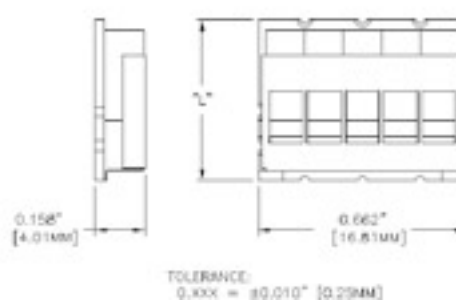
TT3P2—P_

0.158" [4.01MM]

0.307" [7.80MM]

TOLERANCE:
0.XXX = ±0.010" [0.25MM]

TT3P3—P_

0.158" [4.01MM]

0.440" [11.18MM]

TOLERANCE:
0.XXX = ±0.010" [0.25MM]

TT3P4—P_

0.158" [4.01MM]

0.540" [13.72MM]

TOLERANCE:
0.XXX = ±0.010" [0.25MM]

TT3P5—P_

0.158" [4.01MM]

0.662" [16.81MM]

TOLERANCE:
0.XXX = ±0.010" [0.25MM]

SMT Filter Length

	Inches	mm
P1	0.434	11
P2	0.512	13
P3	0.590	15
P4	0.669	17
P5	0.748	19
P6	0.827	21
P7	0.906	23

TT3P6—P_

0.158" [4.01MM]

0.784" [19.91MM]

TOLERANCE:
0.XXX = ±0.010" [0.25MM]
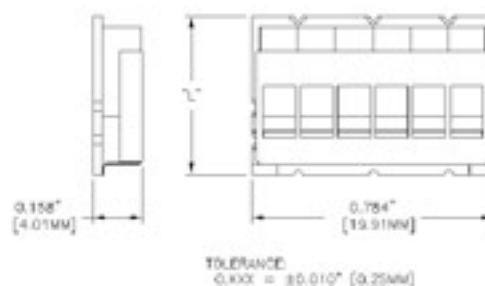
Note: Dimension 'L' will vary in length dependent upon filter's frequency

*All dimensions are in inches

4mm SMT

TT4P2—P_
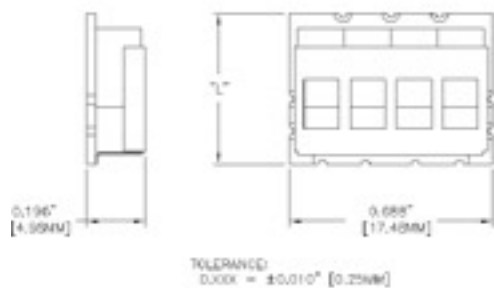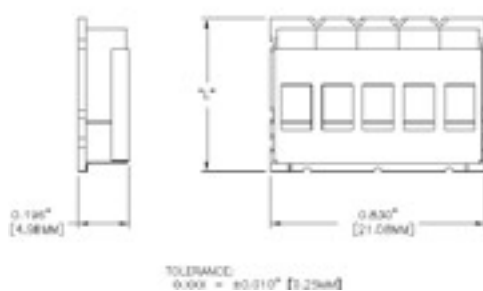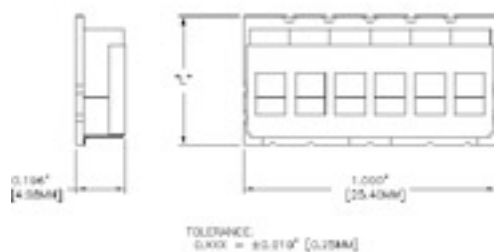
0.196"
[4.99MM]

0.360"
[9.16MM]

TOLERANCE:
0.XXX = ±0.010" [0.25MM]

TT4P3—P_

0.196"
[4.99MM]

0.518"
[13.16MM]

TOLERANCE:
0.XXX = ±0.010" [0.25MM]

TT4P4—P_

0.196"
[4.99MM]

0.688"
[17.48MM]

TOLERANCE:
0.XXX = ±0.010" [0.25MM]

TT4P5—P_

0.196"
[4.99MM]

0.830"
[21.08MM]

TOLERANCE:
0.XXX = ±0.010" [0.25MM]

TT4P6—P_

0.196"
[4.99MM]

1.000"
[25.40MM]

TOLERANCE:
0.XXX = ±0.010" [0.25MM]

SMT Filter Length

	Inches	mm
P1	0.434	11
P2	0.512	13
P3	0.590	15
P4	0.669	17
P5	0.748	19
P6	0.827	21
P7	0.906	23

Note: Dimension 'L' will vary in length dependent upon filter's frequency

6mm SMT

TT6P2—P＿

TT6P3—P＿

TT6P4—P＿

TT6P5—P＿
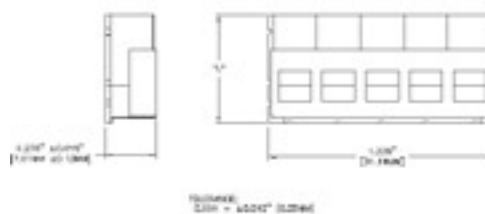
SMT Filter Length

	Inches	mm
P1	0.434	11
P2	0.512	13
P3	0.590	15
P4	0.669	17
P5	0.748	19
P6	0.827	21
P7	0.906	23

TT6P6—P＿
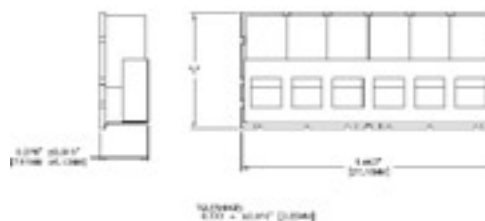
Note: Dimension 'L' will vary in length dependent upon filter's frequency

*All dimensions are in inches

4mm Flat Pack (F)

TT4P2—F
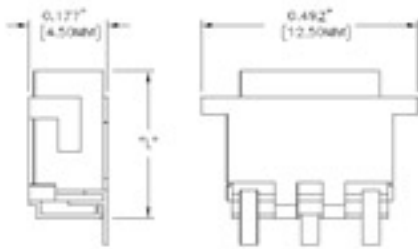
TOLERANCE:
0.XXX = ±0.005" [0.13MM]

TT4P3—F
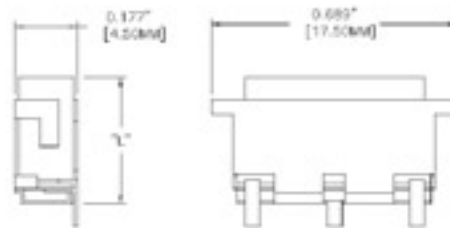
TOLERANCE:
0.XXX = ±0.005" [0.13MM]

6mm Flat Pack (F)

TT6P2—F
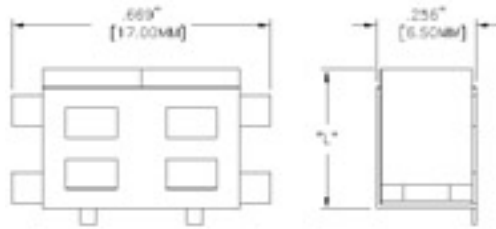
TOLERANCE:
0.XXX = ±0.005" [0.13MM]

TT6P3—F
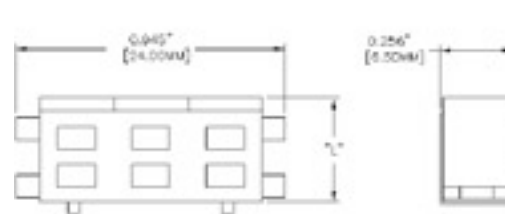
TOLERANCE:
0.XXX = ±0.005" [0.13MM]

6mm Thru-Hole (T)

TT6P2—T
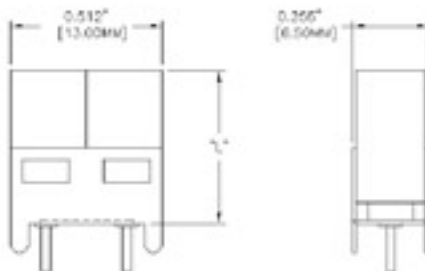
TOLERANCE:
0.XXX = ±0.005" [0.13MM]

TT6P3—T
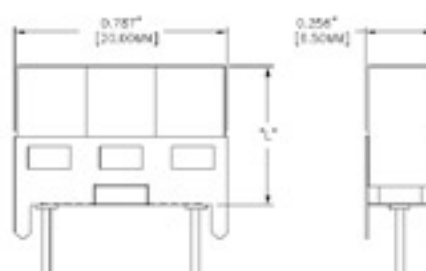
TOLERANCE:
0.XXX = ±0.005" [0.13MM]

Note: Dimension 'L' will vary in length dependent upon filter's frequency

An Overview of
Ferrite and
Applications
Garnet Materials
for Microwave

Microwave Magnetic and Dielectric Materials for Circulators & Isolators
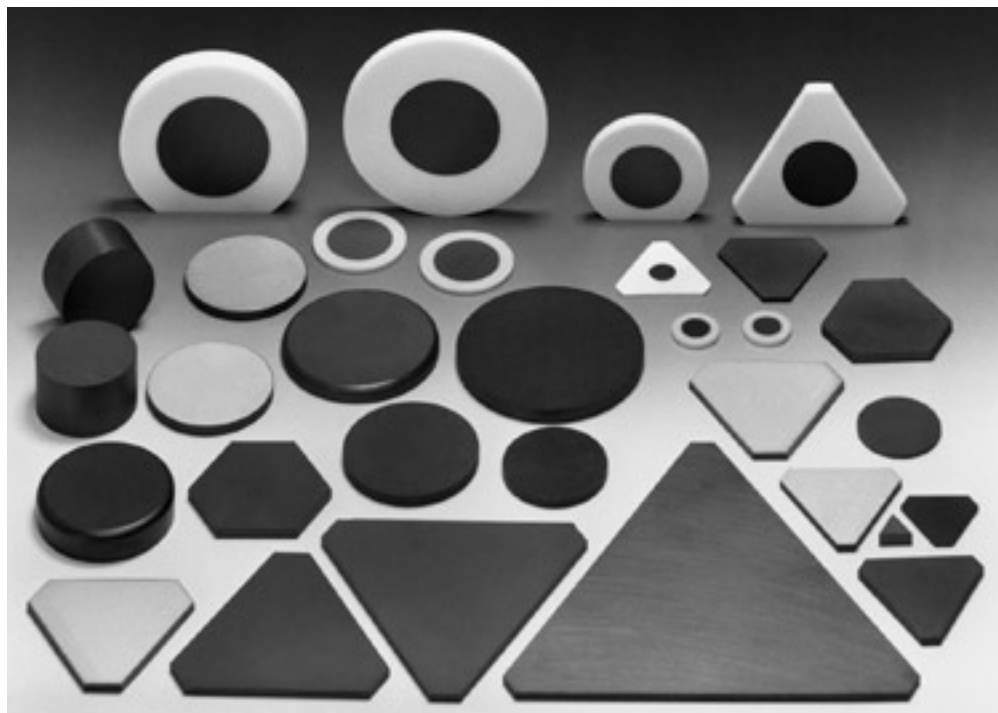
Features
- Broad $4\pi M_s$ Range
- Metallized Ground (optional)
- Precision Machining
- Variety of ΔH, ΔH_k, B_r, H_c, μ

Benefits
- Performance Tailored for Frequency
- Reduced Insertion Loss
- Close Tolerances for Precision Packaging
- Trade-Offs to Optimize Performance

Introduction
With almost 50 years of experience Trans-Tech continues to be the supplier of choice of major OEM's for microwave magnetic and dielectric materials for circulators and isolators. Trans-Tech offers a wide variety of materials, shapes and sizes that can be machined to customer specifications or supplied as an as-fired part.

Intended Applications
Materials are designed to meet the demands of circulator and isolator designs in the 200 MHz to 100 GHz frequency range,to optimize bandwidth, VSWR, insertion loss isolation, temperature and size.

Metallization
Disks and triangles are available with thick film metallization for ground planes. Dielectrics for composites, see section 1, pages 1-30 and 1-31.

General Characteristics
- Wide Selection of $4\pi M_s$ values
- Low Loss
- Low and High Power Material
- Temperature Stability

Availability
The selection of microwave magnetic material is a challenging technical problem, and involves trade-off of one or more performance parameters. High power handling may be obtained at the expense of low-power insertion loss; loss may be improved if temperature performance is not critical. Frequency of operation may force a compromise. Trans-Tech offers a broad range of materials for the designer to choose from. We control the entire process from powder blending to final machining, and can manufacture simple yet precise geometries such as discs or triangles for commercial circulators and isolators.

Guidelines for Below-Resonance Circulator Design

The Lowest Frequency of Operation is Dependent on 4πMs

With F_o in MHz
$$\overline{}$$

$4\pi M_s \ \times \ y \ < \ F_o$ in MHz
$y = 2.8$ MHz \ Oe

Estimated Size of Ferrite Disk
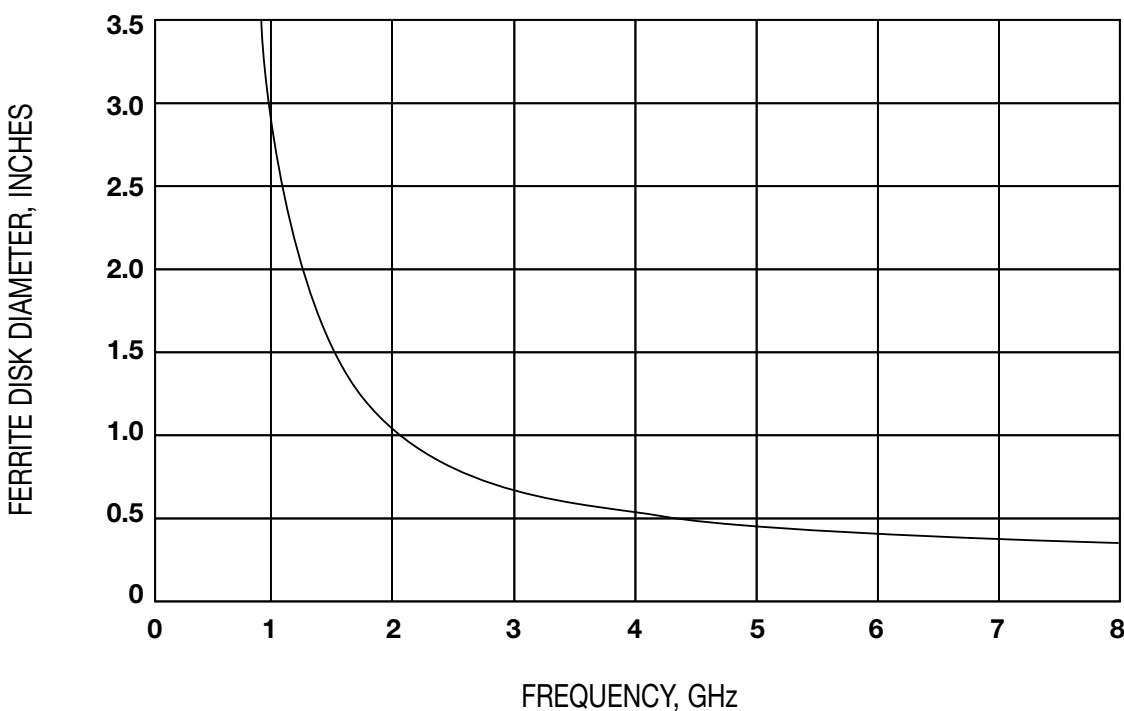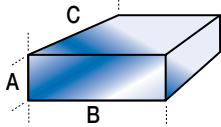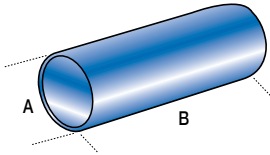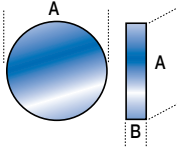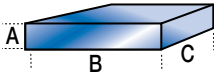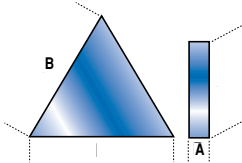
Suggested ferrite disk diameters for below resonance circulators from Simon.

In above resonance applications, choice of $4\pi M_s$ and size is dependent on Gias conditions; therefore, no general approximation is appropriate.

Standard Shapes and Sizes

As Fired Parts

A wide variety of shapes can be produced. The table below shows the shapes and dimensions available as a fired part.

Shapes & Dimensions Available

		MINIMUM SIZE		MAXIMUM SIZE	
Bars		A	.250"	A	1.00"
		B	1"	B	2"
		C	6"	C	6"
Rods		A	.250"	A	1"
		B	6"	B	6"
Disks		A	.500"	A	4"
		B	.050"	B	.150"
Substrates		A	.065"	A	.065"
		B	1"	B	2"
		C	1"	C	2"
Triangles		A	.050"	A	.150"
		B	.500"	B	4"

Machined Parts

Please contact or send specifications to Trans-Tech.

Microwave Substrates
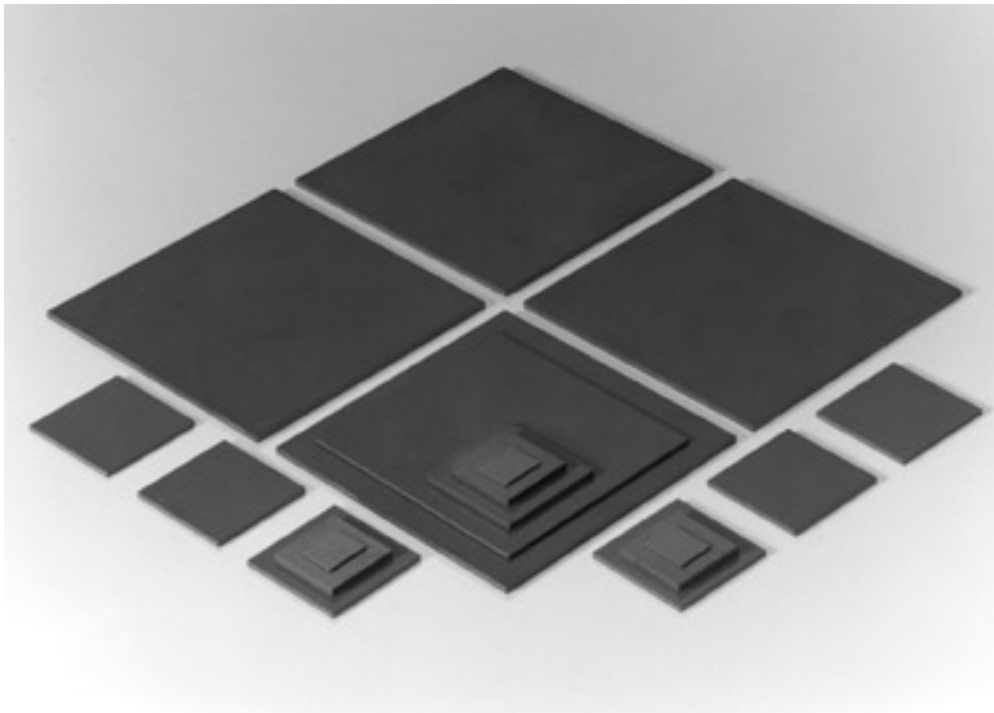
Features
- Wide Selection of $4\pi M_s$
- Small Size
- Weight
- Height

Benefits
- Frequency Design 200 MHz/100 GHz
- No Connectors
- No Housing
- Ease of Integration with Dielectric Substrate

General Characteristics
- Wide Selection of $4\pi M_s$ values
- Low Loss
- Smooth and Flat surfaces
- High Density

Intended Applications

These substrates are designed to meet the demands of devices in the UHF - microwave frequency range. They offer low loss characteristics, temperature stability, and reduced size and weight enabling for circuit miniaturization. Substrates can be metallized for thick film applications.

Available Grades

A selection of magnetic ceramic substrates are available in three standard surface finish grades with custom specifications provided on request.

Grade 4 - Fine Matte   4-8 µ"

Designed for thin film MIC applications that require superior surface perfection and flatness. Grade 4 substrates are also 100% inspected for all important parameters.

Grade 2 - Lapped   <16 µ"

Designed for both thick and thin film MIC applications where cost is a consideration yet controlled electrical and mechanical properties are required.

Grade 1 - Surface Ground   <32 µ"

Designed for thick film MIC application where cost is a consideration and surface perfection is not required.

Other materials, surface finishes, and thicknesses may be requested and should be specified on the drawing. Consult the factory for price and availability.

Inspection Table per ASTM-F-109-73

VISUAL CRITERIA	GRADE 4	GRADE 2	GRADE 1
Surface Finish(RMS)	4-8 µ"	16 µ"	<32µ"
Camber	<.0005"/inch	<.001"/inch	<.002"/inch
Chip (W/D)	*No Single Chip to Exceed .040" Along Edge or .020" at Deepest Point*		
Hole, Pit, Pock	.010" Max.Dia	.015" Max.Dia.	.025" Max.Dia.
Blemishes	*Max. Diameter .030" -- Max. 6/Side or 2/Sq. Inch*		
Crack	None	None	None
Ridges	None	None	None
Inspection Level	100% visual	1% AQL level 2	1% AQL level 2
Length	±.010"	±.010"	±.010"
Width	±.010"	±.010"	±.010"
Thickness	±.001"	±.001"	±.001"
Perpendicularity	.005"/inch	.005"/inch	.005"/inch
Parallelism	.001"/inch	.001"/inch	.001"/inch
Radius of Corners	.010" max.	<.010" max	.010" max

Thinnest Available by Dimension

Garnet & Dielectric Materials are available in the following minimum thickness:
1" x 1" = .010 min.
1" x 2" = .010 min
2" x 2" = .020 min

Ferrite materials are available in the following minimum thickness:
1" x 1" = .015 min.
1" x 2" = .020 min
2" x 2" = .025 min

Visual Criteria
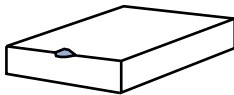
Chip - An area along an edge or corner where the material has broken off: w=width, l=length, d=depth

Crack - A line of fracture without complete separation

Hole, Pit, or Pock - A deep depression or void

Ridge - A long narrow protrusion on the surface

Substrate Cleaning Procedure:

The cleanliness of the oxide substrate strongly influences adhesion of thick and thin film metallization. The cleaning procedures that are widely used for alumina (aluminum oxide) are not directly applicable to other ceramic materials such as titanates, ferrites, and garnets. Many of these procedures incorporate hot strong acids (HCl, HF, HNO3, H2SO4) which, in most cases, are detrimental to these substrates. Others make use of hot strong bases (NaOH, KOH) as cleansing agents which are also harmful and require extensive rinsing for complete removal. The damage may result in degradation of surface finish which causes problems with metallization.

Therefore it is recommended that only mild acidic (pH 2.5-5) and alkaline (pH 9-12) detergents be used to clean substrates. In all cases, we recommend cleaning and thorough rinsing with deionized water at about 60° with ultrasonic agitation. The cleaning should start with an alkaline cleanser followed by an acidic one with an intermediate rinse with dionized water. The final rinse is best accomplished with a cascading set-up (2-3 baths in series). Substrates should be mounted vertically and separately from each other in a suitable holder such that the major surfaces are totally exposed to the aqueous cleaner and the ultrasonic agitation. Substrates should be removed directly from the hot rinse and placed in a clean chamber of hot air dryer (forced draft) set at 70-80°C. For thin film metallization we recommend that the clean substrates be thermally annealed at about 1000°C prior to metal deposition.

For additional information contact factory.

Ordering Information:

Material Type: _____
Grade: _____
Thickness (A): _____
Length (B): _____
Width (C): _____
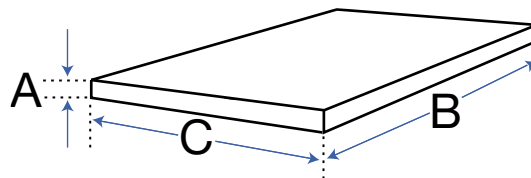
Phase Shifters
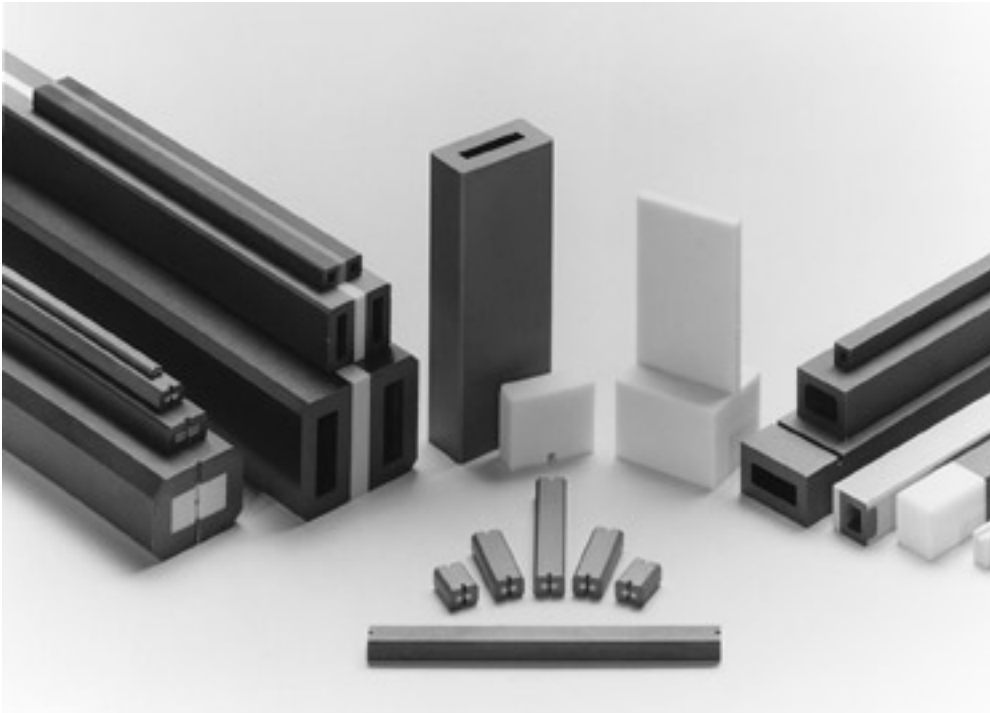
Features
- Wide Selection of $4\pi M_s$
- Low Dielectric Loss
- Square Hysteresis Loop Properties
- Temperature Stabilized
- Controlled Coercive Force
- Controlled ΔH_k

Benefits
- Frequency Design 1.5GHz/35GHz
- Low Insertion Loss
- Maximum Phase Shift
- Wide Temperature
- Low Switching Energy
- High Power Handling

General Characteristics
- Wide Selection of Materials Systems
- Diverse Selection of Material Type
- Low Magnetic and Dielectric Loss
- Controlled $4\pi M_s$ Versus Temperature
- Wide Range of Spin Wave Line Width
- Square Hysteresis Loop Properties

Intended Applications
Phase shifter materials are designed to meet the demands of latching type devices such as phase shifters, switches and latching circulators to optimize phase shift, insertion loss, temperature and size.

Availability
The selection of microwave magnetic material is a science and involves trade-offs of one or more performance parameters. High power handling may be obtained at the expense of low-level insertion loss. Loss may be improved if temperature performance is not critical. Frequency of operation may force a compromise. Trans-Tech offers a broad range of materials for the designer to choose from. The entire process is controlled from powder blending to final machining of phase shifter toroids to ensure reproducible properties. We have consistently shown this fact for +20 years in Aegis and other high volume, long term programs.

Quality Assurance
Throughout manufacturing, random lot samples are tested after key stages of production to guarantee conformance to all electrical and mechanical requirements. In addition, the finished ferrite phase shifter toroid is submitted to an especially rigorous series of quality assurance tests before delivery to the customer. At Trans-Tech, QA testing is the culmination of an overall process ensuring quality control. The final Quality Assurance tests measure the electrical properties of the toroid to assure reproducibility and performance. Using sample toroids from every batch of material, four principal electrical QA measurements are made:

- Complex dielectric constant and loss tangent
- Line width and gyromagnetic ratio
- Saturation magnetization
- Hysteresis loop properties

All finished pieces are 100% tested to verify precise dimensions. By rigorously adhering to quality control standards, Trans-Tech complies with all the specifications applicable to the prime and subcontract requirements for MIL-I-45208, and other Military Specifications.

Microwave Garnets

*For any composition the minimum line width is fixed by KI/Ms. For some shapes and sizes, line widths even closer to the theoretical limit are possible. Typical value for this series is 20oe which is available in some shapes and sizes.

NOTE: Bars and Rods are Available for All Material Types, as well as discs, triangles, and composites.

COMPOSITION AND TYPE NUMBER	PAGE NUMBER	SATURATION MAGNETIZATION $4\pi M_S$ (Gauss)	LANDE' § g-FACTOR g-eff	LINE WIDTH § ΔH oe @-3dB	DIELECTRIC* CONSTANT ε'	DIELECTRIC LOSS TANGENT Tan δ = ε"/	CURIE TEMPERATURE Tc (°C)	SPIN WAVE LINE WIDTH ΔH_k oe	REMANENT INDUCTION* B_r (Gauss)	COERCIVE Force* H_c (oe)	INITIAL PERMEABILITY† μo
		(NominalValue)					(NominalValue)	(NominalValue)	(NominalValue)	(NominalValue)	(NominalValue)
ALUMINUM DOPED											
G-1009	68	175 ± 25g	2.03	≤50	13.8 ± 5%	≤.0002	85	1.5	40	0.90	11
G-250	68	250 ± 25g	2.02	≤45	13.8 ± 5%	≤.0002	105	1.4	123	0.62	34
G-300	68	300 ± 25g	2.02	≤45	14.0 ± 5%	≤.0002	120	2.0	162	0.62	46
G-350	69	350 ± 25g	2.01	≤45	14.0 ± 5%	≤.0002	130	1.4	213	0.66	31
G-400	69	400 ± 25g	2.01	≤45	14.1 ± 5%	≤.0002	135	1.4	224	0.69	41
G-475	69	475 ± 25g	2.01	≤45	14.1 ± 5%	≤.0002	140	1.4	310	0.60	40
G-510	70	550 ± 5%	2.00	≤48	14.3 ± 5%	≤.0002	155	1.3	398	0.55	37
G-610	70	680 ± 5%	2.00	≤48	14.5 ± 5%	≤.0002	185	1.5	515	0.70	50
GADOLINIUM DOPED											
G-1005	70	725 ± 5%	2.02	≤300	15.4 ± 5%	≤.0002	280	7.6	357	1.51	26
G-1003	71	870 ± 5%	2.00	≤186	15.4 ± 5%	≤.0002	280	6.4	543	1.10	36
G-1002	71	1000 ± 5%	1.99	≤132	15.4 ± 5%	≤.0002	280	5.8	672	0.93	48
G-1001	71	1200 ± 5%	1.99	≤96	15.2 ± 5%	≤.0002	280	4.3	717	1.00	72
G-1600	72	1600 ± 5%	1.98	≤66	15.1 ± 5%	≤.0002	280	3.8	986	0.83	116
GADOLINIUM ALUMINUM DOPED											
G-1006	72	400 ± 25g	2.01	≤78	14.2 ± 5%	≤.0002	150	4.2	185	1.00	23
G-500	72	550 ± 5%	2.00	≤78	14.4 ± 5%	≤.0002	180	3.5	280	0.80	28
G-600	73	680 ± 5%	2.00	≤72	14.6 ± 5%	≤.0002	200	4.0	375	0.69	34
G-1004	73	800 ± 5%	2.00	≤90	14.8 ± 5%	≤.0002	240	5.2	493	0.93	38
G-800	73	800 ± 5%	2.00	≤66	14.7 ± 5%	≤.0002	230	4.3	504	0.69	60
G-1000	74	1000 ± 5%	1.99	≤66	14.7 ± 5%	≤.0002	250	3.6	641	0.97	56
G-1021	74	1100 ± 5%	1.99	≤108	15.2 ± 5%	≤.0002	280	5.4	722	0.76	54
G-1200	74	1200 ± 5%	1.98	≤60	15.1 ± 5%	≤.0002	260	3.2	795	0.83	65
G-1400	75	1400 ± 5%	1.98	≤60	15.1 ± 5%	≤.0002	265	3.1	918	0.69	89
HOLMIUM DOPED											
G-4260	75	550 ± 5%	2.00	≤120	14.4 ± 5%	≤.0002	180	8.5	280	0.80	28
G-4259	75	800 ± 5%	2.00	≤132	14.8 ± 5%	≤.0002	240	8.1	493	0.93	38
G-4258	76	1000 ± 5%	1.99	≤156	15.4 ± 5%	≤.0002	280	8.9	672	0.93	48
G-4257	76	1200 ± 5%	1.99	≤120	15.2 ± 5%	≤.0002	280	8.1	717	1.00	72
G-4256	76	1600 ± 5%	1.98	≤84	15.1 ± 5%	≤.0002	280	5.4	986	0.83	116
G-113	77	1780 ± 5%	1.97	≤25	15.0 ± 5%	≤.0002	280	1.4	1277	0.45	134
G-810	77	800 ± 5%	1.99	≤25	14.6 ± 5%	≤.0002	200	1.5	543	0.62	46
G-1010	77	1000 ± 5%	1.99	≤25	14.7 ± 5%	≤.0002	210	1.4	694	1.55	66
G-1210	78	1200 ± 5%	1.98	≤25	14.8 ± 5%	≤.0002	220	1.3	784	0.69	87
CALCIUM VANADIUM DOPED											
TTVG-800	78	800 ± 5%	2.00	≤15	13.9 ± 5%	≤.0002	192	2.0	560	0.60	129
TTVG-930	78	930 ± 5%	2.00	≤10	14.0 ± 5%	≤.0002	188	2.0	380	0.40	225
TTVG-1000	79	1000 ± 5%	2.00	≤10	14.0 ± 5%	≤.0002	199	2.0	320	0.30	210
TTVG-1100	79	1100 ± 5%	2.00	≤10	14.1 ± 5%	≤.0002	205	2.0	600	0.60	209
TTVG-1200	79	1200 ± 5%	2.00	≤10	14.4 ± 5%	≤.0002	208	2.0	635	0.30	221
TTVG-1400	79	1400 ± 5%	2.00	≤10	14.5 ± 5%	≤.0002	215	2.0	825	0.30	263
TTVG-1600	79	1600 ± 5%	2.00	≤10	14.6 ± 5%	≤.0002	220	2.0	1000	0.60	227
TTVG-1850	79	1850 ± 5%	2.00	≤10	14.8 ± 5%	≤.0002	200	2.0	1232	0.50	388
TTZ1950	—	1950 ± 5%	2.00	≤15	15.0 ± 5%	≤.0002	235	2.0	—	—	—

§ Measured @ 9.4GH$_z$ † Measured @ 1KH$_z$ * Measured @ 60H$_z$ or 2KH$_z$ with H$_{app}$=5xH$_c$

G-1009 Aluminum Doped

0.5" O.D. by 0.4" I.D. by 0.5" length toroid
Temperature: 25°C.
Frequency: 2KHz
Drive Field: 5.0 oe

B_m = 84
B_r = 40
H_c = .90

H Oersteds
Hysteresis Loop

Temperature °C
Hysteresis Loop

G-250 Aluminum Doped

0.5" O.D. by 0.4" I.D. by 0.5" length toroid
Temperature: 25°C.
Frequency: 2KHz
Drive Field: 5.0 oe

B_m = 168
B_r = 123
H_c = .62

H Oersteds
Hysteresis Loop

Typical performance curves are shown

Temperature °C
Hysteresis Loop

G-300 Aluminum Doped

0.5" O.D. by 0.4" I.D. by 0.5" length toroid
Temperature: 25°C.
Frequency: 2KHz
Drive Field: 5.0 oe

B_m = 207
B_r = 162
H_c = .62

H Oersteds
Hysteresis Loop

Temperature °C
Hysteresis Loop

Trans-Tech · Phone: **301-695-9400** · Fax: 301-695-7065 · E-mail: sales@trans-techinc.com

G-350 Aluminum Doped

0.5" O.D. by 0.4" I.D. by 0.5" length toroid
Temperature: 25°C.
Frequency: 2KHz
Drive Field: 5.0 oe

$B_m = 269$
$B_r = 213$
$H_c = .66$

G-400 Aluminum Doped

0.5" O.D. by 0.4" I.D. by 0.5" length toroid
Temperature: 25°C.
Frequency: 2KHz
Drive Field: 5.0 oe

$B_m = 291$
$B_r = 224$
$H_c = .69$

G-475 Aluminum Doped

0.5" O.D. by 0.4" I.D. by 0.5" length toroid
Temperature: 25°C.
Frequency: 2KHz
Drive Field: 5.0 oe

$B_m = 360$
$B_r = 310$
$H_c = .60$

G-510 Aluminum Doped

0.5" O.D. by 0.4" I.D. by 0.5" length toroid
Temperature: 25°C.
Frequency: 2KHz
Drive Field: 5.0 oe

$B_m = 448$
$B_r = 398$
$H_c = .55$

B GAUSS
H Oersteds
Hysteresis Loop

$B_r, B_m, 4\pi M_s$ GAUSS
H_c OERSTEDS
Temperature °C
Hysteresis Loop

$4\pi M_s$
B_m
B_r
H_c

G-610 Aluminum Doped

0.5" O.D. by 0.4" I.D. by 0.5" length toroid
Temperature: 25°C.
Frequency: 2KHz
Drive Field: 5.0 oe

$B_m = 582$
$B_r = 515$
$H_c = .70$

B GAUSS
H Oersteds
Hysteresis Loop

$B_r, B_m, 4\pi M_s$ GAUSS
H_c OERSTEDS
Temperature °C
Hysteresis Loop

$4\pi M_s$
B_m
B_r
H_c

G-1005 Gadolinium Doped

0.5" O.D. by 0.4" I.D. by 0.5" length toroid
Temperature: 25°C.
Frequency: 2KHz
Drive Field: 10 oe

$B_m = 439$
$B_r = 357$
$H_c = 1.51$

B GAUSS
H Oersteds
Hysteresis Loop

Typical performance curves are shown

$B_r, B_m, 4\pi M_s$ GAUSS
H_c OERSTEDS
Temperature °C
Hysteresis Loop

$4\pi M_s$
B_m
B_r
H_c

G-1003 Gadolinium Doped

0.5" O.D. by 0.4" I.D. by 0.5" length toroid
Temperature: 25°C.
Frequency: 2KHz
Drive Field: 5.0 oe

$B_m = 616$
$B_r = 543$
$H_c = 1.10$

B GAUSS vs H Oersteds — Hysteresis Loop

B_r, B_m, $4\pi M_s$ GAUSS vs Temperature °C / H_c OERSTEDS — Hysteresis Loop
($4\pi M_s$, B_m, B_r, H_c)

G-1002 Gadolinium Doped

0.5" O.D. by 0.4" I.D. by 0.5" length toroid
Temperature: 25°C.
Frequency: 2KHz
Drive Field: 5.0 oe

$B_m = 756$
$B_r = 672$
$H_c = .93$

B GAUSS vs H Oersteds — Hysteresis Loop

B_r, B_m, $4\pi M_s$ GAUSS vs Temperature °C / H_c OERSTEDS — Hysteresis Loop
($4\pi M_s$, B_m, B_r, H_c)

4

G-1001 Gadolinium Doped

0.5" O.D. by 0.4" I.D. by 0.5" length toroid
Temperature: 25°C.
Frequency: 2KHz
Drive Field: 5.0 oe

$B_m = 851$
$B_r = 717$
$H_c = 1.0$

B GAUSS vs H Oersteds — Hysteresis Loop

B_r, B_m, $4\pi M_s$ GAUSS vs Temperature °C / H_c OERSTEDS — Hysteresis Loop
($4\pi M_s$, B_m, B_r, H_c)

G-1600 Gadolinium Doped

0.5" O.D. by 0.4" I.D. by 0.5" length toroid
Temperature: 25°C.
Frequency: 2KHz
Drive Field: 5.0 oe

B_m = 1165
B_r = 986
H_c = .83

H Oersteds
Hysteresis Loop

Temperature °C
Hysteresis Loop

G-1006 Gadolinium Aluminum Doped

0.5" O.D. by 0.4" I.D. by 0.5" length toroid
Temperature: 25°C.
Frequency: 2KHz
Drive Field: 5.0 oe

B_m = 235
B_r = 185
H_c = 1.0

H Oersteds
Hysteresis Loop

Temperature °C
Hysteresis Loop

G-500 Gadolinium & Aluminum Doped

0.5" O.D. by 0.4" I.D. by 0.5" length toroid
Temperature: 25°C.
Frequency: 2KHz
Drive Field: 10 oe

B_m = 336
B_r = 280
H_c = 1.4

H Oersteds
Hysteresis Loop

Temperature °C
Hysteresis Loop

Typical performance curves are shown

Trans-Tech · Phone: **301-695-9400** · Fax: 301-695-7065 · E-mail: sales@trans-techinc.com

G-600 Gadolinium & Aluminum Doped

0.5" O.D. by 0.4" I.D. by 0.5" length toroid
Temperature: 25°C.
Frequency: 2KHz
Drive Field: 5.0 oe

$B_m = 482$
$B_r = 375$
$H_c = .69$

H Oersteds
Hysteresis Loop

Temperature °C
Hysteresis Loop

$4\pi M_s$
B_m
B_r
H_c

G-1004 Gadolinium & Aluminum Doped

0.5" O.D. by 0.4" I.D. by 0.5" length toroid
Temperature: 25°C.
Frequency: 2KHz
Drive Field: 5.0 oe

$B_m = 560$
$B_r = 493$
$H_c = .93$

H Oersteds
Hysteresis Loop

Temperature °C
Hysteresis Loop

$4\pi M_s$
B_m
B_r
H_c

G-800 Gadolinium & Aluminum Doped

0.5" O.D. by 0.4" I.D. by 0.5" length toroid
Temperature: 25°C.
Frequency: 2KHz
Drive Field: 5.0 oe

$B_m = 594$
$B_r = 504$
$H_c = .69$

H Oersteds
Hysteresis Loop

Temperature °C
Hysteresis Loop

$4\pi M_s$
B_m
B_r
H_c

G-1000 Gadolinium & Aluminum Doped

0.5" O.D. by 0.4" I.D. by 0.5" length toroid
Temperature: 25°C.
Frequency: 2KHz
Drive Field: 5.0 oe

B_m = 729
B_r = 641
H_c = .97

H Oersteds
Hysteresis Loop

Temperature °C
Hysteresis Loop

G-1021 Gadolinium & Aluminum Doped

0.5" O.D. by 0.4" I.D. by 0.5" length toroid
Temperature: 25°C.
Frequency: 2KHz
Drive Field: 5.0 oe

B_m = 823
B_r = 722
H_c = .76

H Oersteds
Hysteresis Loop

Temperature °C
Hysteresis Loop

G-1200 Gadolinium & Aluminum Doped

0.5" O.D. by 0.4" I.D. by 0.5" length toroid
Temperature: 25°C.
Frequency: 2KHz
Drive Field: 5.0 oe

B_m = 930
B_r = 795
H_c = .83

H Oersteds
Hysteresis Loop

Temperature °C
Hysteresis Loop

Typical performance curves are shown

G-1400 Gadolinium & Aluminum Doped

0.5" O.D. by 0.4" I.D. by 0.5" length toroid
Temperature: 25°C.
Frequency: 2KHz
Drive Field: 5.0 oe

B_m = 1075
B_r = 918
H_c = .69

H Oersteds
Hysteresis Loop

Temperature °C
Hysteresis Loop

G-4260 Gadolinium & Aluminum Holmium Doped

0.5" O.D. by 0.4" I.D. by 0.5" length toroid
Temperature: 25°C.
Frequency: 2KHz
Drive Field: 10 oe

B_m = 336
B_r = 280
H_c = 1.4

H Oersteds
Hysteresis Loop

Temperature °C
Hysteresis Loop

G-4259 Gadolinium & Aluminum Holmium Doped

0.5" O.D. by 0.4" I.D. by 0.5" length toroid
Temperature: 25°C.
Frequency: 2KHz
Drive Field: 5.0 oe

B_m = 560
B_r = 493
H_c = .93

H Oersteds
Hysteresis Loop

Temperature °C
Hysteresis Loop

Trans-Tech · Phone: **301-695-9400** · Fax: 301-695-7065 · E-mail: sales@trans-techinc.com

G-4258 Gadolinium & Holmium Doped

0.5" O.D. by 0.4" I.D. by 0.5" length toroid
Temperature: 25°C.
Frequency: 2KHz
Drive Field: 5.0 oe

B_m = 756
B_r = 672
H_c = .93

Left graph: B GAUSS vs H Oersteds — Hysteresis Loop

Right graph: B_r, B_m, $4\pi M_s$ GAUSS and H_c OERSTEDS vs Temperature °C — Hysteresis Loop (B_m, $4\pi M_s$, B_r, H_c)

G-4257 Gadolinium & Holmium Doped

0.5" O.D. by 0.4" I.D. by 0.5" length toroid
Temperature: 25°C.
Frequency: 2KHz
Drive Field: 5.0 oe

B_m = 851
B_r = 717
H_c = 1.0

Left graph: B GAUSS vs H Oersteds — Hysteresis Loop

Right graph: B_r, B_m, $4\pi M_s$ GAUSS and H_c OERSTEDS vs Temperature °C — Hysteresis Loop ($4\pi M_s$, B_m, B_r, H_c)

G-4256 Gadolinium Holmium Doped

0.5" O.D. by 0.4" I.D. by 0.5" length toroid
Temperature: 25°C.
Frequency: 2KHz
Drive Field: 5.0 oe

B_m = 1165
B_r = 986
H_c = .83

Left graph: B GAUSS vs H Oersteds — Hysteresis Loop

Right graph: B_r, B_m, $4\pi M_s$ GAUSS and H_c OERSTEDS vs Temperature °C — Hysteresis Loop ($4\pi M_s$, B_m, B_r, H_c)

G-113 Yttrium

0.5" O.D. by 0.4" I.D. by 0.5" length toroid
Temperature: 25°C.
Frequency: 2KHz
Drive Field: 5.0 oe

B_m = 1449
B_r = 1277
H_c = .45

B GAUSS — H Oersteds
Hysteresis Loop

B_r, B_m, $4\pi M_s$ GAUSS — H_c OERSTEDS
Temperature °C
Hysteresis Loop

G-810 Aluminum Doped

0.5" O.D. by 0.4" I.D. by 0.5" length toroid
Temperature: 25°C.
Frequency: 2KHz
Drive Field: 5.0 oe

B_m = 644
B_r = 543
H_c = .62

B GAUSS — H Oersteds
Hysteresis Loop

B_r, B_m, $4\pi M_s$ GAUSS — H_c OERSTEDS
Temperature °C
Hysteresis Loop

G-1010 Aluminum Doped

0.5" O.D. by 0.4" I.D. by 0.5" length toroid
Temperature: 25°C.
Frequency: 2KHz
Drive Field: 5.0 oe

B_m = 773
B_r = 694
H_c = .55

B GAUSS — H Oersteds
Hysteresis Loop

B_r, B_m, $4\pi M_s$ GAUSS — H_c OERSTEDS
Temperature °C
Hysteresis Loop

Trans-Tech · Phone: **301-695-9400** · Fax: 301-695-7065 · E-mail: sales@trans-techinc.com

G-1210 Aluminum Doped

0.5" O.D. by 0.4" I.D. by 0.5" length toroid
Temperature: 25°C.
Frequency: 2KHz
Drive Field: 5.0 oe

B_m = 896
B_r = 784
H_c = .69

H Oersteds
Hysteresis Loop

$4\pi M_s$
B_m
B_r
H_c

Temperature °C
Hysteresis Loop

TTVG-800 Narrow Line Width Garnet

B_m
$4\pi M_s$
B_r
H_c

Temperature °C
Hysteresis Loop

TTVG-930 Narrow Line Width Garnet

$4\pi M_s$
B_m
B_r
H_c

Temperature °C
Hysteresis Loop

TTVG-1000 Narrow Line Width Garnet

Temperature °C
Hysteresis Loop

TTVG-1400 Narrow Line Width Garnet

Temperature °C
Hysteresis Loop

TTVG-1100 Narrow Line Width Garnet

Temperature °C
Hysteresis Loop

TTVG-1600 Narrow Line Width Garnet

Temperature °C
Saturation Magnetization

TTVG-1200 Narrow Line Width Garnet

Temperature °C
Hysteresis Loop

TTVG-1850 Narrow Line Width Garnet

Temperature °C
Hysteresis Loop

Trans-Tech · Phone: **301-695-9400** · Fax: 301-695-7065 · E-mail: sales@trans-techinc.com

Microwave Ferrites

	COMPOSITION AND TYPE NUMBER	PAGE NUMBER	SATURATION MAGNETIZATION $4\pi M_S$ (Gauss)	LANDE' § g-FACTOR g-eff	LINE WIDTH § ΔH oe @ -3dB	DIELECTRIC § CONSTANT ε'	DIELECTRIC § LOSS TANGENT Tan δ = ε"/ε'	CURIE TEMPERATURE Tc (°C)	SPIN WAVE § LINE WIDTH Δ Hk oe	REMANENT INDUCTION* B_r (Gauss)	COERCIVE FORCE* H_c (oe)	INITIAL PERMEABILITY† μ_0
								(Nominal Value)	(Nominal Value)	(Nominal Value)	(Nominal Value)	(Nominal Value)
MAGNESIUM FERRITES	TT1-414	82	750 ± 5%	1.98	≤144	11.3 ± 5%	≤.00025	90	5.1	544	0.48	120
	TT1-1000	82	1000 ± 5%	1.98	≤120	11.6 ± 5%	≤.00025	100	3.1	627	0.62	93
	TT1-109	82	1300 ± 5%	1.98	≤162	11.8 ± 5%	≤.00025	140	2.5	940	0.87	30
	TT1-1500	83	1500 ± 5%	1.98	≤216	12.0 ± 5%	≤.00025	180	2.3	968	0.99	51
	TTI-105	83	1750 ± 5%	1.98	≤270	12.2 ± 5%	≤.00025	225	2.2	1220	1.20	55
	TTI-2000	83	2000 ± 5%	1.98	≤300	12.4 ± 5%	≤.00025	290	2.1	1385	1.60	52
	TT1-390	84	2150 ± 5%	2.04	≤648	12.7 ± 5%	≤.00025	320	2.5	1288	1.80	50
	TT1-2500	84	2500 ± 5%	2.03	≤624	12.9 ± 5%	≤.00025	275	3.0	1410	1.33	57
	TT1-2650	84	2650 ± 5%	2.02	≤636	13.0 ± 5%	≤.0005	245	2.8	1511	1.33	85
	TT1-2800	85	2800 ± 5%	2.01	≤648	13.1 ± 5%	≤.0005	225	2.2	1477	0.83	140
	TT1-3000	85	3000 ± 5%	1.99	≤228	12.9 ± 5%	≤.0005	240	3.2	2100	0.85	54
NICKEL FERRITES	TT2-113	85	500 ± 10%	1.54	≤190	9.0 ± 10%	≤.0008	120	–	140	2.00	23
	TT2-125	86	2100 ± 10%	2.30	≤575	12.6 ± 5%	≤.0010	560	6.1	1426	4.42	26
	TT2-102	86	2500 ± 10%	2.25	≤610	12.7 ± 5%	≤.0020	570	6.9	1485	4.42	23
	TT2-2750	86	2750 ± 10%	2.20	≤540	12.8 ± 5%	≤.0025	580	9.0	1130	3.00	20
	TT2-101	87	3000 ± 10%	2.19	≤375	13.0 ± 5%	≤.0025	585	12.4	1853	5.70	17
	TT2-3250	87	3250 ± 10%	2.10	≤440	12.8 ± 5%	≤.0025	550	10.5	1200	2.20	36
	TT2-3500	—	3500 ± 10%	2.10	≤500	12.8 ± 5%	≤.0025	540	9.0	1260	2.40	50
	TT2-4000	87	4000 ± 10%	2.22	≤425	12.3 ±10%	≤.0025	470	7.0	1800	3.00	93
MILLIMETER WAVE FERRITES	TT2-111	88	5000 ± 10%	2.11	≤200	12.5 ±10%	≤.0010	375	6.0	1956	0.96	317
	TT71-4800	88	4800 ± 5%	2.01	≤240	14.5 ± 5%	≤.0015	400	–	3360	0.89	–
	TT86-6000	88	5000 ± 5%	2.11	≤200	12.5 ± 5%	≤.0002	363	6.0	3800	1.50	317

NOTE: Bars and Rods are Available for All Material Types
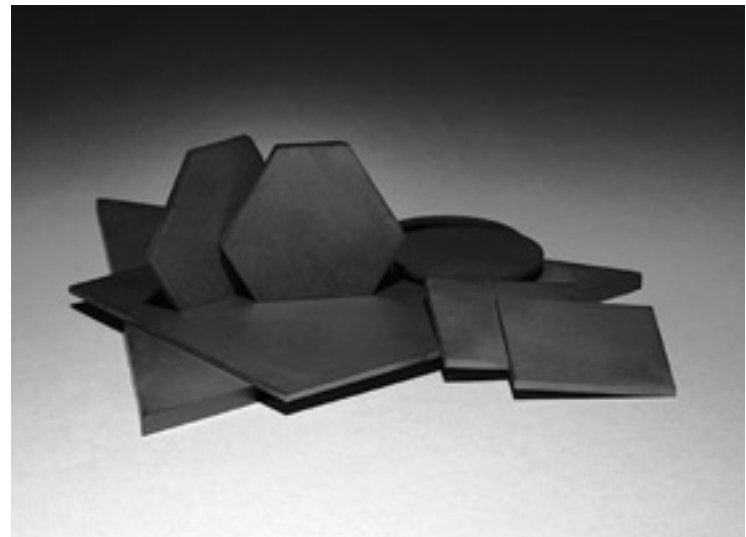
§ Measured @ 9.4GHz   † Measured @ 1KHz   * Measured @ 60Hz or 2KHz with H_{app}=5xH_c ** Anneal @ 1100° C in oxygen after machining

Trans-Tech · Phone: **301-695-9400** · Fax: 301-695-7065 · E-mail: sales@trans-techinc.com

TT1-414 Magnesium

0.5" O.D. by 0.4" I.D. by 0.5" length toroid
Temperature: 25°C.
Frequency: 2KHz
Drive Field: 5.0 oe

B_m = 650
B_r = 544
H_c = .48

B GAUSS

H Oersteds
Hysteresis Loop

B_r, B_m, $4\pi M_s$ GAUSS

H_c OERSTEDS

$4\pi M_s$
B_m
B_r
H_c

Temperature °C
Hysteresis Loop

TT1-1000 Magnesium

0.5" O.D. by 0.4" I.D. by 0.5" length toroid
Temperature: 25°C.
Frequency: 2KHz
Drive Field: 5.0 oe

B_m = 728
B_r = 627
H_c = .62

B GAUSS

H Oersteds
Hysteresis Loop

B_r, B_m, $4\pi M_s$ GAUSS

H_c OERSTEDS

$4\pi M_s$
B_r
B_m
H_c

Temperature °C
Hysteresis Loop

TT1-109 Magnesium

0.5" O.D. by 0.4" I.D. by 0.5" length toroid
Temperature: 25°C.
Frequency: 2KHz
Drive Field: 5.0 oe

B_m = 1053
B_r = 940
H_c = .87

B GAUSS

H Oersteds
Hysteresis Loop

*Typical performance
curves are shown*

B_r, B_m, $4\pi M_s$ GAUSS

H_c OERSTEDS

$4\pi M_s$
B_m
B_r
H_c

Temperature °C
Hysteresis Loop

TT1-1500 Magnesium

0.5" O.D. by 0.4" I.D. by 0.5" length toroid
Temperature: 25°C.
Frequency: 2KHz
Drive Field: 5.0 oe

B_m = 1075
B_r = 968
H_c = .99

Hysteresis Loop

Hysteresis Loop

TT1-105 Magnesium

0.5" O.D. by 0.4" I.D. by 0.5" length toroid
Temperature: 25°C.
Frequency: 2KHz
Drive Field: 5.0 oe

B_m = 1343
B_r = 1220
H_c = 1.16

Hysteresis Loop

Hysteresis Loop

TT1-2000 Magnesium

0.5" O.D. by 0.4" I.D. by 0.5" length toroid
Temperature: 25°C.
Frequency: 2KHz
Drive Field: 5.0 oe

B_m = 1450
B_r = 1385
H_c = 1.6

Hysteresis Loop

Hysteresis Loop

TT1-390 Magnesium

0.5" O.D. by 0.4" I.D. by 0.5" length toroid
Temperature: 25°C.
Frequency: 2KHz
Drive Field: 5.0 oe

B_m = 1420
B_r = 1288
H_c = 1.80

B GAUSS — H Oersteds
Hysteresis Loop

$4\pi M_s$
B_r
B_m
H_c

B_r, B_m, $4\pi M_s$ GAUSS — H_c OERSTEDS
Temperature °C
Hysteresis Loop

TT1-2500 Magnesium

0.5" O.D. by 0.4" I.D. by 0.5" length toroid
Temperature: 25°C.
Frequency: 2KHz
Drive Field: 5.0 oe

B_m = 1612
B_r = 1410
H_c = 1.33

B GAUSS — H Oersteds
Hysteresis Loop

$4\pi M_s$
B_m
B_r
H_c

B_r, B_m, $4\pi M_s$ GAUSS — H_c OERSTEDS
Temperature °C
Hysteresis Loop

TT1-2650 Magnesium

0.5" O.D. by 0.4" I.D. by 0.5" length toroid
Temperature: 25°C.
Frequency: 2KHz
Drive Field: 5.0 oe

B_m = 1779
B_r = 1511
H_c = 1.33

Typical performance curves are shown

B GAUSS — H Oersteds
Hysteresis Loop

$4\pi M_s$
B_m
B_r
H_c

B_r, B_m, $4\pi M_s$ GAUSS — H_c OERSTEDS
Temperature °C
Hysteresis Loop

TT1-2800 Magnesium

0.5" O.D. by 0.4" I.D. by 0.5" length toroid
Temperature: 25°C.
Frequency: 2KHz
Drive Field: 5.0 oe

B_m = 1947
B_r = 1477
H_c = 0.83

H Oersteds
Hysteresis Loop

Temperature °C
Hysteresis Loop

TT1-3000 Magnesium

0.5" O.D. by 0.4" I.D. by 0.5" length toroid
Temperature: 25°C.
Frequency: 2KHz
Drive Field: 5.0 oe

B_m = 2250
B_r = 2000
H_c = 0.85

H Oersteds
Hysteresis Loop

Temperature °C
Hysteresis Loop

TT2-113 Nickel

0.5" O.D. by 0.4" I.D. by 0.5" length toroid
Temperature: 25°C.
Frequency: 2KHz
Drive Field: 25 oe

B_m = 340
B_r = 140
H_c = 2.0

H Oersteds
Hysteresis Loop

Temperature °C
Hysteresis Loop

Trans-Tech · Phone: **301-695-9400** · Fax: 301-695-7065 · E-mail: sales@trans-techinc.com.

TT2-125 Nickel

0.5" O.D. by 0.4" I.D. by 0.5" length toroid
Temperature: 25°C.
Frequency: 2KHz
Drive Field: 25 oe

B_m = 1714
B_r = 1426
H_c = 4.42

TT2-102 Nickel

0.5" O.D. by 0.4" I.D. by 0.5" length toroid
Temperature: 25°C.
Frequency: 2KHz
Drive Field: 25 oe

B_m = 1753
B_r = 1485
H_c = 4.42

TT2-2750 Nickel

0.5" O.D. by 0.4" I.D. by 0.5" length toroid
Temperature: 25°C.
Frequency: 2KHz
Drive Field: 25 oe

B_m = 1760
B_r = 1130
H_c = 3.0

*Typical performance
curves are shown*

TT2-101 Nickel

0.5" O.D. by 0.4" I.D. by 0.5" length toroid
Temperature: 25°C.
Frequency: 2KHz
Drive Field: 25 oe

B_m = 2239
B_r = 1853
H_c = 5.7

H Oersteds
Hysteresis Loop

$4\pi M_s$
B_m
B_r
H_c

Temperature °C
Hysteresis Loop

TT2-3250 Nickel

0.5" O.D. by 0.4" I.D. by 0.5" length toroid
Temperature: 25°C.
Frequency: 2KHz
Drive Field: 25 oe

B_m = 1812
B_r = 1200
H_c = 2.2

H Oersteds
Hysteresis Loop

$4\pi M_s$
B_m
B_r
H_c

Temperature °C
Hysteresis Loop

TT2-4000 Nickel

0.5" O.D. by 0.4" I.D. by 0.5" length toroid
Temperature: 25°C.
Frequency: 2KHz
Drive Field: 18 oe

B_m = 2500
B_r = 1800
H_c = 3.0oe

H Oersteds
Hysteresis Loop

$4\pi M_s$
B_r
B_m
H_c

Temperature °C
Hysteresis Loop

Trans-Tech · Phone: **301-695-9400** · Fax: 301-695-7065 · E-mail: sales@trans-techinc.com

TT2-111 Nickel

0.5" O.D. by 0.4" I.D. by 0.5" length toroid
Temperature: 25°C.
Frequency: 2KHz
Drive Field: 5.0 oe

B_m = 3595
B_r = 1956
H_c = .963

B GAUSS — H Oersteds
Hysteresis Loop

B_r, B_m, $4\pi M_s$ GAUSS — H_c OERSTEDS — Temperature °C
$4\pi M_s$
B_m
B_r
H_c
Hysteresis Loop

TT86-6000 Nickel

0.5" O.D. by 0.4" I.D. by 0.5" length toroid
Temperature: 25°C.
Frequency: 2KHz
Drive Field: 10 oe

B_m = 4100
B_r = 3800
H_c = 1.5

B GAUSS — H Oersteds
Hysteresis Loop

B_r, B_m, $4\pi M_s$ GAUSS — H_c OERSTEDS — Temperature °C
$4\pi M_s$
B_m
B_r
H_c
Hysteresis Loop

TT71-4800 Lithium Zinc

0.5" O.D. by 0.25" I.D. by 0.1" length toroid
Temperature: 25°C.
Frequency: 2KHz
Drive Field: 10 oe

B_m = 3743
B_r = 2843
H_c = .89

B GAUSS — H Oersteds
Hysteresis Loop

B_r, B_m, $4\pi M_s$ GAUSS — H_c OERSTEDS — Temperature °C
$4\pi M_s$
B_m
B_r
H_c
Hysteresis Loop

*Typical performance
curves are shown*

Trans-Tech · Phone: **301-695-9400** · Fax: 301-695-7065 · E-mail: sales@trans-techinc.com

An Overview of Absorbing Materials
and Inductors for UHF and
Microwave Applications.

High Frequency Absorbers and Inductors
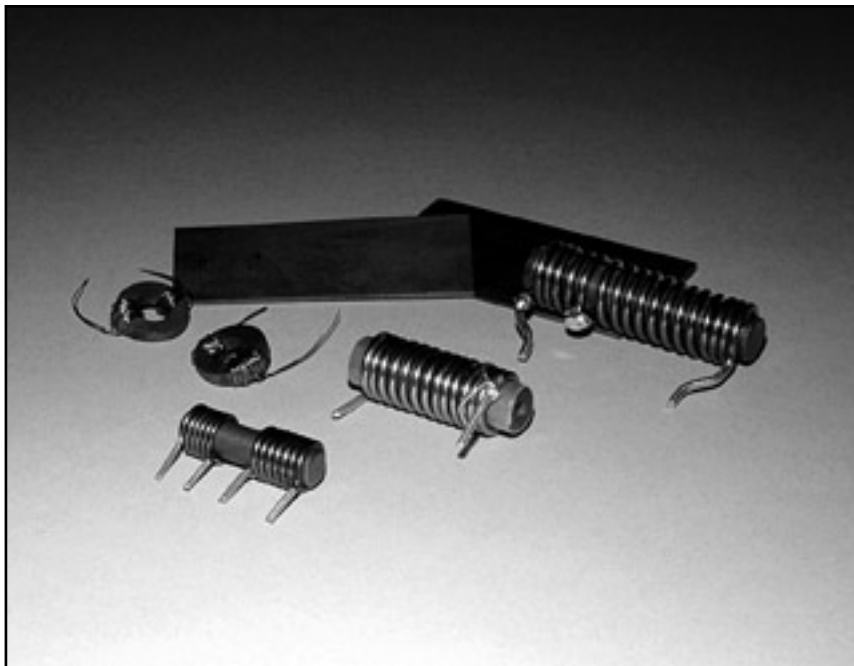
Introduction

Trans Tech Ferrite Materials can be used as either absorbers or inductors in the UHF and Microwave region.

Ferrite materials with $4\pi Ms$ values of up to 5000 Gauss will absorb microwaves up to Y x $4\pi Ms$ MHz, where Y is 2.8MHz /Oe ,i.e. up to 14 GHz.. By combining lossy dielectric properties with magnetic losses, this absorption can be enhanced. These materials become absorptive at frequencies approaching their Snoek limit, which for spinel ferrites are usually much less than 200 MHz . Ferrites operating well below their Snoek limit are useful as inductors or as high permeability substrates for VHF/UHF circuits and antennas. Some examples of spinel based Absorbers and Inductors from TT's large range are given below. Hexagonal Ferrites have Snoek limits extending well into the microwave region, and therefore can be used as inductors or circuit elements into the low end of the microwave region. They can be used as absorbers at higher frequencies, into the millimetric region as the permeability and Q fall. TransTech makes a range of hexagonal ferrites, one of which is included in the permeability versus frequency graphs shown on page 91.

Examples of Trans-Tech Absorbers

(>200MHz to < 12GHz)
TT2-111
Ferrite 50

Examples of Trans-Tech Inductors/Absorbers

TT2-101
TT2-4000
TT2-111
TT86-6000
TT Hexagonal

Permeability vs. Log Fr(MHz)

Permeability vs. Log Fr(MHz)

Log Frequency

Q vs. Log Frequency
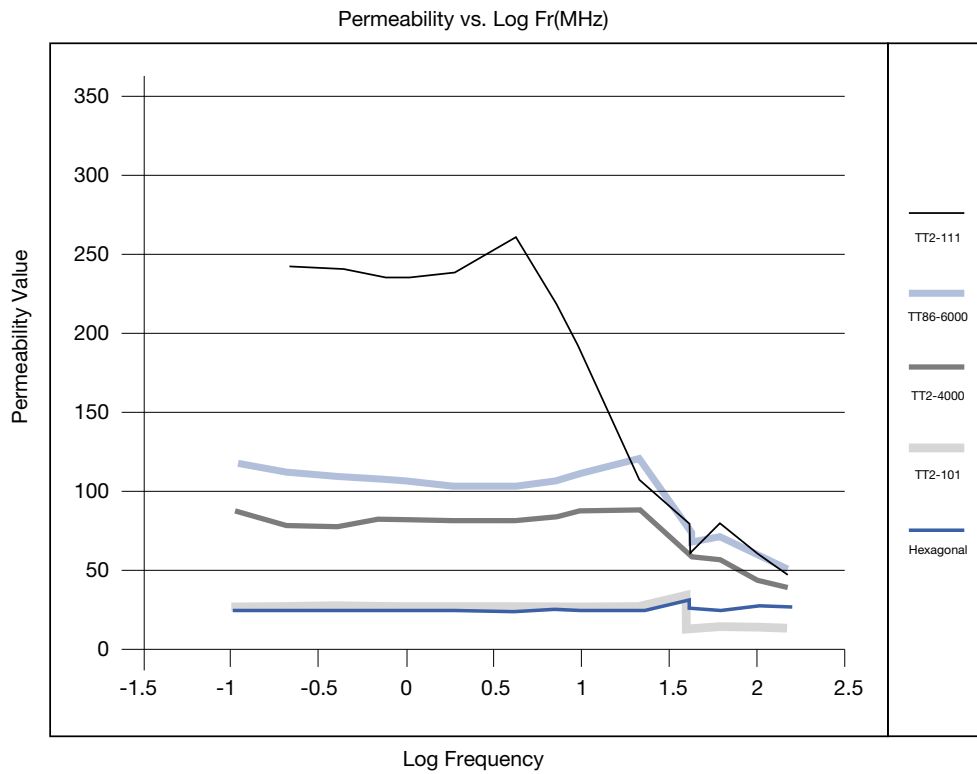
Q vs. Log Frequency

Log Frequency (MHz)
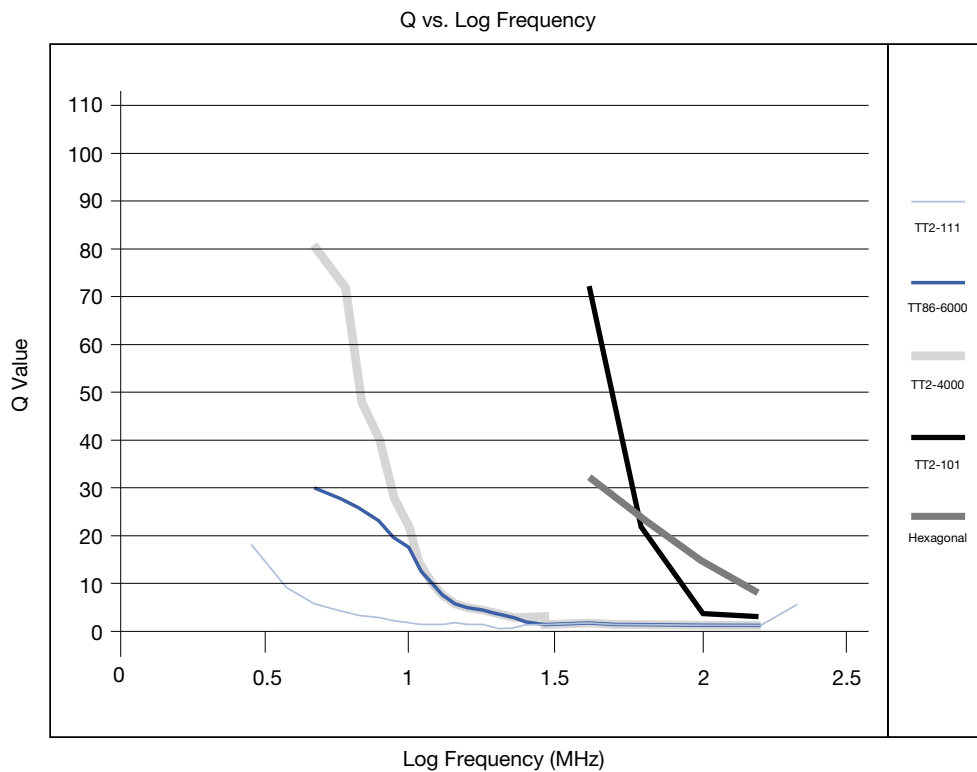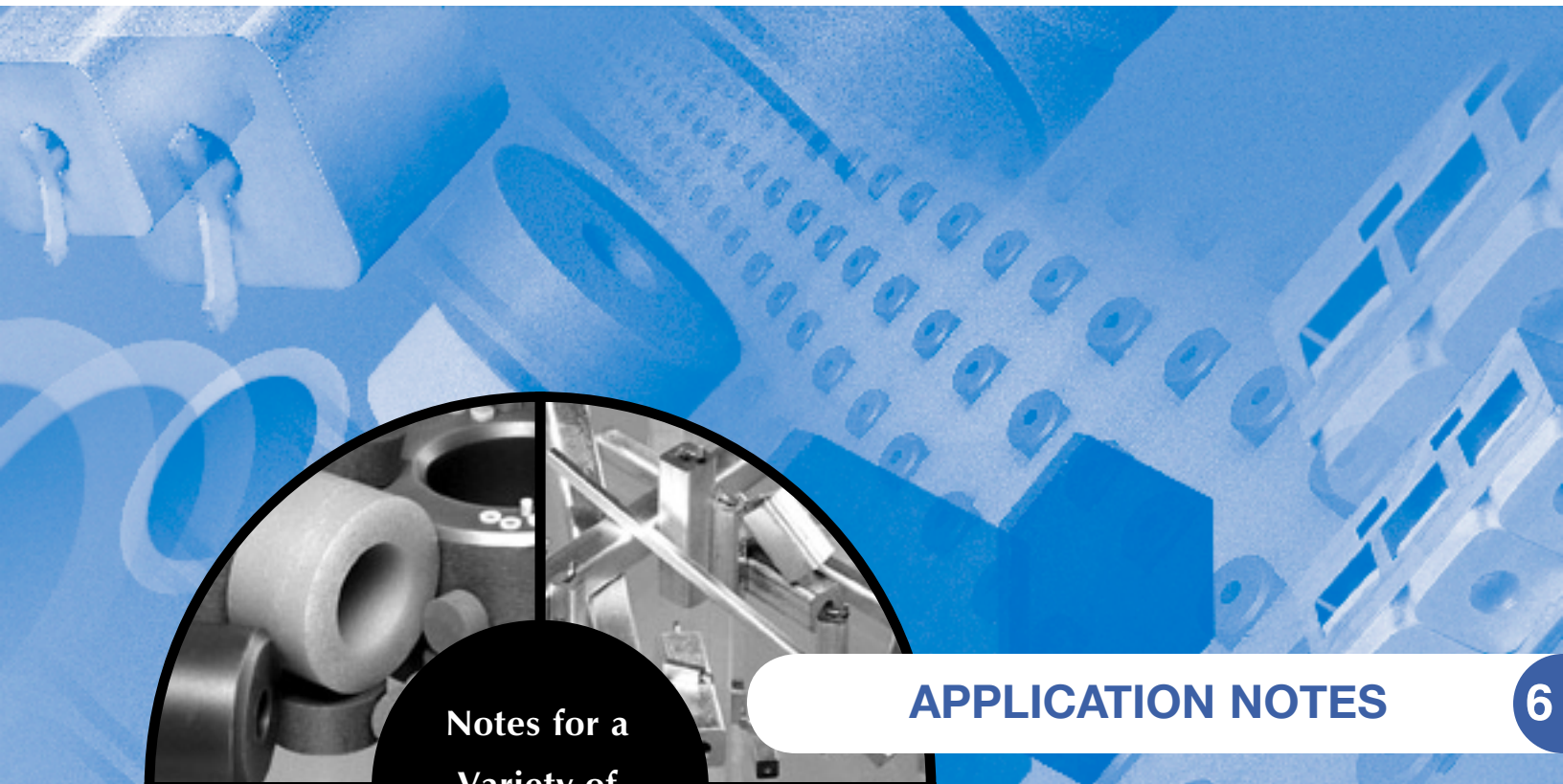
Notes for a
Variety of
Applications

Table of Contents for Application Notes

Dielectric Resonators

Brief Historical Background

In 1939, R.D. Richtmyer[1] showed that unmetallized dielectric objects can function similarly to metallic cavities which he called dielectric resonators (D.R.s). Practical applications of D.R.s to microwave circuits, however, began to appear only in the late 60's as resonating elements in waveguide filters[2]. Recent developments in ceramic material technology have resulted in improvements including small controllable temperature coefficients of resonant frequency over the useful operation temperature range and very low dielectric losses at microwave frequencies. These developments have revived interest in D.R. applications for a wide variety of microwave circuit configurations and subsystems[3,4].

Some of the advantages of the substitution of conventional resonators by D.R.s are:

1. Smaller circuit sizes.

2. Greater degree of circuit and subsystem integration, due to simpler coupling schemes from microwave integrated circuits (MICs) to D.R.s.

3. Better circuit performance, when compared to MIC line resonators, with regard to both temperature and losses.

4. Reduction of overall circuit cost for comparable performances.

Basic Properties

The important material properties for D.R. applications are:

a) The temperature coefficient of resonant frequency(τ_f), which combines three independent factors: temperature coefficient of the dielectric constant ($\tau\epsilon$), thermal expansion of the material (α_s) and thermal expansion of the environment in which the resonator is mounted.

Resonant frequency shifts due to intrinsic material parameters are related by the temperature coefficients given in equation (1).

$$\tau_f \quad -1/2\, \tau\epsilon \ - a\Lambda \qquad \text{Equation 1}$$

b) The unloaded Q factor (Q_o, which depends strongly on both dielectric losses and environmental losses. Q_o is defined by the ratio between the stored energy to the dissipated energy per cycle.

c) The dielectric constant of the material, which will ultimately determine the resonator dimensions. At present, commercially available temperature stable D.R. materials exhibit dielectric constants of about 36 to 40.

Cylindrical Resonator Design

Among the theoretically explored geometrics, the cylindrical shape has been widely accepted as the most advantageous one.

Practical circuit applications often require mounting the resonator in the proximity of conducting walls and/or other dielectric materials, therefore, an accurate prediction of the resonant frequency is possible only when all these boundary perturbations are taken into account in the theoretical analysis[5].

Figure 2 shows the general effect of conducting parallel plates on both the resonant frequency and unloaded Q of the fundamental mode ($TE_{01\delta}$) of cylindrical resonators. As L/H decreases, the resonant frequency of the dielectric resonator can be varied in a controllable manner. The exact point at which the Q degrades to 75% of the nominal unperturbed value depends on both the operating frequency and the conductivity of the plates, but will fluctuate around L/H = 2.

It is important to notice that tuning the frequency by means of approaching conducting surfaces is achieved at the cost of reduction in both unloaded Q and temperature stability. The decrease in temperature stability is due to the increasing slope of the tuning curve as the distance between the resonator and plates decrease[5].

The effects of the presence of a dielectric coated conductor plane, such as a micro-strip substrate, were shown[5] to be negligible (less than 1% shift in the frequency). This occurs when the thickness of the substrate is less than a quarter of the D.R. thickness, and the dielectric constant of the substrate is less than one half that of the d.R. dielectric constant. Similarly, side walls were shown to exhibit little or no effect whenever placed at a distance greater than the D.R. diameter.

The D.R. aspect ratio (thickness/diameter) can also exercise some effect on tuning and Q, but a choice of H/D = 0.4 is recommended for both optimum Q and minimum interference of spurious modes[3].
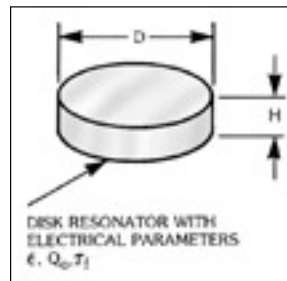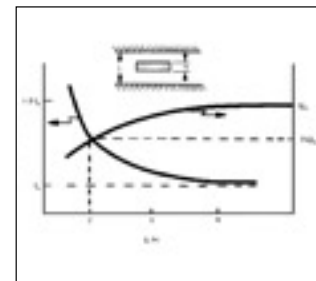

Figure 1.	Figure 2.

References

(1) Richtmyer, R.D., "*Dielectric Resonators,*" J. Appl. Phys., Vol. 10, pp. 391-398, June 1939.

(2) Cohn, S.B., "*Microwave Bandpass Filters Containing Hi-Q Dielectric Resonators.*" IEEE TMTT< pp. 218-227, April 1968.

(3) Plourde, J.K. and Ren, C.L., "*Application of Dielectric Resonators in Microwave Components,*" IEEE TMTT, pp. 754-770, August 1981.

(4) Bonetti, R.R. and Atia, A.E., "*Analysis of Microstrip Circuits Coupled to Dielectric Resonators,*" IEEE TMTT, pp. 1333-1337, December 1981.

(5) Bonetti, R.R. and Atia, A.E., "Design of Cylindrical Dielectric Resonators in Inhomogeneous Media," IEEE TMTT, pp. 323-327, April 1981.

No. 831 Temperature Coefficients of Dielectric Resonators

Introduction

Our previous Tech-Brief[1] detailed some of the advantages of the substitution of conventional microwave resonators by dielectric resonators (D.R.s). Better circuit performance with respect to temperature variations was mentioned among others. The design of D.R. temperature compensated circuits involves an understanding of the relationship between the different temperature coefficients. The purpose of this Tech-Brief is to present an introduction to the definitions, properties and measurements of the temperature coefficients of cylindrical D.R.s.

Definitions

There are four temperature coefficients (T.C.): T.C. of dielectric constant, T.C. of the cavity, T.C. of thermal expansion, and T.C. of resonant frequency which is a function dependent on the other three. Their definitions are (relative to Figure 1)

$$\tau_\epsilon = \frac{1}{\epsilon_\tau} \frac{\Delta \epsilon_\tau}{\Delta T} \cdots$$

T.C. of dielectric constant

$$\tau_c = \frac{1}{L} \frac{\Delta L}{\Delta T} \cdots$$

T.C. of the cavity

$$\alpha_L = \frac{1}{H} \frac{\Delta H}{\Delta T} = \frac{1}{D} \frac{\Delta D}{\Delta T} \cdots$$

T.C. of thermal expansion

$$\tau_f = \frac{1}{f_o} \frac{\Delta f_o}{\Delta T} \cdots$$

T.C. of resonant frequency

where Δf_o is the total frequency variation corresponding to the temperature shift ΔT, $\Delta \epsilon_\tau$ is the variation of the dielectric constant, ΔL the cavity expansion and ΔH, ΔD the resonator material linear expansions.

The usual units employed in the measurement of any of the above coefficients is $10^{-6}/°C$ or ppm/°C.

Temperature Coefficient of Resonant Frequency τf

As mentioned previously[1], the resonant frequency of cylindrical D.R.s depends on the resonator's geometric and physical parameters as well as the environment surrounding it. Therefore, the computation of the overall effect of temperature variation will have to include the variations of all the materials employed to hold and shield the D.R.

For the configuration shown in *Figure 1*, the effects of the holder can be neglected if it is manufactured of a material with low dielectric constant and low coefficient to thermal expansion (such as fused silica). If the effects of radial expansion are also neglected (only true for cavities which are large relative to the D.R.), the relationship between the temperature coefficients and τ_f is:

$$\tau_f i = 3/4 \ (A\tau_\epsilon + B\alpha_L + C_\tau c) \tag{5}$$

where A ~ 1/2, B ~ 1. C is dependent on the position of the D.R. relative to the top and bottom cavity walls. The typical range of values for C is between 0.05 and 1.0.

Figure 2 shows a typical variation of resonant frequency as a function of cavity length. Note how the same variation in the cavity dimension, $\Delta L_1 = \Delta L_2$, can lead to different frequency variations, $\Delta f_1 = \Delta f_2$. This change depends on the initial cavity size. This feature, together with the availability of materials with an appropriate range of τ_ϵ's can lead to the desired value of τ_f via a careful choice of the parameters in Equation 5.

Measurement

The measurement of τ_f can be easily performed in any test setup capable of precise resonant frequency measurements. A resolution of at least seven digits read out in the GHz range is required. *Figure 3* is an example using the impedance method to track the change in resonant frequency of the D.R. with temperature. The microwave signal is coupled to the D.R. located in a cylindrical test cavity via a H-field probe.

Values of τ_f given in Trans-Tech specifications bulletins are measured on test samples of 0.500" dia. by 0.200" thickness. The sample is centered in a cavity of 1.500" dia. by 1.050" height. The room temperature resonant frequency of the cavity plus D.R. is about 4.2 GHz. A practical example of the strong effect of the top and bottom cavity walls on the temperature coefficient of resonant frequency is given for Trans-Tech dielectric resonator type D-8512. In a parallel plate cavity with the metallic walls in contact with the D.R., a τ_f of +9 ppm/°C is obtained. When measured in the quality control standard cylindrical cavity described above, the value of τf is reduced to +4.0 ppm/°C. It is worthwhile noting that manufacturers measure the Q of dielectric resonators at different frequencies. A general phenomenological equation can be utilized to estimate the Q at any frequency.

$$f_o \bullet Q = 40,000 \tag{6}$$

where f_o is the resonant frequency. For example, a material with a Q of 10,000 at 4 GHz will have a Q of 5,000 at 8 GHz.

In summary, care must be exercised in selecting a D.R. material of correct value to obtain overall device temperature stability.
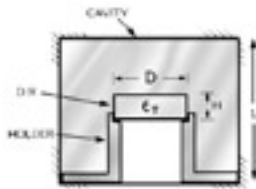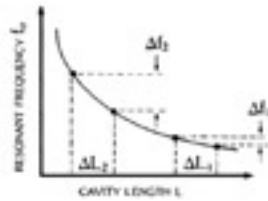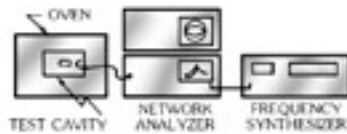
Figure 1

Figure 2

Figure 3

Trans-Tech compliments its product line of Dielectric Resonators by offering materials with various temperature coefficients of Resonant Frequency, abbreviated τ_r. The purpose of offering a variety of τ_r is to allow the designer control of frequency drift vs. temperature.

The τ_r is expressed in ppm/°C. In this context, the meaning is 1 Hz change for each MHz of operating frequency. For example, if an oscillator running at 10,750 MHz (10.750 GHz) decreases in frequency by a total of 1.5 MHz over a -20°C to + 70°C temperature range, the temperature coefficient of the oscillator circuit, T_c, is

$$t_c = \frac{-1.5 \times 10^6 \text{ Hz}}{10750 \text{ MHz}} \times \frac{1}{(70 - -20)}$$

$$= -1.55 \text{ ppm/°C}$$

This oscillator could be compensated for near-zero temperature drift by changing the τ_r of the dielectric resonator by + 2ppm/°C.

TTI recommends that first design iterations begin with zero coefficient, $\tau_r = 0$.

References:
(1) Tech-Brief No. 821 - An Introduction to Dielectric Resonators.

No. 851 Tuning & Exciting Dielectric Resonator Modes

Introduction

The many advantages found in the substitution of conventional resonators by dielectric resonators[1] (D.R.s) have been leading part of the microwave community into a continuous race to explore further potentials of this promising new area. New applications range from simple, low cost, oscillators for small earth stations[2] to spacecraft filters and multiplexers[3,4] Different devices require different structures to excite and tune the resonator, especially when employing higher order resonant modes. The purpose of this Tech-Brief is to introduce the microwave engineer to some of the definitions, properties, coupling structures, and tuning schemes pertaining to the cylindrical dielectric modes used in most applications.

Definitions and Properties

The natural modes of a cylindrical sample of high dielectric constant material can be classified into four categories: TE_{opg}, TM_{opg}, HE_{ngg}, and EH_{npg} where n and p are integers which describe the standing wave pattern in the azimuthal and radial directions respectively while g is in general a real number; reflecting the fact that the two circular boundary surfaces do not contain an integer number of half wavelengths as in metallic cavities. For the fundamental TE mode, g is usually substituted by the greek ($TE_{01\delta}$) and assumes values in the range 0.5 to 1.0.

TE and TM modes do not contain electric and magnetic fields in the axial directions (z) respectively. The HE and EH modes are called hybrid, because all six field components are present in both. Snitzer[5] suggested a simple scheme to classify the hybrid modes based on the value of the amplitude coefficient ratio of axial components of electric and magnetic fields:

$$P = \frac{\varpi\mu_o}{\beta} \frac{Hz}{E_zHz} \quad (1)$$

where β is the axial wave number, w is the angular frequency and μ_o the free space permeability. The modes for which P is positive are designated as EH and those for which it is negative as HE. The great majority of practical applications employ either the $TE_{01\delta}$ mode or the HE_{11g} mode, which are the first two to resonate when the D.R. is placed between conducting walls and air gaps left in between. *Figure 1* shows a sketch of the fields for these two modes in the cross section of the resonator.

The ratio between the D.R. diameter and its length (D/H) together with the exterior boundary conditions such as tuning elements, holders, shields, and substrates determines which of the two modes has the lowest resonant frequency. For most configurations[6] the $TE_{01\delta}$ mode is dominant when D/H > 1.42.

Exciting the Resonator

The choice of an appropriate structure to couple energy in and out of a D.R. will depend on the following considerations:

- which mode is to be excited
- which transmission medium is to be utilized (waveguide, coaxial line, microstrip line, etc. . . .
- how much coupling is desired

Modes with strong exterior magnetic fields such as the $TE_{01\delta}$ are more effectively excited through coupling loops, which can assume, for example, the form of a bent coaxial probe, a circular sector microstrip line, or an offset straight line as illustrated in Figs. 2a, b, and c respectively.
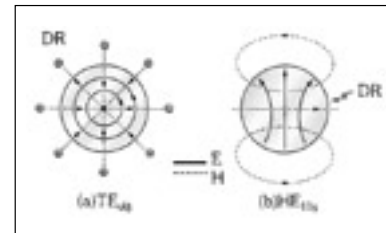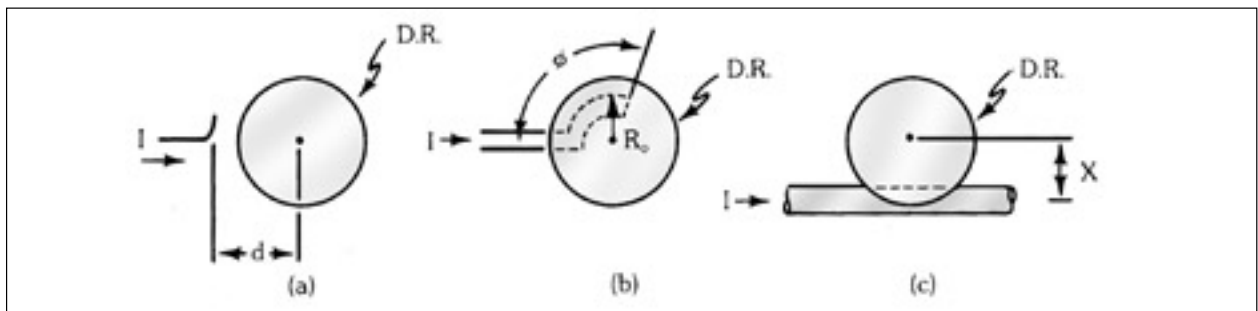

Figure 1

The amount of coupling obtained in any one structure can be quantitatively measured by the external Q, defined as:

$$Q = \frac{\text{(stored energy per cycle)}}{\text{(energy delivered to the load per cycle)}} \quad (2)$$

For side-coupled resonators (Figure 2a), Q_e will decrease as "d" decreases. In the microstrip couplings (Figs. 2b and 2c), Q_e will decrease as the D.R. approaches the substrate in the z direction, but in the plane of the pictures, Q_e achieves a minimum[4] (maximum coupling) when the following relations hold:

$$R_o = 0.32D \quad X = 0.35D \tag{3}$$

In the case of the curved microstrip probe, Q will decrease with the angle →, but will achieve minimum when the length of the line (→R_o) approaches a quarter wavelength in its substrate.[4]

Hybrid modes are more effectively coupled via a straight probe[3] and Q_e will decrease proportionally to the probe length.

Tuning the Resonator

Tuning a D.R. means adjusting its resonant frequency to a prescribed value. Several techniques can be used to achieve that, namely:

- changing either the diameter or length of the D.R.
- perturbing the fringing fields outside the D.R. via screws, plungers, dielectric, or ferromagnetic materials, etc.
- perturbing the D.R. shape through moving a piece of its own, or other material in and out of a hole made in the D.R.

The choice of a particular method will have to consider the following factors:

- the mode to be tuned
- the mechanical configuration of the final device, and
- the amount of tuning desired and its direction (to lower or higher frequencies)

A detailed discussion on the merits of each tuning technique is out of the scope of this Tech-brief, but some general principles will be helpful to acquaint the engineer with the capabilities of each method. For example, the tuning of TE modes is easily achieved via perturbations on the fringing fields performed by metallic or dielectric bodes placed parallel to the circular surface. The tuning of HE modes is best done by screws running perpendicular to the z axis of the D.R. *Figure 3* exhibits a schematic of the general effect the above-mentioned methods will have on the unperturbed resonant frequency. Metallic plungers approaching the D.R. will pull the frequency up for both TE and HE modes and dielectric ones will push it down. Side screws will also push down the frequency of HE modes as they approach the D.R.

The amount of tuning that can be obtained by any of these methods can reach up to ±20% of the unperturbed value of f_o, however, it is good practice to restrict this amount to below 5% in order to prevent degradations[1] on both temperature coefficient and unloaded Qs.
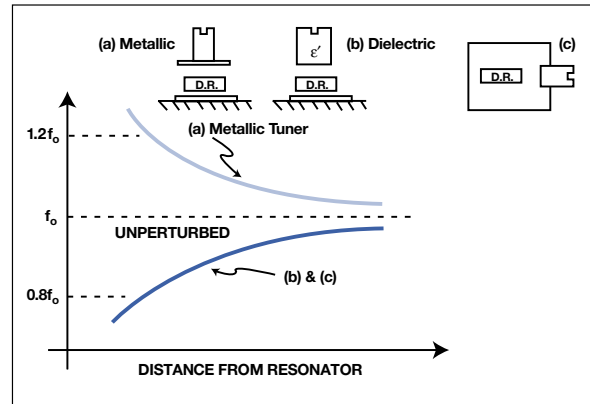

Figure 3.

References

(1) Tech-Brief No. 821 An Introduction to Dielectric Resonators.

(2) *"Integrated SHF Converter Simplifies Satellite Broadcasting,"* Microwave Systems News, pp. 55-57, June 1979.

(3) S.J. Fiedziuszro, *"Dual Mode Dielectric Resonator Cavity Filters,"* IEEE GMTT Vol. MTT 30, No. 9, pp. 311-316, September 1982.

(4) Bonetti, R.R. and Atia, A.E., *"Generalized Dielectric Resonator Filters,"* COMSAT Technical Review, Vol. 11, No. 2, Fall 1981.

(5) Snitzer, E., *"Cylindrical Dielectric Waveguide Modes,"* J. Opt. Soc. Amer., Vol. 51, No. 5, pp. 491-4398, May 1961.

(6) Guillon, P. and Garault, Y., *"Accurate Resonant Frequencies of Dielectric Resonators,"* IEEE TMTT pp. 916-922, Vol. MTT-25, November 1977.

Optimize DRO's for Low Phase Noise
This circuit trick provides an extra "hand" and a fast qualitative indicator of best resonator position.

Designers of free-running Dielectric Resonator (DR) oscillators ultimately face the task of fine-tuning the best DR "puck" position adjacent to the microstrip. Frequently, the goal is to minimize phase noise at a specified offset from the carried. Through trial and error and many observations on a spectrum analyzer, it's possible to strike a compromise between low noise and good power output. Low phase noise is dependent upon the choice of active device, its operating bias point, the supporting circuit components, and the unloaded quality factor of the resonator--all contribute to the loaded Q (Q_L) of the oscillator unit.

Q_L has been measured by load-pull or injection-locking techniques, but Q_L isn't the bottom line. The technique described here minimizes noise and simultaneously monitors relative e power output. The pushing figure, or sensitivity of the oscillating frequency to changes in supply voltage is also tied to Q_L. So it's possible to observe pushing as a qualitative indicator of the puck position which gives the optimum Q_L, and therefore good phase noise.

Instead of manually varying the supply voltage, suppose the supply is modulated, approximately a half volt p-p, at a low audio rate. If the bench supply can't be programmed to do this directly, insert the secondary of a miniature audio transformer (Radio Shack variety) between the supply and the circuit - after the voltage regulator, if any - and rive the transformer primary form an audio source such as a function generator. The modulation will push or "fm" the oscillator. Adjust the spectrum analyzer to view the fm. Experiment with the x, y and z position of the DR puck, and the supply voltage (or active device current).

As a high Q_L point is approached, the fm deviation will minimize. The dB amplitude (power output) change can be observed, too. Make a few correlations of "minimum fm deviation: puck position with close-in phase noise - don't forget to turn off the modulation - and watch this tuning trick help zero in on the best DR placement.
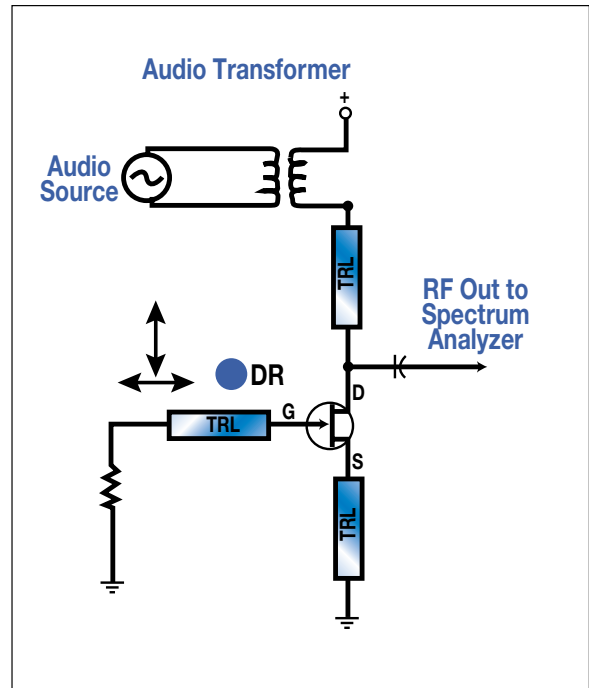
Coaxial Resonators

Using Coaxial Line Elements as Inductors

Coaxial (or coax) line elements can be used below resonance to simulate high-Q, temperature-stable, compact inductors. More precisely, shorted coax lines will exhibit an inductive reactance when used below quarter-wave resonance, and will approximate the behavior of an ideal inductance or "coil" over a limited frequency range. As the operating frequency approaches the SRF of the coax line element, the approximation will be less valid. An exact equivalent circuit is complex and would include parasitic elements resulting from a transition from the printed wiring board to the interior of the coax line. In this note, a first-order model includes only the ceramic coax line and an estimate of the inductance due to the physical length of the center conductor tab. The tab inductance will appear in series with the coax line's input impedance. An ideal, lossless transmission line is assumed to simplify the calculations. Minor corrections to part length may be evident from prototype circuit performance.

Let the desired inductive reactance at the design frequency f_o be approximated by

$$Z_{input} = Z_o \tan(\Theta) \text{ ohms}$$

where:

Z_{input}	=	impedance at the coax line terminals (ohms)
Z_o	=	coax line characteristic impedance (ohms)
Θ	=	$\dfrac{2\pi\ell}{\lambda_g}$ coax electrical length (radians)
ℓ	=	coax line physical length (inches)
λ_g	=	wavelength in the dielectric at f_o inches

The characteristic impedance, Z_o, is established by the coax dimensions and the material dielectric constant ε_r, as shown in Table 1. The cross-section width, W and hole diameter, d, differ from final catalog part sizes by an allowance of .001" for conductor metallization thickness.

Table 1. Coax Lines Properties vs. Profile and Material

Profile	1000 (10.5 ± 0.5)	2000 (20.6 ± 1)	8800 (39 ± 1.5)	9000 (90 ± 3)	Tab Inductors
HP	25.3 Ω	18.1 Ω	13.1 Ω	8.6 Ω	1.8nH
EP	22.5 Ω	16.1 Ω	11.7 Ω	7.7 Ω	1.0nH
SP	18.3 Ω	13.1 Ω	9.5 Ω	6.3 Ω	1.0nH
LS	18.4 Ω	13.1 Ω	9.5 Ω	6.3 Ω	0.9nH
LP	27.4 Ω	19.6 Ω	14.2 Ω	9.4 Ω	1.0nH
SP	25.7 Ω	18.4 Ω	13.3 Ω	8.8 Ω	0.6nH
SM	18.4 Ω	13.1 Ω	9.5 Ω	6.3 Ω	0.6nH

The Z_o values in Table 1 were computed from the approximation[1]

$$Z_o = \frac{60}{\sqrt{\varepsilon_r}} \ \ell n\left(1.079 \frac{W}{d}\right)$$

The wavelength in the dielectric, λ_g, can be calculated from the expression in Table 2, with f_o as the design frequency in MHz.

Table 2. Wavelength (λ_g) in Dielectric

Material	ε_r	Wavelength Formula for λ_g (inches)
1000	10.5 ± 0.5	3642 / f_o
2000	20.6 ± 1	2601 / f_o
8800	39 ± 1.5	1890 / f_o
9000	90 ± 3	1244 / f_o

Figure 10

Note that the shorted transmission line model requires the constant of the material filling the coax line. Inductance-Per-Unit-Length formulas are useful only when the line is very short compared to a wavelength, and are inaccurate as f_o approaches SRF. The equation for input impedance can be rearranged to determine the part length for a desired inductive reactance.

$$\iota = \frac{\lambda_g}{2\pi} \tan^{-1}\left(\frac{Z_{input}}{Z_o}\right)$$

The SRF must lie within the recommended frequency range[2] for the same profile and material when used as a coaxial resonator. This restriction places constraints upon the range of inductive reactance which can be realized by this technique, although arbitrarily high reactance values can be achieved close to SRF. The designer should prudently analyze the circuit response when f_o is near SRF.

SRF may be calculated from previously determined values.

$$SRF = \frac{\lambda_g f_o}{4} \bullet \frac{1}{\ell}$$

The center conductor tab will present a small additional series inductance which may be included in the total desired inductive reactance. The tab influence has not been measured, but suggested approximate values are given in Table 1.

Q, or quality factor, may be estimated from:

$$Q = K\sqrt{f_o}\frac{\ln\left(\frac{W}{d}\right)}{\left(\frac{1}{W} \bullet \frac{1}{d}\right)}$$

where: K = 240 for 8800 material
= 200 for 9000 material

and W, d and f_o have been defined earlier

Refer to pages 67-69 for Design Examples.

References

(1) H. Riblet, "An Accurate Approximation of the Impedance of a Circular Cylinder Concentric with an External Square Tube," IEEE Trans. Microwave Theory Tech., vol. MTT-31, pp. 841-844, Oct. 1983
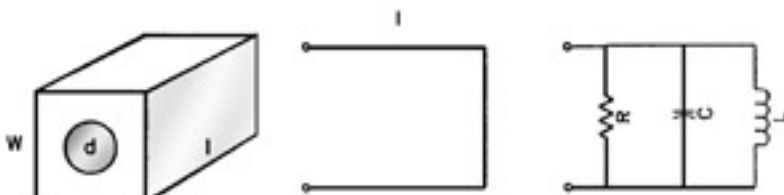
Coaxial Resonators for VCO Applications

Many engineers choose to design their own VCO circuits to reduce cost, size, and power consumption. Development of high-Q ceramic coaxial resonators simplifies the VCO design process. When a Trans-Tech coaxial resonator (transmission line) is the frequency determining element of a VCO, it typically replaces a discrete inductor. The rugged ceramic resonator has enormous benefits over traditional coils by offering better temperature stability, higher Q, and no microphonics. This application note introduces the designer to Trans-Tech's coaxial resonator, outlines its use in a VCO, and details the method of selecting the correct part.

Coaxial Resonator & Transmission Line Basics

At high frequencies, the distributed inductance and capacitance of a coaxial transmission line is efficient as a circuit element. Short sections of transmission lines with reflecting terminations exhibit inductive reactance when operated below the Self Resonant Frequency (SRF) of the line, and exhibit capacitance reactance when operated slightly above SRF. When SRF is reached, the transmission line may be approximated by the following:[1,2]

$$L = \frac{8Z_o l \sqrt{\epsilon_r}}{\pi^2 c} \qquad C = \frac{l\sqrt{\epsilon_r}}{2cZ_o} \qquad R = \frac{4Z_o Q}{\pi} \qquad Z_o = \frac{60}{\sqrt{\epsilon_r}} \ln\left(1.079\frac{W}{d}\right)$$

6

Transmission Line as an Inductance

Below resonance, coaxial line elements simulate high-Q, temperature-stable, compact inductors. More precisely, shorted coax lines will exhibit an inductive reactance when used below quarter-wave resonance, and will *approximate* the behavior of an ideal inductance or "coil" over a limited frequency range. As the operating frequency (f_o) approaches the self-resonant frequency (SRF) of the coax line element, the approximation will be less valid.
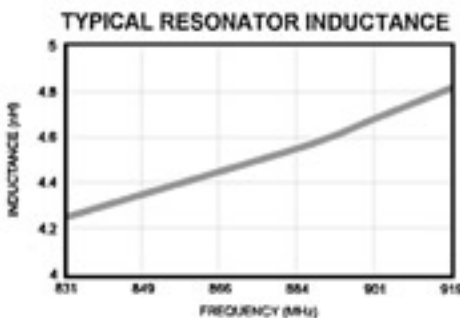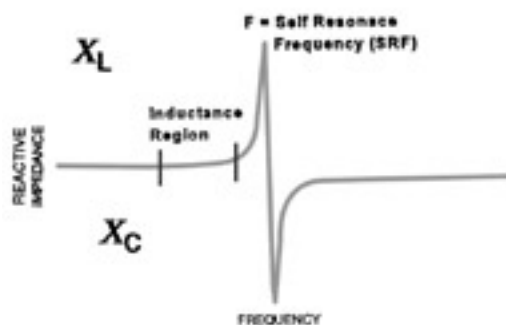
The formula below may be used to approximate the inductive reactance at the VCO operating frequency (f_o). The coaxial element's tab inductance will appear in series with the coax line's input impedance. An ideal, lossless transmission line is assumed to simplify the calculations. Minor corrections to part length may be evident from prototype circuit performance.

Let the desired inductive reactance at the design frequency f_o be approximated by:[3]

$$\mathbf{Z_{input} = X_L = Z_o \tan(\Theta)} \qquad 0 \geq \lambda \geq \lambda/4$$

where:

$\mathbf{Z_{input}}$ = impedance at the coax line terminals (ohms)

$\mathbf{Z_o}$ = coax line characteristic impedance (ohms)

Θ = $\dfrac{2\pi\iota}{\lambda_g}$ coax electrical length (radians)

ℓ = coax line physical length (inches)

λ_g = $\dfrac{11803}{f_o \sqrt{\varepsilon_r}}$ wavelength in the dielectric at f_o inches

VCO Basics

A varactor diode is the most widely used method to vary the operating frequency of an oscillator. Because a shorted transmission line will look inductive when operated below the Self Resonant Frequency (SRF) of the line, a varactor can tune the following circuit.
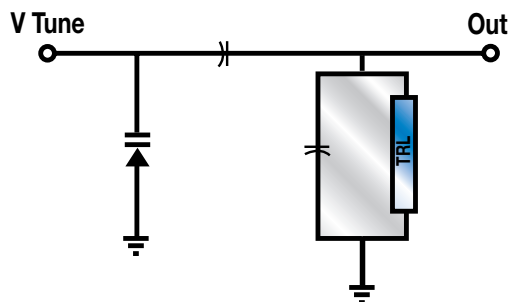
*Transmission Line in
Varactor Tuned Resonant Circuit*

Typical VCO Circuit Using a Trans-Tech Resonator

The circuit below shows typical DC biasing and load circuits added to the VCO circuit.[4] The major frequency determining components are: D1, C2, TRL, C3 and C8. The tuning range of the VCO is determined by the varactor coupling capacitor, C2. As the value of C2 is increased, the tuning range will increase at the expense of circuit Q.[5] It is important to note that component parasitics are significant at these operating frequencies, and should be estimated and included if computer modeling is used.[6]
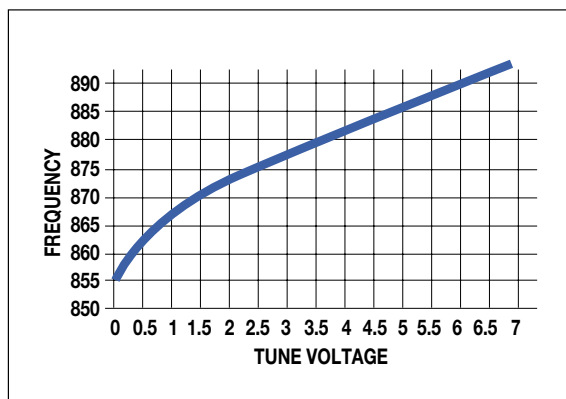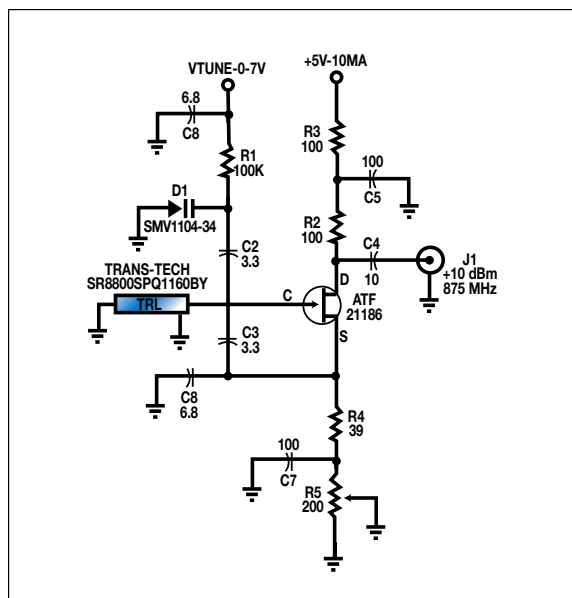
Selecting the Correct Trans-Tech Part

Select a Trans-Tech coaxial resonator that has a higher SRF than the operating frequency of the VCO. The designer may refer to Trans-Tech's "*Coaxial Resonator Design Program for Windows™*" or page 56 for frequency, material, and size guidelines. The following pages also provide a step-by-step process to specify the proper Trans-Tech

1. Determine a desired inductance or circuit impedance (Z_{input}).

2. Choose an operating frequency.

3. Select an initial profile and material from Table 2 below.

4. Calculate the length of the part using:

$$\iota = \frac{\lambda_g}{2\pi} \tan^{-1}\left(\frac{Z_{input}}{Z_o}\right) \text{ inches}$$

where Z_0 and λ_g can be obtained from Tables 1 and 2 below.

5. Choose the final profile.

Table 1.
Wavelength (λ_g) in Dielectric

Material	ε_r	Wavelength Formula for λ_g (inches)
1000	10.5 ± 0.5	3642 / f_o
2000	20.6 ± 1	2601 / f_o
8800	39 ± 1.5	1890 / f_o
9000	90 ± 3	1244 / f_o

Table 2.
Coax Line Properties vs. Profile and Material

Profile	1000	2000	8800	9000	Tab Inductors
HP	25.3Ω	18.1Ω	13.1Ω	8.6Ω	1.8nH
EP	22.5Ω	16.1Ω	11.7Ω	7.7Ω	1.0nH
SP	18.3Ω	13.1Ω	9.5Ω	6.3Ω	1.0nH
LS	18.4Ω	13.1Ω	9.5Ω	6.3Ω	0.9nH
LP	27.4Ω	19.6Ω	14.2Ω	9.4Ω	1.0nH
SP	25.7Ω	18.4Ω	13.3Ω	8.8Ω	0.6nH
SM	18.4Ω	13.1Ω	9.5Ω	6.3Ω	0.6nH

Selecting the Correct Trans-Tech Part (continued)

The SRF must lie within the recommended frequency range for a coaxial resonator of the same profile and material (see pg. 2-35). This manufacturing restriction places constraints upon the range of inductance reactance which can be realized by this technique, although arbitrarily high reactance values can be achieved close to SRF. The designer should prudently analyze the circuit response when f_o is near SRF.

SRF may be calculated from previously determined values:

$$SRF = \frac{\lambda_g f_o}{4} \cdot \frac{1}{\ell} \text{ MHz}$$

The center conductor tab will present a small additional series inductance which may be included in the total desired inductive reactance. The tab inductance has been measured with values given in Table 2.

Design Example 1

Use a shorted coax line element to give an inductive reactance of 25 ohms at 900 MHz. Smallest height is required.

The SM profile is chosen with 8800 material, $\varepsilon_r = 39$ The 0.6 nH tab inductance contributes 3.4 Ω and is subtracted from the 25 Ω to give 21.6 Ω. From Table 1, the wavelength in the dielectric at 900 MHz is:

$$\lambda_g = 1890 / 900 = 2.1 \text{ inches}$$

With $Z_0 = 9.2 \, \Omega$ from Table 2, we have

$$\ell = \frac{2.111}{2\pi} \tan^{-1}\left(\frac{21.6}{9.5}\right) = 0.392 \text{ inches}$$

also,

$$SRF = \frac{(2.1)\,(900)}{(4)\,(0.392)} = 1205 \text{ MHz}$$

Notice that the coax line is $0.392 / 2.111 = 0.186\lambda_g$ long. This part could be ordered from Trans-Tech as Part Number SR8800SMQ1210BY. It would be manufactured and tested for self-resonance at 1210 MHz.

Design Example 2

Use a shorted coax line element to give an inductive reactance equivalent to that of an ideal 4.0 nH coil at 800 MHz. Low loss is required, but part must be less than .250" high.

Choose an SP profile (.238" high) in 8800 material, ε_r = 38.6. The 1.0 nH tab inductance is subtracted from the desired inductance, allowing 4.0 - 1.0 = 3.0 nH equivalent inductance from the coax line. An inductive reactance of 2π (800 x 10^6) (3.0 x 10^{-9}) = 15.1Ω is required. From Table 1, the wavelength in the dielectric at 800 MHz is:

With Z_0 = 9.4 Ω from Table 2, we have:

$$\iota = \frac{2.375}{2\pi}\tan^{-1}\left(\frac{15.1}{9.4}\right) = 0.383 \text{ inches}$$

$$= 240\sqrt{800}\frac{\ln\left(\frac{.236}{.097}\right)}{\left(\frac{1}{.236} + \frac{1}{.097}\right)} = 415$$

$$SRF = \frac{(2.375)\ (800)}{(4)\ (0.383)} = 1239 \text{ MHz}$$

The coax line is 0.383 / 2.375 = 0.161 λ_g long. This part could be ordered from Trans-Tech as Part Number SR8800SPQ1239BY. It would be manufactured and tested for self-resonance at 1239 MHz.
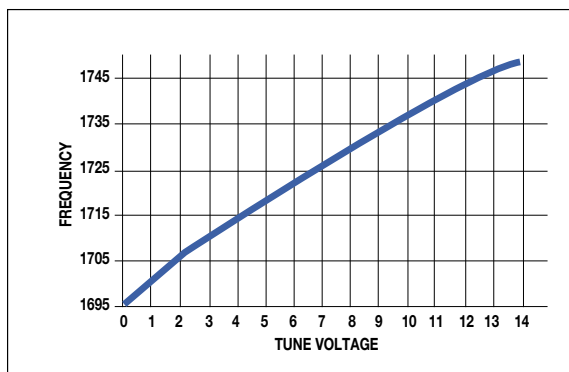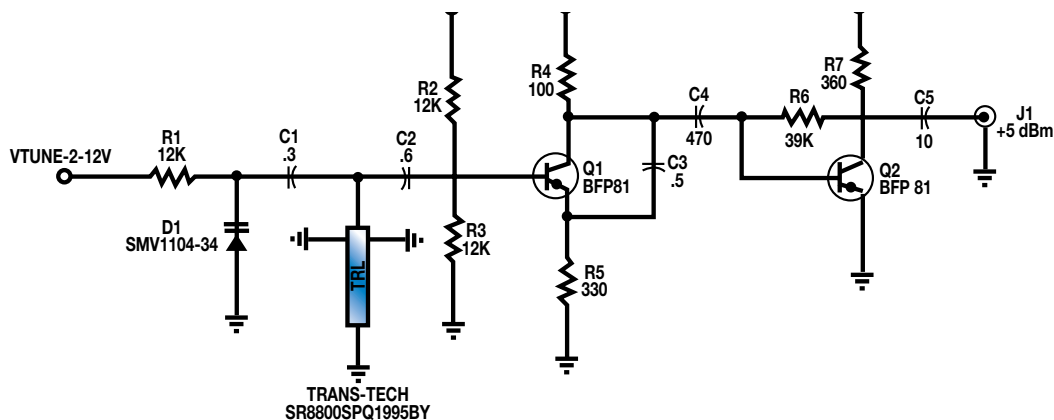
Typical VCO Using Trans-Tech Resonator [5]

References

1. H. Riblet, "An Accurate Approximation of the Impedance of a Circular Concentric with an External Square Tube," *IEEE Trans. Microwave Theory Tech.,* vol. MTT-31, pp. 841- 844, Oct. 1983.

2. Theodore Moreno, *Microwave Transmission Design Data* (1948; Norwood: Artech House, 1989) p.40.

3. W. Johnson, *Transmission Lines and Networks*, McGraw-Hill, 1950.

4. Used by permission of Les Reading, Scientific Research Labs, Santa Maria, CA.

5. Brendan Kelly. "1.8 GHz Direct Frequency VCO with CAD Assessment" *RF Design*, p.29, Feb. 1993.

6. Randdell Rhea, *Oscillator Design & Computer Simulation* (1990; Englewood Cliffs: Prentice Hall).

Additional Reading

Ulrich Rohde, "Oscillator Design for Lowest Phase Noise," *Microwave Engineering Europe*, p. 31, May 1994.

Ulrich Rohde, C.R. Chang, "The Accurate Simulation of Oscillator and PLL Phase Noise in RF Sources," *Proceedings of the Second Annual Wireless Symposium*, Santa Clara, CA, February 15-18, 1994.

6

Computer Simulation of Coaxial Resonators

Trans-Tech's coaxial resonators are a ceramic filled transmission line with a reflecting termination. Some electronic simulation programs will support round coaxial transmission line models, however, Trans-Tech's coaxial resonators have a square outer conductor and have been successfully modeled using the following:

If the part is a quarter wavelength and shorted on one end, use Short-Circuited Physical Transmission Line (TLPSC) with the following parameters:

$$\mathbf{Z} = \text{characteristic impedance} = \mathbf{Z_o} = \frac{60}{\sqrt{\varepsilon_r}} \ln\left(1.079\,\frac{W}{d}\right)$$

Characteristic Impedance vs. Profile and Material

Profile	1000	2000	8800	9000
HP	25.3 Ω	18.1 Ω	13.1 Ω	8.6 Ω
EP	22.5 Ω	16.1 Ω	11.7 Ω	7.7 Ω
SP	18.3 Ω	13.1 Ω	9.5 Ω	6.3 Ω
LS	18.4 Ω	13.1 Ω	9.5 Ω	6.3 Ω
LP	27.4 Ω	19.6 Ω	14.2 Ω	9.4 Ω
MP	25.7 Ω	18.4 Ω	13.3 Ω	8.8 Ω
SM	18.4 Ω	13.1 Ω	9.5 Ω	6.3 Ω

$$\mathbf{L} = \text{length} = \frac{\lambda_g}{4} = \frac{c}{4\,f_o\sqrt{\varepsilon_r}}$$

$$\mathrm{K} = \varepsilon_r = \text{dielectric constant } (8800 = 38.6 \pm 1.5),\ (9000 = 88.5 \pm 3.0)$$
$$(1000 = 10.5 \pm 0.5),\ (2000 = 20.6 \pm 1.0)$$

$$\mathbf{A} = \text{attenuation} = \alpha\ \frac{\beta}{2Q} = \frac{2\pi\lambda_g}{2Q} = \frac{8.68\,\pi\,\sqrt{\varepsilon_r}\,f_o}{cQ}$$

Simulation Example

To model Trans-Tech's SR8800KLPQ1200BY,

$Z = 14\Omega$

$$L = \frac{11803}{4 \; 1200 \; \sqrt{38.6}} = .396 \text{ inches}$$

$K = 38.6$

$$A = \frac{8.68 \, \pi \, \sqrt{\varepsilon_r} f_o}{c \, Q} = \frac{8.68 \, \pi \, \sqrt{38.6} \; 1200}{11803 \; 407}$$

6

Q specification = 354, Q typical = 407

Therefore the circuit file would read:

TLPSC   n1   n2   Z=14   L=.396   K=38.6   A=.04   F=1200

Frequency Tuning of Coaxial Resonators

The space-saving design and mechanical ruggedness of Trans-Tech's high Q coaxial resonators make them ideal for use in stable oscillators as well as in filter applications. Often it is desired to shift the Self Resonant Frequency (SRF) of the resonator when testing circuit prototypes. This note demonstrates three mechanical methods of tuning a coaxial resonator.

In most applications, the SRF of the coaxial resonator will be loaded by stray and parallel capacitances. In an oscillator, this will usually lead to a shift in the resonant frequency to a lower value.

The SRF of the resonator can be increased by removing the silver metallization from the open end. Start by removing 10-50 mils from the top, and continue to remove metallization from each side if necessary. Depending on the length of the part, the SRF can be increased 10-20% without degrading the unloaded Q.

The SRF of the resonator can be decreased by removing the silver metallization from the shorted end of the resonator or by varying the position of the grounding plane. Removing the silver metallization from the shorted end of the resonator perturbs the current and will result in a degradation of Q.

Once the designer produces a resonator that works well in his circuit, the SRF can be measured using the method described in Trans-Tech's "Measuring SRF and Q of Coaxial Resonators" Note #1015, or the part can be returned to Trans-Tech to characterize and provide new samples.

Remove metallization to increase Self Resonant Frequency (SRF)
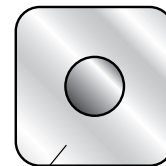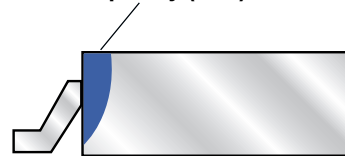
Remove metallization to decrease SRF

Characteristic Impedance of Coaxial Resonators

The characteristic impedance of a dielectric filled coaxial transmission line with a square outer conductor can be found using the following formula:

$$Z_o = \text{characteristic impedance} = Z_o = \frac{60}{\sqrt{\varepsilon_r}} \ln\left(1.079\, \frac{W}{d}\right)$$

where:

W = width of resonator

d = diameter of inner conductor

ε_r = dielectric constant

This formula shows that changes in W, d, and ε_r will effect the characteristic impedance. Using Trans-Tech's manufacturing tolerances, an analysis of characteristic impedance follows:

| Profile	Width (W)	diameter (d)	Z_o for Materials (ε_r)			
			1000	2000	8800	9000
HP (12mm)	0.476 ± 0.005	0.131 ± 0.004	25.3 Ω	18.1 Ω	13.1 Ω	8.6 Ω
EP (8mm)	0.316 ± 0.005	0.101 ± 0.004	22.5 Ω	16.1 Ω	11.7 Ω	7.7 Ω
SP (6mm)	0.237 ± 0.004	0.095 ± 0.004	18.3 Ω	13.1 Ω	9.5 Ω	6.3 Ω
LS (4mm)	0.155 ± 0.004	0.062 ± 0.004	18.4 Ω	13.1 Ω	9.5 Ω	6.3 Ω
LP (4mm)	0.155 ± 0.004	0.038 ± 0.003	27.4 Ω	19.6 Ω	14.2 Ω	9.4 Ω
MP (3mm)	0.119 ± 0.004	0.032 ± 0.003	25.7 Ω	18.4 Ω	13.3 Ω	8.8 Ω
SM (2mm)	0.080 ± 0.003	0.032 ± 0.003	18.4 Ω	13.1 Ω	9.5 Ω	6.3 Ω

Measuring SRF and Q of Coaxial Resonators

Trans-Tech's coaxial resonators are ceramic filled transmission lines supporting TEM waves. Accurate characterization of these microwave resonators are essential for their effective use. The important parameters required to fully describe a resonator are:

Self Resonant Frequency SRF

Coupling coefficient β

Quality factor Q

Several measurement methods are possible, but we will describe here a simple reflection technique using the impedance locus on the Smith Chart. A small slotted brass slug can be used to capacitively couple to the coaxial resonator.

One side of the slot acts as a plate of the coupling capacitor, with the resonator's tab acting as the other plate. The complete fixture is constructed using a SMA panel mount connector (M/A Com 2052-1201-02) and an aluminum block.
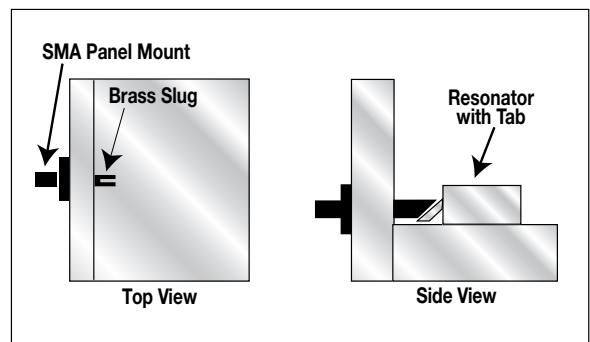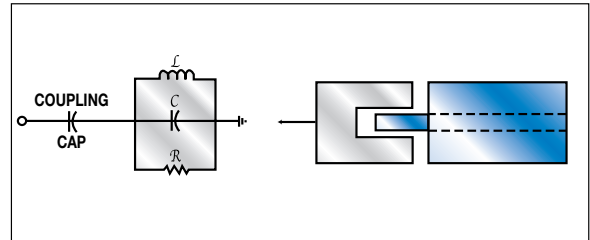
Procedure:

Find the approximate SRF using:

$$\text{SRF} = \frac{c}{4\,l\,\sqrt{\varepsilon_r}} = \text{Quarterwave shorted}$$

or

$$\text{SRF} = \frac{c}{2\,l\,\sqrt{\varepsilon_r}} = \text{Halfwave open}$$

Where C = speed of light, and er = 38.5 (8800 materials) or 88.5 (9000 material)

Set the network analyzer to measure S_{11}, Center frequency = SRF, Span = 80 MHz, Number of points = 801, Format = Smith Chart. Calibrate response open.

Insert the tab into the brass slot until critical coupling (β= 1, R = Z_0) is achieved.

Over coupled

Critical coupled

Under coupled

S_{11}
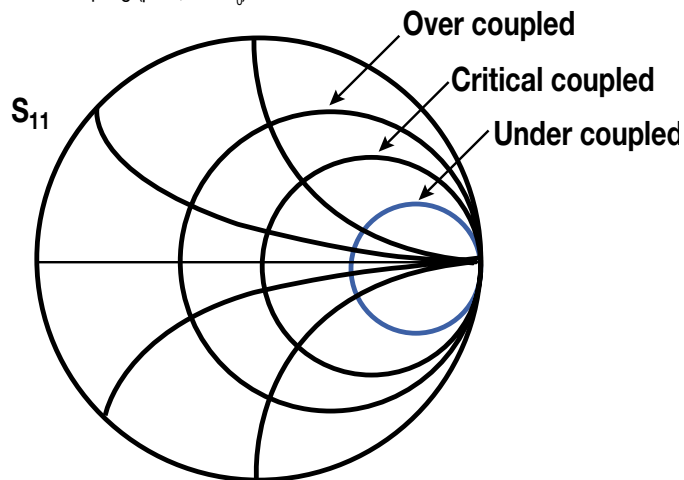
The resonant frequency is defined at this critical coupled condition or at the point of maximum return loss.

- 7 db

$f1$ ▼   ▼$f2$

▼

f_o
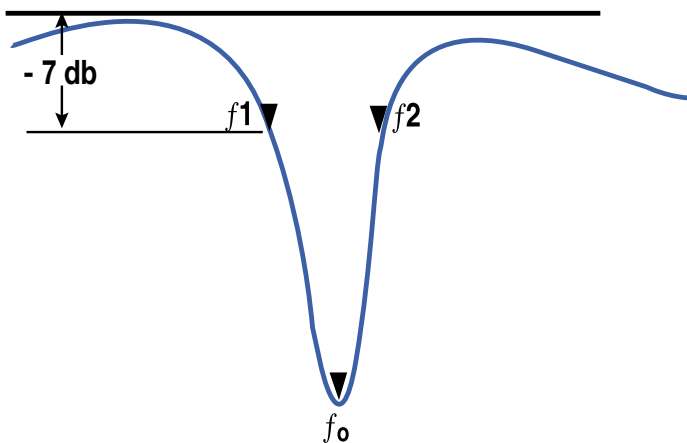
The half power bandwidth will correspond to the - 7 dB return loss points (R = ±X), therefore, Q can be found using:

$$Q = \frac{f_o}{f_2 - f_1}$$

The Influence of Coaxial Inductors on VCO Tuning Bandwidth

Ceramic coaxial transmission lines are commonly used to resonate with a varactor in voltage-controlled oscillator (VCO) circuits. When short-circuited at one end and used below self-resonant frequency (SRF), the coax line presents an inductive reactance to the VCO. Performance advantages of the coax inductor vs. discrete wire coils or chip inductors are acknowledged [1]. Less obvious is the influence of the coax inductor on VCO tuning rate, expressed in MHz/volt.

Unlike an ideal inductor whose reactance varies linearly with frequency, the coax inductor reactance increases in a non-linear (tangent-function) manner as the frequency approaches SRF, as shown in the figure.

The varactor governs the tuning bandwidth when inductance is constant. But *the effective inductance of the coaxial* line increases with frequency - as SRF *is approached* - and opposes the varactor's control. The varactor must be "pushed" further to overcome the increase in effective inductance. For a given control voltage swing, the VCO frequency change will be less than with the ideal coil. The tuning bandwidth will be reduced when the coaxial inductor is operated near SRF. Two coax lines of different characteristic impedance (Z_0), but same SRF would have different effective inductance at F0. It can be seen from the figure that for a specified nominal reactance XL at the VCO frequency F_0, a lower coax line Z0 leads to a lower SRF and a more rapid reactance change in the vicinity of F_0. This component will give a lower SRF and a more rapid reactance change in the vicinity of F_0. This component will give a lower tuning bandwidth than either a higher-impedance coax line or an ideal inductor.
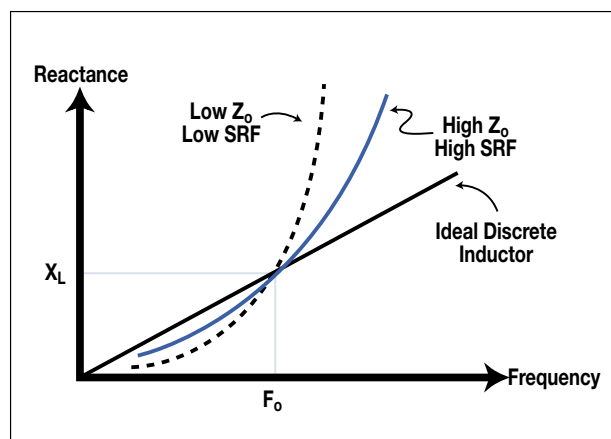
We can state the following guidelines:

♦ **For Widest Tuning Bandwidth** - choose a coax inductor with an SRF as far as possible above the VCO operating frequency (F_o). Coax lines with highest Z_o and lowest dielectric constant (ε_r) will have the highest SRF.

♦ **To Restrict Tuning Sensitivity** - use a part with SRF near F_o. Choose a coax inductor with low Z_0 and high ε_r.

Reference

1. Brendan Kelly, "1.8 GHz Direct Frequency VCO with CAD Assessment" *RF Design*, p29 Feb. 1993.

Empirically Determining the VCO Inductor

Many engineers are not familiar with the analytical techniques of using coaxial resonators in VCO circuits. Typically, the designer needs the equivalent of a high-Q inductor to resonate with his varactor, and an excellent choice is a ceramic coax line with a SRF approximately 15% higher than the VCO's center frequency (F_o). If a circuit simulation isn't used to determine the exact input impedance of the coax line that the active circuit wants to "see", a few resonator samples *could* be ordered with SRF's somewhat higher than F_o. This wait-and-try cycle can be slashed by using conventional 50-ohm coax that's readily available, such as .085" semi-rigid cable. This interim measure won't give the great Q, temperature performance, or even the same tuning slope as the ceramic resonator, but it will nail down the impedance at F_o, and it will provide a very good estimate for specifying the ceramic coax prototype.

This technique works for circuit topologies where one end of the VCO circuit "inductor" is at RF ground, but not *necessarily d-c ground*. This is because the ceramic coax line is preferably mounted on the circuit board with its outer metallization at RF ground. Otherwise, the outer conductor will be RF "hot," and could radiate to nearby circuits, defeating the desirable self-shielding nature of the coax resonator. It may not be obvious, but the coax line can be *either* short or open-circuited at one end, and with the correct length, will still present an inductive reactance at the active circuit end. This allows a short piece of 50-ohm coax to work nicely in the breadboard circuit, but remember to provide a complete d-c path for the varactor bias. An example will illustrate the technique.

Figure 1 shows a typical VCO schematic. The "temporary" 50-ohm coax line's center conductor is connected to the junction of the 3.3 pF capacitors, and the shield at the same end of the coax is connected to a good RF ground point. Grounding the shield along its entire length is optional, and if the far end is left free, the line length can be progressively snipped off at the open end until the circuit oscillates at 900 MHz. How long should the coax be? Start with a half wavelength ($\lambda_g/2$), at 900 MHz, in the coax dielectric. Then as the open-ended line is trimmed shorter than a half-wave, its presents an equivalent inductance at the active circuit end. Suppose the coax dielectric constant (ε_r) is 2.01, then a half wave at 900 MHz is a length of coax:

$$\lambda_g = \frac{11,803}{2F_o\sqrt{\varepsilon_r}} = \frac{11,803}{2\,(900)\sqrt{2.01}} = 4.625 \text{ inches}$$

Once the line is trimmed to run the VCO at 900 MHz, unsolder the 50-ohm coax and measure its impedance at the circuit connection end. A network analyzer will give the equivalent inductive reactance at 900 MHz. No analyzer available? Measure the trimmed coax jacket length (l) and approximate the equivalent reactance with:

$$X_{eqv} = \text{-j} \frac{Z_o}{\tan\left(\frac{\pi l}{\lambda_g/2}\right)} \text{ ohms}$$

6

where the value of λ_g was determined by Equation 1. Remember that the argument of the tangent is in *radians*. For example, suppose the 50-ohm (Z_o) coax trimmed length is 3.137 inches, then $X_{eqv} = j31.33$ ohms, which is also equivalent to 5.54 nH at 900 MHz. This value can be used with TTI's CARD/COAX software in the **inductor** mode to specify a ceramic coax resonator. The software will include the effects of the ceramic resonator's tab inductance, giving choices of parts that will provide X_{eqv}. Choose the part which makes the ceramic coax line element SRF as high as possible above 900 MHz. In this case, the best choice for $X_{eqv} = j28.75$ ohms at 900MHz is TTI's part number SR8800LPQ1308BY, with SRF at 1308 MHz and an unloaded Qu of 308. Or, if better Qu is necessary, an alternate choice is SR8800SPQ1160BY, with SRF at 1160 MHz and Qu = 442.

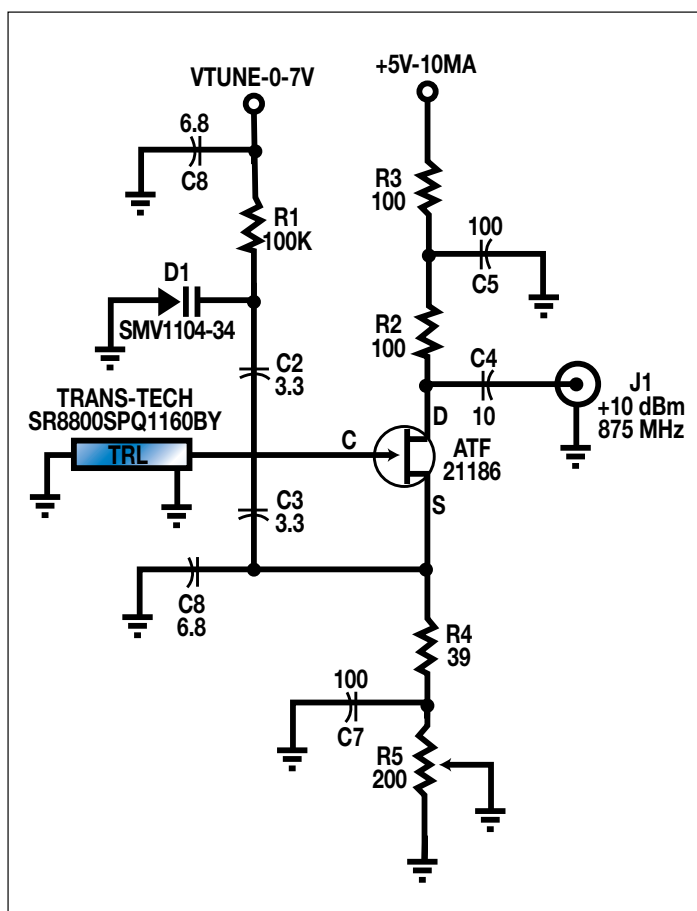*Figure 1:*
Example 900 MHz VCO Schematic

Tolerance Analysis of Coaxial Inductors

Quite often, VCO designers will specify a coaxial inductor by designating a catalog *resonator*. Trans-Tech's coaxial resonator part numbering scheme includes the ceramic material designator, the physical profile, and the self-resonant frequency (SRF). The part is operated below SRF, so that it presents an inductive reactance to the VCO active circuit. Whether analytically or empirically determined, specifying SRF alone - specifically SRF tolerance - does not guarantee the same tolerance on the *equivalent inductance* (L_{eq}) value. Unfortunately, there is no way short of a tolerance analysis that will disclose the possible L_{eq} variations. Results are unique to the application, particularly the separation between the SRF and VCO frequency. Fortunately, the analysis is not difficult, and it can forewarn the designer how much the part's nominal value of L_{eq} can vary, unit to unit.

An approximation to the equivalent inductance, L_{eq}, can be modeled by a small lumped tab inductance (L_{tab}) plus the contribution of the shorted ceramic transmission line.

$$L_{eq} = L_{tab} + \frac{60{,}000}{2\pi F_{vco}\sqrt{\varepsilon_r}} \, \ln\!\left(1.079\,\frac{W}{d}\right) \tan\!\left(\frac{\pi F_{vco}}{2F_{SRF}}\right)$$

where:

L_{eq}	=	total equivalent inductance of the coaxial inductor (nH)
L_{tab}	=	tab inductance (nH)
F_{VCO}	=	VCO center frequency, in MHZ
ε_r	=	dielectric constant of the ceramic
W	=	coaxial line width (inches)
d	=	coaxial line inner diameter (inches)
F_{SRF}	=	coaxial line self-resonant frequency (SRF) in MHZ

The tangent function argument is evaluated in radians. For a given VCO center frequency, the components of L_{eq} which are variable are the SRF, the dimensions (W, d), and the dielectric constant ε_r. SRF is usually specified with 1% or 0.5% accuracy. Dielectric constants of 8800 and 9000 material are given in Table 1. Values and tolerances for W, d, and the tab inductance are given in Table 2. Due to skin effect, RF current flows in the metallization at the ceramic-metal interface. The (W,d) values here are *ceramic* dimensions, which differ from Trans-Tech's catalog (metallized) values. A spread-sheet can be developed with the above formula as its core, to test the contributions of the variables and the cumulative variance in L_{eq}. As a rule, L_{eq} will vary least when:

a) The SRF is as far as possible above F_{vco}. This is achieved by using a part with the lowest ε_r and the highest characteristic impedance (Z_o). TTI's series SR8800LPQ (4 mm) resonators has ε_r = 38.6, and Z_o = 14 ohms.

b) The part geometry is large enough where the effect of dimensional tolerances is minimized. This implies that L_{eq} varies most with very small (2 mm and 3 mm) resonators.

6

Table 1.

Dielectric Constants (εr) of Coaxial Material

Material	εr
1000	10.5 ± 0.5
2000	20.6 ± 1.0
8800	39.0 ± 1.5
9000	90.0 ± 3.0

Table 2.

Dimensions and Tab Inductance vs. Profile

Profile	Width(W) (inches)	Diameter(d) (inches)	L_{tab}(nH)
HP (12mm)	0.476 ± 0.005	0.131 ± 0.004	1.8
EP (8mm)	0.316 ± 0.005	0.101 ± 0.004	1.0
SP (6mm)	0.237 ± 0.004	0.095 ± 0.004	1.0
LS (4mm)	0.155 ± 0.004	0.062 ± 0.004	0.9
LP (4mm)	0.155 ± 0.004	0.038 ± 0.003	1.0
MP (3mm)	0.119 ± 0.004	0.032 ± 0.003	0.6
SM (2mm)	0.080 ± 0.003	0.032 ± 0.003	0.6

An example will illustrate the analysis technique. Suppose a VCO design with center frequency of 915 MHZ requires an equivalent inductance of 10.0 nH. Table 3 shows two coaxial resonators satisfying this L_{eq}, Trans-Tech's parts SR9000SMQ0986BY (2 mm) and SR8800LPQ1098BY (4 mm).

Table 3.

Resonator comparisons for Leq=10.0 nH @ 915 MHZ

Parameter	Symbol	Resonators	
		SR9000SMQ0986BY (2mm)	**SR8800LPQ1098BY (4mm)**
Tab Inductance (nH)	L_{tab}	0.6	1.0
Dielectric Constant	$ε_r$	90 ± 3	39 ± 1.5
Width (Inches)	W	0.080 ± 0.003	0.155 + 0.004
Diameter (inches)	d	0.032 ± 0.003	0.038 ± 0.003
Resonant Frequency (MHz)	F_{SRF}	986	1098
Sensitivity to $ε_r$	$\Delta L_{eq} \Delta e_r$	± 1.6%	± 1.8%
Sensitivity to W	$\Delta L_{eq} \Delta W$	± 3.4%	± 1.6%
Sensitivity to d	$\Delta L_{eq} \Delta d$	± 8.4%	± 4.6%
Sensitivity to F_{SRF}	$\Delta L_{eq} \Delta F_{SRF}$	±14.4%	± 5.1%

The above results demonstrate the importance of the separation between F_{VCO} and F_{SRF}. The *components* of sensitivity may be statistically manipulated with a Monte-Carlo process or other analysis method. If the tolerance on F_{SRF} were reduced from 1% to 0.5%, the $\Delta Leq/\Delta F_{SRF}$ component reduces from the above figures to ± 6.65% and ± 3.88% for the 2 mm and 4 mm parts, respectively. An alternative solution might be to shunt-load the resonator with a small capacitor, then the required equivalent inductance would be smaller, which would also raise F_{SRF}. The effect of the additional capacitance on the MHZ/volt sensitivity of the VCO should then be circuit-analyzed, because that performance is also influenced by the placement of F_{SRF}.

Ceramic Filters
A Bandpass Filter Using Coaxial Resonators

Coaxial resonators can be used as high Q circuit elements in the design of filters. This application note demonstrates the Touchstone simulation of a 3 pole filter using quarter-wave resonators.

1670 MHz Capacitive Coupled Bandpass Filter
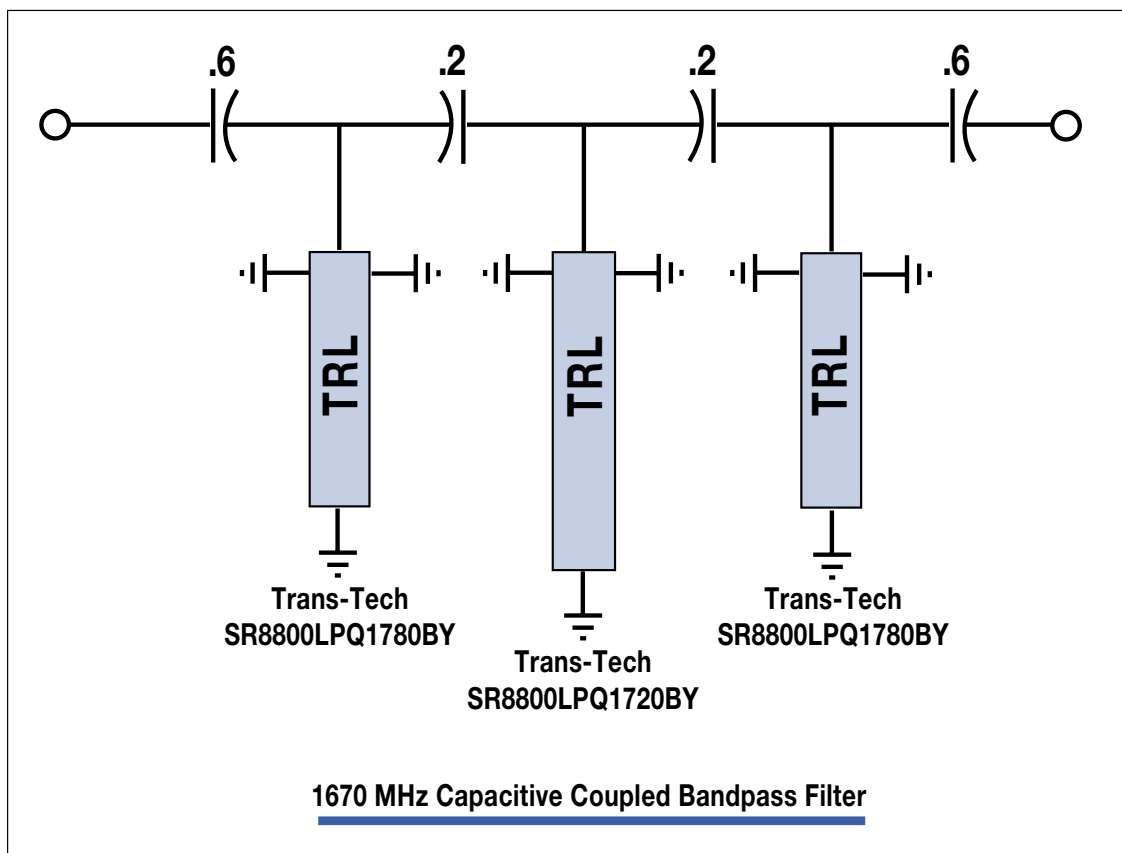
The center shunt resonator is loaded less than the input and output shunt resonators; therefore it has a lower Self Resonant Frequency (SRF). The TouchTone circuit file and output plot is contained on the following page.

A Bandpass Filter Using Coaxial Resonators

The Touchstone™ Circuit File

DIM

FREQ	MHz
CAP	PF
LNG	IN

VAR

C1 =	.6	!	series cap input and output
C2 =	.2	!	series coupling caps
L1 =	.267	!	length of input and output resonator
L2 =	.276	!	length of center resonator

CKT

CAP	1	2	C^C1				!	INPUT CAP
TLPSC	2	0	Z=14	L^L1 K=38.6 A=.05 F=1781			!	INPUT SHUNT LINE
CAP	2	4	C^C2				!	COUPLING CAP
TLPSC	4	0	Z=14	L^L2 K=38.6 A=.05 F=1717			!	CENTER SHUNT LINE
CAP	4	6	C^C2				!	COUPLING CAP
TLINP	6	0	Z=14	L^L1 K=38.6 A=.05 F=1781			!	OUTPUT SHUNT LINE
CAP	6	8	C^C1				!	OUTPUT CAP
DEF2P	1	8	RESP					

FREQ

SWEEP	1420	1920	1

OUT

RESP	DB	[S11]	GR1
RESP	DB	[S21]	GR1

GRID

RANGE	1420	1920	50
GR1	0	-60	10
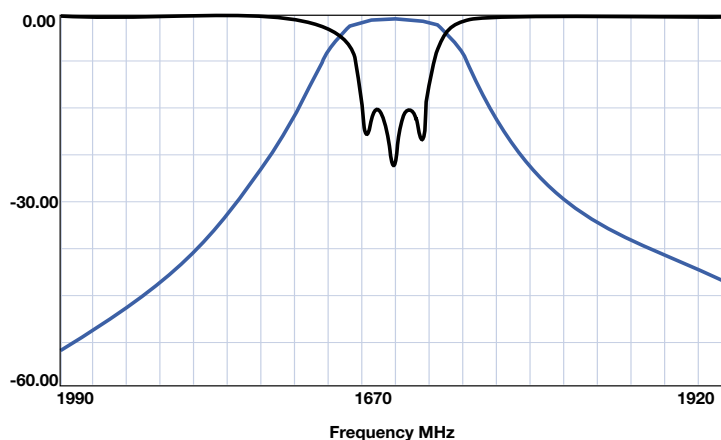
Glossary of Terms

Coaxial Resonator. A component in which standing waves are established in a ceramic coaxial line, short- or open-circuited at the end, remote from the drive. These resonators can be either 1/4 wavelength or 1/2 wavelength type.

Coupling. The method by which a dielectric resonator is electromagnetically connected to the external environment.

Cylindrical Resonator. A disc type resonator with a centered hole used for ease of mounting and improved mode separation.

DBS - Direct Broadcast Satellite. A satellite broadcast system which operates in the range of 10 to 40 GHz in different world locations.

Dielectric Constant (ε_r). The ratio of electric displacement in a medium to that which would be produced in free space by the same field.

Dielectric Resonator (DR). An unmetallized dielectric ceramic which functions similarly to a mechanical resonant cavity at microwave frequencies, but has a greatly reduced size because of its high dielectric constant.

Disc Resonator. A solid cylindrical ceramic body with a height to diameter ratio of approximately .4.

DRO - Dielectric Resonator Oscillator. In this type of oscillator, a dielectric resonator is used as a frequency-determining element for a microwave oscillator to achieve high stability.

GPS - Global Positioning System. A satellite system for determining accurate location. It is employed in land, sea, and air applications, other commercial and military.

Loss Tangent (tanδ). The reciprocal of the Q of the dielectric resonator. (See Q factor definition.)

Q Factor = (1/tanδ). The figure of merit for assessing the performance or quality of a resonator, the Quality factor, is a measure of energy loss or dissipation per cycle as compared to the energy stored in the fields inside the resonator. Q factor is defined by:

$$Q = 2p \; X \; \frac{\text{max energy stored}}{\text{average energy dissipated per cycle}}$$

Q_o Unloaded Q. Q_o is the value of Q obtained when only the incidental dissipation of the system elements is present. Q_o is defined by the following equation:

$$\frac{1}{Q_o} = \frac{1}{Q_c} + \frac{1}{Q_d} + \frac{1}{Q_r}$$

where:

Q_c = Q of conductor
Q_d = Q of dielectric
Q_r = Radiation Q factor

Q_L Loaded Q. Q_L is the value of Q obtained when the system is coupled to an external device that dissipates energy. Q_L is defined by the following equation:

$$\frac{1}{Q_L} = \frac{1}{Q_c} + \frac{1}{Q_d} + \frac{1}{Q_r} + \frac{1}{Q_{ext}}$$

Resonant Frequency (f_o) of Dielectric Resonator. The frequency which the dielectric resonator can store the electromagnetic signal for time periods that are long compared to the period of the frequency being applied.

Spurious Mode. Output from a dielectric resonator caused by a signal or signals having frequencies other than the resonant frequency desired. The presence of higher resonant modes close to the resonant frequency of the principle mode will interfere with filter or oscillator performance.

Temperature Coefficient of Dielectric Constant (τ_f). The change of the dielectric constant of "' of the resonator as a function of temperature.

Temperature Coefficient of Resonant Frequency τ_f (ppm/°C). The shift in resonant frequency of the dielectric resonator due to the linear expansion of the material plus the change in its dielectric constant as a function of temperature.

Thermal Coefficient of Expansion. The linear expansion of a dielectric resonator in all directions with temperature.

Tuning Device. A mechanical mechanism used to adjust the resonant frequency of the dielectric resonator up to 5% by perturbing the external electromagnetic fields.

TVRO - Television Receive Only. A satellite broadcast system which operates in the 3.7 to 4.2 GHz range. It is employed in North and South America.

6

Tech Notes for Magnetic Materials

A Discussion of Ferrite Material Characteristics in Waveguide Digital Phase Shifters

#652 DIGITAL PHASE SHIFTERS

Introduction

Currently the interest in large electronically scanned Radar Antenna Arrays has sparked a renewed interest in ferrite phase shifters. Several types of phase shifters have received intensive study during the past year or two. This article will discuss ferrite material characteristics relevant to one type, the wave guide digital ferrite phase shifter.

Digital Phase Shifter

The most recent type of ferrite device of interest to the microwave industry is the digital phase shifter. One type is shown in Figure 1. The principal feature

DIGITAL PHASE SHIFTER
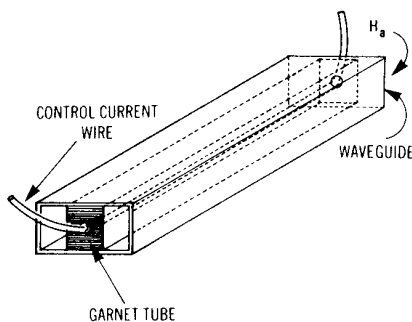
Figure 1

involves the squareness of the hysteresis loop. Borrowing a bit of technology from the computer industry, one relies on the ability of the ferrite or garnet to remember past history of magnetization. A typical hysteresis loop for yttrium iron garnet is shown in Figure 2. The memory, which may be defined as B_r/B_{max}, the remanent magnetic moment divided by the maximum moment, is typically 0.75 for a toroidal shape. The control magnetic field is supplied by the axial wire running through the garnet tube which acts like a thick toroid. If a positive pulse of current is sent through the wire, creating sufficient field to latch the ferrite, it will remain magnetized at the plus remanent value. Now, if a negative pulse is sent through the wire, the material will latch in the opposite direction.
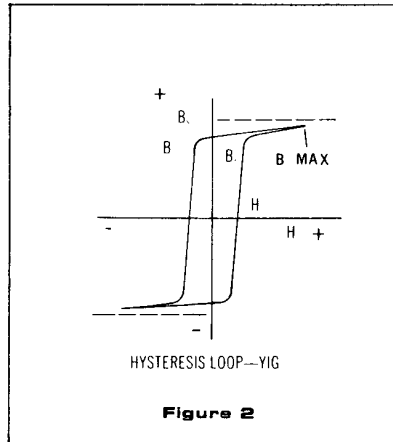

HYSTERESIS LOOP—YIG

Figure 2

DIFFERENTIAL PHASE SHIFT
AS A FUNCTION OF CONTROL CURRENT

Figure 3

The digital ferrite phase shifter can be analyzed as a form of the transversely magnetized twin slab ferrite phase shifter since components of the circumferential magnetization are in effect anti-parallel and transverse to the direction of propagation.

Referring to Figure 1, to the right of the waveguide center line, the remanent magnetization is downward, while to the right, magnetization is upward. These regions each contain components of r-f magnetic field that are circularly polarized in opposite sense. With the r-f power flow in one direction, the direction of r-f polarization has the same sense on both sides with respect to the steady remanent magnetization, and this corresponds to one state of permeability, say ($\mu+$). Reversing the magnetization or the direction of power flow will alter the polarization with respect to the r-f field and provides a different state of permeability ($\mu-$).

The differential phase shift is non-reciprocal then, and is given in terms of the difference between ($\mu+$) and ($\mu-$), generally,

$$\triangle \varnothing \quad = \quad \mu+ \quad - \quad \mu-$$

Consequently, two values of phase shift are available from each length of material in the waveguide. The behavior is as shown in Figure 3. Note that the B/H curve resembles the $\triangle\varnothing$ vs I curve. With currently available materials, it is possible to build a 360° phase shifter with an insertion loss of approximately 0.5 db in this configuration. Stated an-
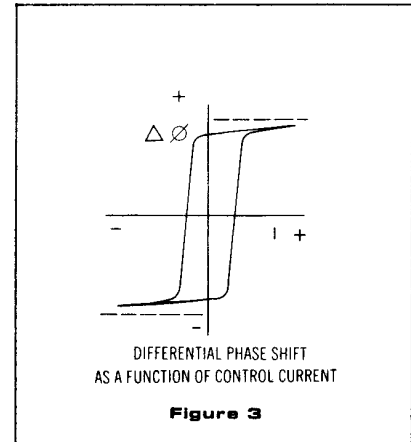
other way, this is an R.F. efficiency of 89%.

By cascading appropriate lengths of tubing, each individually switched by current pulses, one can assemble a phase shifter having as many discrete values as required. Each value can be switched in or out in nanoseconds with no holding field or power required.

Material Requirements

From the above it is apparent that ferrite or garnet material with the usual criteria of low field loss properties at the frequency of operation is essential for low insertion loss. This indicates that the proper saturation moment must be chosen and a narrow linewidth material, having a small anisotrophy field, is best. Magnesium-manganese ferrite and yttrium-iron-garnet with aluminum and/or gadolinium substitution for control of saturation moment satisfy this criteria to the highest degree.

In addition to the above, the material must also have a high remanent magnetization and possess a small coercive force to minimize the control power requirement. In other words, it should have good square loop properties. Fortunately, the best r-f materials for this application also have very tolerable hysteresis loop properties as well with squareness ratios between 0.75 and 0.90 and coercive force values of between 0.25 and 2.0 oersteds depending upon the saturation value chosen.

Permeability Spectra of Ferrimagnetic Materials

#658 FERRITE BASIC PHYSICS

Introduction

We have seen that ferrimagnetic materials employed in microwave applications exhibit high insulating and passive dielectric properties. Propagating electromagnetic waves are thus able to couple efficiently with the magnetic characteristic enabling us to obtain device action. In this article we will describe some of the properties of ferrite permeability.

The relationships between R.F. magnetic field (h) and R.F. magnetic induction (b) inside of a ferrite are dependent upon its state of static magnetization and the frequency of operation. Also, a time varying magnetic field will generally dissipate energy. The relationship between the h and b fields defined as the permeability (μ) may be described in terms of a scalar or tensor quantity depending upon the conditions of operation.

Basic Theory

The origin of ferrimagnetism is found in the cooperative behavior of electronic spins. Strong exchange forces between the electrons of the constituent magnetic ions enforce a spatial ordering of their spin orientations within the ferrite. This results in large volumes of material, called domains, being spontaneously magnetized. In a macroscopically demagnetized sample these domains are arranged with haphazard orientations. When a static field is applied, the domain magnetization tends to orient parallel to it. This increases the observed magnetism by the amount $(\mu-1)H$.

1. Scalar permeability

If we apply a small R.F. magnetic field to a demagnetized ferrite specimen so as to avoid hysteresis losses, the relationship between h and b can be described by the introduction of a factor μ_i known as the initial permeability. This factor is complex to account for residual losses.

$$b = \mu_i h \qquad \mu_i = \mu_i' - j\mu_i'' \qquad (1)$$

where μ_i' is the real part of the permeability. Energy dissipation is usually expressed as $\tan \delta_m = \mu_i''/\mu_i'$. The energy loss is then proportional to μ_i'' and both components of μ_i can vary with frequency.

A typical spectrum of initial permeability is shown in *Figure 1*. Microwave ferrites
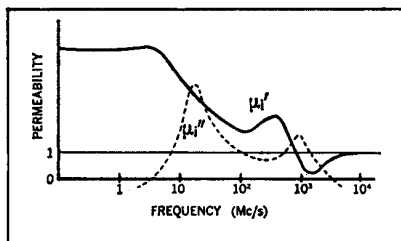

Figure 1

exhibit low frequency μ_i' values between about 10 and 100. Two regions of dispersion and absorption are generally observed. They are attributed to domain wall and rotational resonance effects at the low and high frequencies, respectively. Note that at frequencies where microwave devices are employed μ_i' is approximately unity.

2. Tensor permeability

The magnetization resulting from an internal static magnetic field (H_i) may be coupled to the R.F. magnetic field through ferromagnetic resonance processes. It is found that components of R.F. magnetic induction can be generated in several directions in this manner. This is the origin of the tensor nature of the permeability and the realization of non-reciprocal microwave devices.

Tensor permeability is most tractable when described in terms of plane wave propagation through an infinite ferrite medium. This theory quite readily predicts the properties exhibited by finite samples inside wave guides. For such a medium, saturated by a field (H_i), we have

$$b = \begin{bmatrix} \mu & -jk & 0 \\ jk & \mu & 0 \\ 0 & 0 & 1 \end{bmatrix} h \qquad (2)$$

Neglecting losses, the components of the tensor permeability are

$$\mu = 1 + \frac{4 \pi M_s H_i \gamma^2}{\gamma^2 H_i^2 - \omega^2} \qquad (3a)$$

$$k = \frac{4 \pi M_s \gamma \omega}{\gamma^2 H_i^2 - \omega^2} \qquad (3b)$$

where (M_s) is the ferrite magnetization and (γ) is the gyromagnetic ratio. Two cases are of interest. These are for a plane wave propagating perpendicular and parallel to the applied static field (H_i).

Case I—For the plane wave propagating perpendicular to H_i, and with the R.F. magnetic field parallel to H_i, the plane wave will see an effective permeability ($\mu_{eff\parallel}$) equal to unity. For the R.F. magnetic field perpendicular to both H_i and the direction of plane wave propagation we have

$$\mu_{eff\perp} = \frac{\mu^2 - k^2}{\mu} \qquad (4)$$

The properties of the effective permeability at constant frequency are shown in *Figure 2*. When H_i has the magnitude required
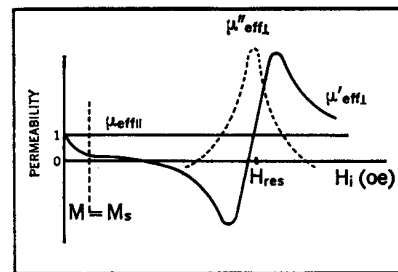

Figure 2

for resonance, $\mu_{eff\perp}$ exhibits large dispersions. Both the real and loss components are indicated. Values of $\mu'_{eff\perp}$ are typically 5 to 40. Below saturation ($M < M_s$) these equations do not strictly apply, but they show qualitatively what occurs as the permeability reverts to its scalar condition.

Case II—When a plane wave propagates parallel to H_i, the observed effects can best be described if we represent the plane wave by two contra-rotating circularly polarized components. Permeabilities can then be defined for the positive and negative sense of rotation. The positive sense is clockwise when viewed in the direction of H_i.

$$\mu_+ = \mu - k \qquad \mu_- = \mu + k \qquad (5)$$

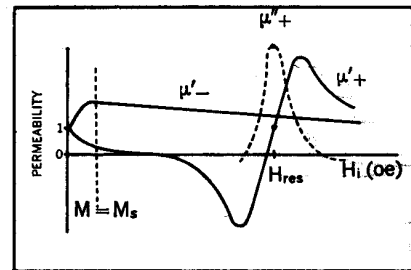The properties of these permeabilities are shown in *Figure 3*. The loss component

Figure 3

μ''_- (not shown) has a form similar to μ'_- but a much smaller magnitude. A negatively circular polarized wave can thus be obtained from a propagating plane wave with sufficient ferrite path length and magnitudes of H_i close to resonance. At low values of H_i, the losses are about equal but a plane wave will experience a change in phase due to the difference in μ'_- and μ'_+. Notice that μ'_+ is qualitatively similar to $\mu'_{eff\perp}$. It is found experimentally that a plane wave propagating perpendicular to H_i exhibits the same effects as a circularly polarized wave propagating parallel to H_i. Regions where the permeability is zero result in reflection of incident waves.

Application

The variation of R.F. permeability is of major importance in the design of microwave ferrite devices. In the unsaturated region the difference in permeability of two circularly polarized waves is utilized to design circulators, isolators, switches, amplitude modulators, single-sideband modulators, and phase shifters in circular waveguide employing Faraday rotation effects. At resonance fields the loss characteristic is used to design isolators, principally in rectangular waveguide. Field displacement and differential phase shift devices such as circulators and duplexer-detectors usually operate between the unsaturated and resonance regions.

Stabilization of Remanent Induction by Thermal Annealing

#691 FABRICATION PROCESSES

Introduction

In recent years microwave device engineers have increasingly employed the hysteresis loop characteristic of ferrimagnetic materials to obtain phase shifter device action. Two major advantages of this design technique are: (1) elimination of external d.c. biasing magnets, and (2) rapid switching between remanent induction states at low switching power.

A number of chemical and ceramic processing techniques are currently being studied to better control the remanent induction of ferrimagnets. The sensitivity of the remanent induction of a ferrimagnet to the fabrication method employed has been of major concern to material scientists because of its effect on device action. It has been found, experimentally, that there is a direct linear relationship between the magnitude of remanent induction and the differential phase shift obtained for a given material.

Machining or lapping and polishing of ferrimagnets into phaser toroids and substrates can result in a large change of the remanent induction from its nominal intrinsic value. This effect is most pronounced when a finished section is less than approximately one-tenth of an inch thick. This Tech-Brief describes a thermal treatment for eliminating deleterious effects which may result from mechanical finishing.

Table I

Magnetostrictive Properties of Ferrites†

	Material	$4\pi M_s$ Gauss	$B_R/B_{R(0)}$** at 3000 psi
Mg-Mn	TT1-414*	680	1.0
	TT1-109	1250	1.0
	TT1-105	1700	1.0
	TT1-390	2150	1.0
	GE 42L	860	1.0
Ni-Co	TT2-116	1400	1.55
	TT2-115	1600	1.21
	TT2-101	3000	0.93
	M-52*	3150	0.84
Garnets	TTG-1002	1000	0.84
	TTG-1001	1200	0.88
	TTG-1200	1200	0.88
	TTG-113	1780	0.95
	SP 286*	1250	0.95

*Prefixes: TT—Trans-Tech, M—Motorola, SP—Sperry, GE—General Electric

**$B_R/B_{R(0)}$ is the ratio of remanent induction at 3000-psi compression over the remanent induction without stress.

†After Stern & Temme

Magnetostriction

Current theory suggests that magneto-strictive effects are the origin of observed variations in the remanent induction of mechanically finished ferrimagnets. Mechanical stress will change the direction of domain magnetization ($4\pi M$) via the magnetostriction. Under mechanical stress a component of magnetoelastic energy (E) exists which can be expressed as

$$E = \frac{3}{2}\lambda s \, \sigma \sin^2 \theta \qquad (1)$$

where λs is the isotropic magnetostrictive constant, σ represents a uniform applied tensile stress, and θ is the angle between the applied stress and the direction of magnetization. Since nature tends to minimize energy, it follows that an alignment of $4\pi M$ and σ is favored when λs is positive while a 90° orientation between $4\pi M$ and σ is favored when λs is negative.

The effect of applied stress on the remanent induction of a number of ferrimagnetic toroids is given in Table I. Notice that Ni-Co ferrites and garnets exhibit greater magnetostrictive properties than Mg-Mn type ferrites. To date Ni-Co type ferrites have not been employed extensively in latching phaser applications because of their relatively large coercive force.

Thermal Annealing

Under the severe conditions encountered at the surface of a ferrimagnet during machining, it appears that a mechanical strain is induced in the material. The hysteresis loop of a machined toroid of garnet material type TTG-1001 is shown in Figure 1a. The remanent induction is severely degraded. This strain can be removed by thermal annealing. In Figure 1b the hysteresis loop of the same toroid is shown after being thermally annealed at 1200°C for one hour. The measured remanent induction value of 651 gauss compares favorably with that of toroids fabricated from the same ferrimagnetic material but not subjected to a machining step.

Although the magnetostrictive coefficients of garnets and nickel-cobalt ferrites are generally greater than those of magnesium-manganese type ferrites, a deterioration in remanent induction of the latter type ferrites may also occur if the part is thin enough.

It appears quite feasible to eliminate deleterious effects resulting from mechanical finishing by means of thermal annealing.

The thermal annealing treatment consists of heating the part in the same atmosphere employed during sintering, which is normally air. For garnets this consists of a heating rate of approximately 100°C per hour up to 1200°C; holding for one hour at 1200°C; and cooling at approximately 100°C per hour to room temperature. For
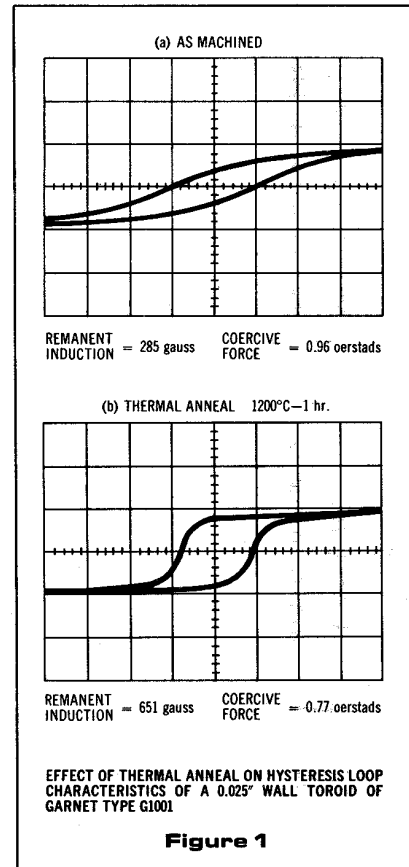

(a) AS MACHINED

REMANENT INDUCTION = 285 gauss   COERCIVE FORCE = 0.96 oerstads

(b) THERMAL ANNEAL   1200°C—1 hr.

REMANENT INDUCTION = 651 gauss   COERCIVE FORCE = 0.77 oerstads

EFFECT OF THERMAL ANNEAL ON HYSTERESIS LOOP CHARACTERISTICS OF A 0.025″ WALL TOROID OF GARNET TYPE G1001

Figure 1

magnesium-manganese type ferrites, the treatment is the same with the exception that an 1100°C hold should be employed. In all cases care should be taken to avoid thermal shock. At these temperatures and heating/cooling rates, the mechanical integrity and chemical nature of the ferrimagnetic part are not affected so that no change in mechanical dimensions or technical properties should be encountered.

Thermal annealing should be considered as part of the fabrication process when a ferrimagnetic part for latched phase operation is mechanically finished to final dimensions of approximately one-tenth of an inch or less. If the microwave device engineer fabricates ferrimagnetic parts from bar stock for similar use, it is also advisable that thermal annealing be employed.

References:

"Magnetostriction Effects in Remanence Phase Shifters", E. Stern and D. Temme, IEEE Trans. MTT, vol. MTT-13, p. 873 (November 1965).

Ferrimagnetic Substrates for Microwave Integrated Circuits

#693 FABRICATION PROCESSES

Introduction

A number of microwave investigators[1,2,3] have succeeded in demonstrating the feasibility of constructing useful microwave components on ferrimagnetic substrates utilizing printed circuit techniques. In this Tech-Brief, methods are described for the ceramic fabrication of microwave ferrite substrates of four square inch area. The economic production of MIC's on ferrimagnetic substrates requires that as-fired geometric tolerances be held within values that are compatible with circuit design requirements. These parts exhibit intrinsic technical properties and as-fired mechanical tolerances suitable for construction of microstrip ferrimagnetic devices. The elimination of machining to obtain usable mechanical tolerances provides for a cost reduction of ferrite parts. Also, methods of improving the surface finish when required are discussed.

Fabrication Methods

When fabricating ceramic parts, the attainable mechanical tolerances depend in considerable measure on the forming method selected which also effects the magnetic and dielectric properties of the final part. At Trans-Tech, it has been found that the best forming powders are obtained by the spray drying method. These powders exhibit good die fill uniformity and require a minimum amount of binder which is important in reducing non-uniform shrinkage and warpage during sintering.

The fraction of spray dried powder employed is 90 to 150 microinch. The substrate compact is then pressed at 6000 psi, resulting in a green density high enough to insure optimum substrate properties. Ejection of the formed substrate under pressure is important in obtaining maximum flatness of the substrate surface. This is accomplished by relieving the upper punch pressure and ejecting with the lower punch, forcing the substrate and upper punch up simultaneously. Parts ejected in this manner show no edge deformation. The green formed substrate is strong enough to be easily handled and prepared for the final sintering operation.

A key step required to hold the mechanical flatness of the substrates to ±0.001 inch involves loading the substrate during sintering with a ceramic cover plate of approximately equal cross sectional area. This plate weighs approximately the same as the substrate it covers. One arrangement used is shown in Figure 1; here the substrate is sandwiched between two plates. Various types of ceramic cover plates can be employed, such as yttria stabilized zirconia for garnets and alumina or mullite for spinel type ferrites. An isotherm is set up across the substrate thickness due to the presence of

Preparation for Sintering Ferrite Substrate
Figure 1
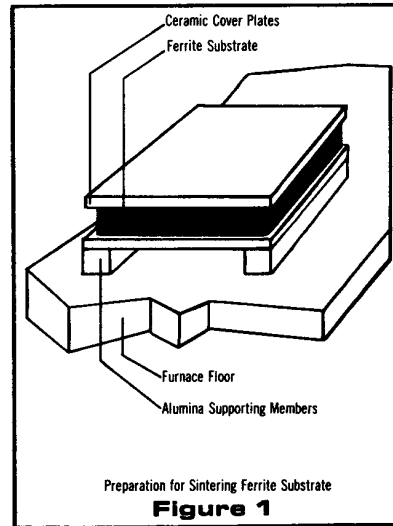
the cover plate. This results in more uniform sintering and better mechanical integrity.

Results

Substrates have been fabricated that exhibit a surface finish (roughness) of 10 to 15 microinches. Surface flatness to within 0.0015" can be obtained on the same substrates. Parallelism between the two flats can be held to ±0.001 inch.

A summary of the mechanical tolerances obtained on the as-fired substrates is given in Table I.

When required, rapid lapping and polishing methods are employed to reduce the surface finish to less than 5 microinches. Lapping and polishing is achieved using a planetary lapping machine which simultaneously removes equal amounts of material from each side of the work. The choice of lapping compound is dependent on surface finish and stock removal desired. All polishing is done with chromic oxide polishing compounds on pellon paper. To decrease polishing time it is necessary that the substrates be lapped flat first using 25 micron lapping compound. Surface finishes of 1 microinch on garnet and 3 microinches on ferrite

Table 1
AS-FIRED FERRITE SUBSTRATE MECHANICAL TOLERANCES

	Tolerance Attained	
	1 sq. in. area	4 sq. in. area
Length, Width (in.)	.005	.010
Thickness (in.)	.001	.001
Total Indicated Run Out (Waviness) (in.)	.003	.003
Surface Finish (Microinch)	10 - 15	10 - 15

have been achieved. Annealing is needed for all magnetostrictive materials after lapping or polishing to remove strains which effect the hysteresis loop. (See Tech Brief #691.)

The technical properties and electrical characteristics of the as-fired substrates when compared to those of substrates cut from bulk material are found to be identical when the surface finishes are the same. Typical methods of forming microstrip components on ferrite substrates have been described in the literature.[1,2,3]

Cost Reduction

A measure of the cost reduction accomplished via the fabrication methods described here is in order. To accomplish this, a typical cost estimate has been made for ten thousand (10,000) substrates of four (4) square inch area, assuming substrates machined from bulk stock vs. substrates formed and sintered to size and for three (3) surface roughness criteria. The results are as follows:

Material	From Bulk Stock	As Formed & Sintered
Garnet	A. $15.45 each	$6.75 each
	B. $16.80 each	$7.05 each
	C. $17.40 each	$7.20 each
Ferrite	A. $6.35 each	$2.20 each
	B. $7.55 each	$2.50 each
	C. $7.60 each	$2.65 each
Surface Roughness:	A $\leq$ 20 microinches	
	B $\leq$ 10 microinches	
	C $\leq$ 5 microinches	

Applications

MIC's find application in areas similar to traditional ferrimagnetic components except that they are smaller and lend themselves to higher reproducibility because of the printed circuit methods employed in fabrication.

To date MIC's exhibit higher insertion loss and lower power handling capability than conventional ferrimagnetic devices. Some typical uses include: phase shifters, isolators, phased arrays, latching circulators, multiple port and other similar devices.

Acknowledgments

References

1. Roome, G. T.; Hair, H. A. and Gerst, C. W.; "Thin Ferrite Phase Shifters for Integrated Microwave Devices," J. App. Physics, vol. 38, p. 1411 (1967).

2. Hershenov, B.; "Microstrip Junction Circulator for Microwave Integrated Circuits," IEEE Trans. MTT, vol. MTT-15, p. 748 (1967).

3. Roome, G. T.; Hair, H. A. and AuMiller, C.; "Ferrite Devices for Microwave Integrated Systems," 1968 ISSCC Digest Technical Papers, p. 52 (1968).

Polycrystalline Grain Size Effects on High Power Non-Linearity in Ferrimagnetic Materials

#657 HIGH POWER MATERIALS

Introduction

One of the characteristics of ferrimagnetic materials used in microwave devices is that non-linear absorption occurs as a function of R.F. power level. At milli-watt power levels, the insertion or absorption loss can be small; but at some higher power level, a sudden increase in absorption is noted and beyond that level, the absorption continues to increase until saturation is encountered. This effect can be used to build devices such as limiters, power levelers, frequency multipliers and parametric amplifiers. Offtimes, however, non-linearity is undesirable as it imposes a limitation on the amount of power that can be propagated through ferrite devices. It is our purpose here to discuss a mechanism, namely, grain size control, that can effectively increase the non-linear threshold or critical power level by an order of magnitude or more.

Non-Linearity Model

Many articles have appeared in the literature[1,2,3,4] concerning the various atomic models used to explain the onset of non-linear absorption in ferrites and garnets. Theoretical studies are continuing that contribute to the still incomplete picture. Each case requires a somewhat different analysis since much depends on the operating point relative to gyromagnetic resonance.

The generally accepted model for explaining the phenomenon is that of spin wave build up in the material. Spin waves are excited when the R.F.$_h$ field exceeds a critical value. The critical field is dependent on many factors, such as geometry, magnetization, R.F. power, main resonance linewidth, the relevant spin wave linewidths, gyromagnetic ratio and operating frequency. The theory provides for a spectrum of spin waves, some having lower critical fields than others. This accounts for the fact that as R.F. power is increased, absorption continues to increase as more spin waves are excited.

It has been found that a number of techniques can be employed to retard the build up of spin waves. For example, in YIG the substitution of rare earth ions, which increases the spin wave linewidth, will effectively increase the non-linear threshold. In both YIG and ferrite, porosity, which effects main resonance linewidth, will do the same. Reduction of the saturation moment for a given case is effective. However, the application of these techniques to a high power problem almost always results in an increase in low power insertion loss or reduction of activity. This means a poor figure of merit for the device design. *Figure 1* shows the effect of substituting holmium in YIG as measured in a digital phase shifter.
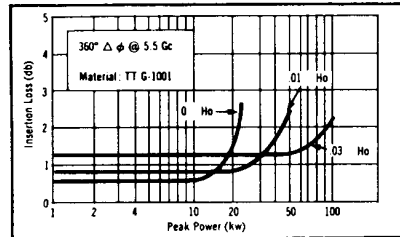

Figure 1

Since spin waves exhibit discrete frequencies and finite wave lengths, another approach to the problem is suggested. Similar to the approach that Rado[5] took in eliminating the domain wall loss in ferrites by reducing the polycrystals to sub-domain size, we have approached the spin wave problem by reducing the grain size to sub-spin wave dimensions. The hypothesis being that the grain boundaries would provide sufficient discontinuity to break up spin waves. With such a model, it is expected that as grain size is progressively reduced the longer λ spin waves will be attenuated first and then the shorter λ spin waves. Thus a progressive increase in threshold is expected as grain size is reduced.

Ferrites and garnets manufactured for the microwave industry normally have grain sizes between 10 and 20 microns. Calculation shows that spin waves having wave lengths as short as 0.1 μ can exist. It seems reasonable, then, that grain sizes as small as 0.01 μ would be useful. At this time, ceramic science has not provided for fabrication of acceptable specimens having grain sizes this small, but good specimens having grain sizes between 0.1 μ and 20 μ have been fabricated and tested. In *Figure 2* we see the results of a set of fine grain experiments with G-1001 garnet for use in a C-band digital phase shifter. The maximum peak power available for the tests was 50 kw. Saturation moment, linewidth, dielectric constant, dielectric loss tangent and effective "g" value was constant within measurement error in all four cases.
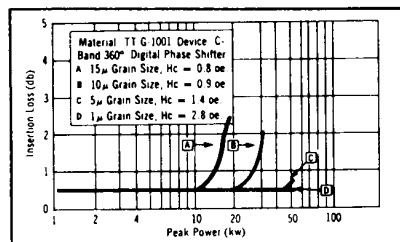

Figure 2

The coercive force is increased by the reduction of grain size due to domain wall involvement. This is a serious consequence for digital devices because the control

energy is increased, or more to the point, the peak drive current is increased. In other type devices, however, the demagnetizing effect of the geometry usually tends to make this an unimportant consideration.

In *Figure 3*, the results obtained in a Reggia-Spencer type analog phase shifter at C-band are shown. In this type of device, the increase in H$_c$ is of no consequence. The two micron material was
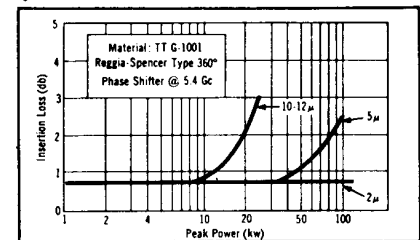

Figure 3

tested to the limit of the available power (115 kwp) without any measurable increase in the insertion loss. It is important to note that the low power insertion loss remained constant.

Conclusions

Reduction in the grain size of polycrystalline ferrites and garnets does increase the high power threshold without increasing the low power insertion loss. An order of magnitude increase in P$_{crit}$ is achievable with present technology. Fine graining does not change low power characteristics of the material, such as main resonance linewidth, magnetization, dielectric properties or Curie temperature. The principal effect is interpreted as an increase in the effective ΔH$_k$ the spin wave linewidth.

Garnet material has been used for the illustrations here, but substantially the same results have been obtained with magnesium and nickel ferrites. The fine grain approach to obtain an increase in the linear power handling capability of ferrimagnetic materials appears equally applicable to ferrites and garnets.

References:

[1]Bloembergen, N., and Wang, S., "Relaxation Effects in Para- and Ferromagnetic Resonance," *Phys. Rev.*, Vol. 93, 1954, p. 72.
[2]Damon, R. W., "Relaxation Effects in Ferromagnetic Resonance," *Rev. Mod. Phys.*, Vol. 25, 1953. p. 239.
[3]Suhl, H., "The Theory of Ferromagnetic Resonance at High Signal Powers," *J. Phys. Chem. Solids*, Vol. 1, 1957. p. 209.
[4]Schlömann, E., Green, J. J., and Milano, D., "Recent Developments in Ferromagnetic Resonance at High Power Levels," *J. Appl. Phys.*, Vol. 31, May 1960, p. 386S.
[5]Rado, G. T., *Rev. Mod. Phys.*, Vol. 25, 1953, p. 81.

Use of Ferrimagnetic Material in Isolators

#6510 MICROWAVE FERRITE

Introduction

It has been found convenient to define three functional classes of non-reciprocal microwave ferrite devices as: (1) isolators, (2) circulators, and (3) gyrators. The realization of these devices stems from the gyromagnetic behavior of the elementary magnetic dipoles, or uncompensated electron spins, of the ferrite material as discussed in preceding Tech-Briefs.

This article will describe the intrinsic material properties and basic geometry criteria required in the design of rectangular waveguide resonance isolators. An isolator is defined as a two port circuit element that exhibits differential, or non-reciprocal, attenuation. The isolator circuit symbol indicates that an R.F. signal may be transmitted with little loss of energy from port 1 to port 2, but will experience

1 ⎯⎯◯⎯⎯ 2

ISOLATOR SYMBOL
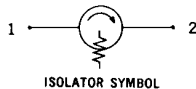
substantial attenuation when transmitted from port 2 to port 1. The great value of isolators is in their ability to decouple energy sources from their loads with little reduction in available output power.

Resonance Isolator Theory

Recall that the main features of the gyromagnetic behavior of a ferrite in the presence of an internal static magnetic field (H_i) and a correctly positioned R.F. magnetic field include:

(a) the magnetic dipoles precess at a frequency that is proportional to the magnitude of the static internal field:

$$\omega = \gamma H_i, \qquad (1)$$

(b) the direction of precession depends on the direction of the static field, and the positive sense is clockwise when viewed in the direction of H_i.

From these conditions it is observed that resonance absorption of propagating electromagnetic energy can take place when the frequency and rotation of the R.F. magnetic field corresponds to that of the elementary magnetic dipoles. For rotations of the R.F. magnetic field in the opposite direction, little, if any, absorption occurs.

Waveguide Isolators

In rectangular waveguide propagating the dominant TE_{10} electromagnetic mode there are geometric locations where the R.F. magnetic field exhibits circular polarization. *Figure 1* represents the R.F. magnetic field observed looking down on the broad face of the waveguide. In effect, the fields at points A and B rotate in the directions shown as a function of time. The rotation at points A and B has a positive sense for a static magnetic field (H_a) out of and into the plane of the page respectively.
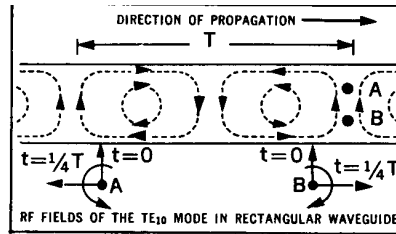

Figure 1

If a thin ferrite slab is located at a distance corresponding to point A from the side wall and biased with a static field (H_a) of proper magnitude, the ferrite will exhibit directional absorption. With H_a directed out of the page and the microwave signal propagating from left to right, the electron spins rotate in the same direction as the R.F. magnetic field. The microwave signal will give up energy to the spin system. If the microwave signal propagates from right to left, the R.F. magnetic field will rotate in an opposite sense to the electron spins and no interaction will occur. These two cases correspond to attenuation in one direction and little or no attenuation in the other.

Note that if the ferrite is moved from point A to point B, the direction of isolation is reversed. If the ferrite is not moved from point A, but the external field is reversed, the isolator acts in the same way as if the ferrite had been moved from A to B. Consequently, reversing the field corresponds to turning the isolator around.

The plot of R.F. magnetic fields in *Figure 1* is valid only for an unloaded waveguide. Insertion of a ferrite slab causes distortion which tends to elliptically polarize the fields. The position of the ferrite is best adjusted experimentally to give an optimum ratio of reverse-to-forward attenuation.

It is appropriate here to describe several elements of resonance isolator design. From equation (1), it is apparent that the static magnetic field required for resonance increases with frequency. Kittel's equation,

$$H_i = \{ [H_a - (N_z - N_x) M_s] [H_a - (N_z - N_y) M_s] \}^{1/2} \quad (2)$$

shows that the internal field can be varied over a wide range by choosing the correct shape factors. Since it is desirable to design the isolator to work with the smallest and cheapest external magnet possible, a geometry should be achieved where the demagnetizing factors boost the external field inside the ferrite.

The geometry shown in *Figure 2* yields demagnetizing factors of $N_x = 4\pi$; $N_y = 0$; $N_z = 0$. Inserting these values in Kittel's equation, we obtain

$$H_i = [H_a^2 + 4\pi M_s H_a]^{1/2} \quad (3)$$

Thus by determining H_i from equation (1), the required H_a from a solution of equation (3) can be found.
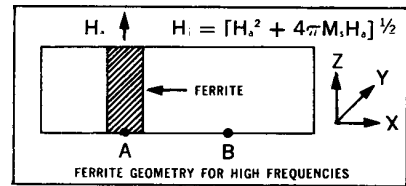

Figure 2

If a wideband isolator is desired, a ferrite with a large linewidth should be chosen; however, this usually results in a lower ratio of reverse-to-forward attenuation. The ratio of the forward attenuation to the reverse attenuation when measured in decibels is defined as the figure of merit (R) of the resonance isolator. A practical formula for any resonance isolator is:

$$R = \left(\frac{4\omega}{\gamma_{eff} \Delta H} \right)^2 \quad (4)$$

It can be seen that the figure of merit is directly proportional to the square of frequency and inversely proportional to the square of the linewidth and the gyromagnetic ratio. This figure of merit represents the theoretical limit of performance. In practice lower values are obtained.

There exists a frequency region below which high device insertion losses occur as a result of the ferrite not being fully magnetized. It is called the low field loss region, and has for its upper limit the frequency

$$\omega_L = \gamma (H_{anis} + 4\pi M_s) \quad (5)$$

where H_{anis} is the anisotropic field associated with the crystal structure; for most microwave ferrites it is of the order of 100 oersteds or less.

If the operating frequency of the isolator is low, the magnetic field required for resonance may be too low to saturate the ferrite. Resonance isolators for operation at low microwave frequencies require either a ferrite material with a saturation magnetization less than (ω_L/γ), or a geometry where a high magnetic field is required for resonance. One useful geometry is shown in *Figure 3*. Here the internal field is always less than the external field.
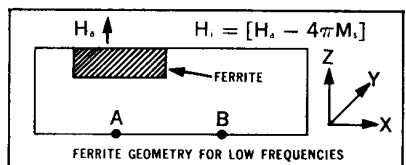

Figure 3

Summary

The essential factors in resonance isolator design are the selection of the proper ferrite geometry, correct location of the ferrite specimen, and the choice of a ferrimagnetic material with suitable intrinsic parameters (γ, ΔH, $4\pi M_s$) for the operating frequency desired. Kittel's equation allows us to readily handle the complex demagnetizing effects resulting from the finite ferrite specimens employed.

# Use of Ferrimagnetic Material in Circulators

#6511 MICROWAVE FERRITE

Introduction

The realization of non-reciprocal microwave ferrite devices stems from the gyromagnetic behavior of the elementary magnetic dipoles, or uncompensated electron spins, of the ferrite material as discussed in preceding Tech-Briefs.

In this article we will describe the material properties and basic geometry criteria required in the design of ferrite junction circulators. We will deal with the three-port version usually called the Y-junction circulator.

The Y-junction circulator is a non-reciprocal device providing transmission of energy from one of its ports to an adjacent port while decoupling the signal from all other ports. The circulator symbol
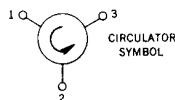
shown indicates that R.F. energy incident on port 1 emerges from port 2, R.F. energy entering port 2 emerges from port 3, and R.F. energy entering port 3 emerges from port 1.

The Y-junction circulator can also be used as an isolator or as a switch. It is simple in construction, compact, and lightweight. Units have been built to operate in frequency bands of approximately 5 to 35 percent from 0.1 Gc to greater than 140 Gc. Good results have been obtained over wide ranges of peak and average power. At VHF, circulators have been operated at about 1 megawatt peak and at greater than 2 Kw average power.

Junction Circulators

The Y-junction circulator can be constructed in either rectangular waveguide or stripline. The waveguide type, shown in *Figure 1a* is used at high microwave frequencies. It consists of three H-plane junc-
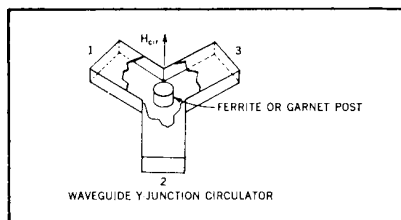

Figure 1a

tions although E-plane circulators can also be made. The stripline version shown in *Figure 1b* is principally applicable to the VHF and low microwave frequencies. It is usually made with coaxial connectors.

In both types, a ferrite element is placed in the center of three symmetrical junctions spaced 120 degrees apart. A ferrite
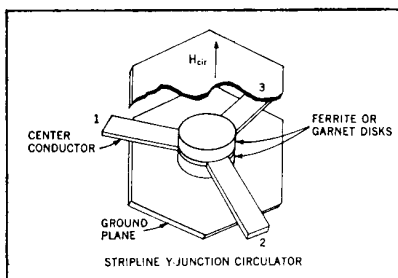

Figure 1b

post is employed in the waveguide version. Two ferrite disks, one located on each side of a metallic center conductor, are used in the stripline type.

Circulator action is obtained by biasing the ferrite element in the axial direction with an internal static field (H_{cir}) of proper magnitude. The circulator can operate at two values of H_{cir}. One is small in magnitude and less than the internal d-c magnetic field required for gyromagnetic resonance. The other is larger than that required for resonance. This property enhances the versatility of ferrite Y-junction circulators.

In general, circulator action is controlled by either of two pairs of independent variables, (1) ferrite post or disk diameter and magnetic field, or (2) saturation magnetization and magnetic field. The operating range can be increased by placing dielectric matching sections in the junction. The direction of circulation is reversed by reversing the static magnetic field.

Operating Principles

Network theorems tell us that reciprocal multi-port junctions can not be matched but that we can match non-reciprocal multi-port junctions. Also, we find that a non-reciprocal, lossless, matched, multi-port junction is a perfect circulator. These theorems led to the development of ferrite Y-junction circulators. Much of the device design has proceeded on an empirical basis. Recently circulator action has been described in terms of electromagnetic field theory.

A cavity type resonance of the ferrite element appears to be an essential feature of circulator operation. The lowest frequency resonance mode of the stripline disk structure is shown in *Figure 2a*. The
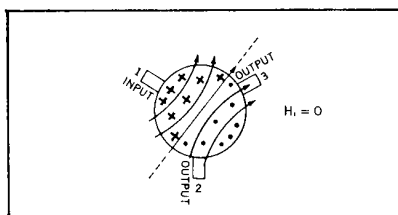

Figure 2a

R.F. electric field vectors are perpendicular to the plane of the disk and the R.F. magnetic field vectors are parallel to the plane of the disk. This mode is excited by an R.F. signal entering port 1 and zero applied static magnetic field. The R.F. signals are 180 degrees out of phase at ports 2 and 3, and about half the input signal magnitude.

When a static magnetic field is applied into the plane of the page, the standing wave pattern will rotate clockwise, as shown in *Figure 2b*. An R.F. signal null
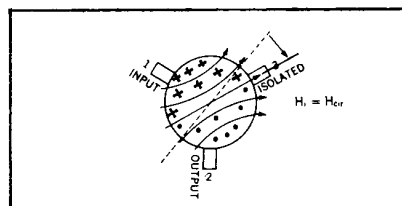

Figure 2b

will appear at port 3 for a certain value of internal static field (H_{cir}). The R.F. signal at port 2 will about equal the input signal at port 1. We can represent the standing wave by two contra-rotating field patterns. The R.F. magnetic fields lie in the plane of the disk. They are circularly polarized at the disk center and linearly polarized at the disk edge. Permeabilities can then be defined for the positive and negative sense of rotation. The positive sense is clockwise when viewed along H_{cir}.

The required disk or post diameter increases as the operating frequency decreases. For operation above gyromagnetic resonance the static magnetic field H_{cir} increases as $4\pi M_s$ increases. For operation below gyromagnetic resonance H_{cir} decreases as $4\pi M_s$ increases.

At low frequencies, circulator operation below gyromagnetic resonance can cause high device insertion loss as a result of the ferrite not being fully magnetized. By operating the circulator above gyromagnetic resonance the ferrite usually will be fully magnetized and the low field loss region avoided.

Design equations exist that relate the ferrimagnetic element size and circulator operating characteristics to the intrinsic material properties ($4\pi M_s$, ΔH, γ_{eff}, $\tan \delta$, ϵ'). Although very tractable, they are rather long and are not given here. The reader is referred to the references given below.

References

H. Bosma, "On Stripline Y-Circulation at UHF", IEEE TRANS. ON MICROWAVE THEORY AND TECHNIQUES, vol. MTT-12, pp. 61-72; January 1964.

C. E. Fay, and R. L. Comstock, "Operation of the Ferrite Junction Circulator", IEEE TRANS. ON MICROWAVE THEORY AND TECHNIQUES, vol. MTT-13, pp. 15-27; January 1965.

Use of Ferrimagnetic Materials in Gyrators

#6512 MICROWAVE FERRITE

Introduction

Non-reciprocal microwave devices are conveniently defined in three functional classes: (1) isolators, (2) circulators, and (3) gyrators. In general, these devices are interchangeable in circuit synthesis because each may be converted into either of the others by combining it with reciprocal elements. We have seen examples of isolators and circulators in preceding Tech-Briefs; now gyrators will be described.
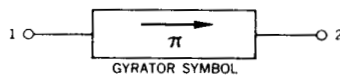
GYRATOR SYMBOL

A gyrator is defined as a two port circuit element that exhibits 180 degrees of differential, or non-reciprocal, phase shift. The gyrator circuit symbol indicates that an R.F. signal transmitted from port 1 to port 2 will undergo 180 degrees phase shift (arrow direction) relative to an R.F. signal transmitted in the reverse direction. For many systems applications, devices that exhibit 45° or 90° of differential phase shift are required. This article will describe the material properties and basic geometry criterion required in the design of rectangular waveguide non-reciprocal phase shifters.

Differential Phase Shift

Recall that a magnetized section of ferrimagnetic material placed in a waveguide at a region of R.F. magnetic field circular polarization, will exhibit a permeability that is different for the two directions of R.F. signal propagation. At low values of internal static field (H_i), the losses are small and about equal but a plane wave will experience a change in phase due to the difference in μ'_- and μ'_+. The differential phase shift ($\Delta\phi$) is non-reciprocal and in general

$$\Delta\phi = (\mu'_+) - (\mu'_-) \qquad (1)$$

to avoid gyromagnetic resonance loss, values of H_i are usually restricted to the region,

$$H_i < H_{res} - 5\ \Delta H$$
$$H_i > H_{res} + 5\ \Delta H \qquad (2)$$

where H_{res} is the internal static field required for gyromagnetic resonance and ΔH is the resonance linewidth of the ferrimagnetic material employed. At low frequencies, gyrator operation above gyromagnetic resonance can be used to avoid the low field loss region.

Waveguide Devices

If a thin slab of ferrimagnetic material is placed in a rectangular waveguide, as shown in *Figure 1*, and biased with a static field (H_a) we can obtain differential phase shift. The internal static field (H_i) is related to H_a by Kittel's equation,
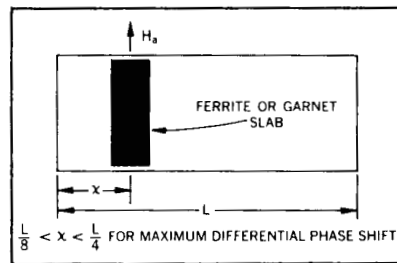

$\frac{L}{8} < x < \frac{L}{4}$ FOR MAXIMUM DIFFERENTIAL PHASE SHIFT

Figure 1

$$H_i = \{[H_a - (N_z - N_x)\ M_s]$$
$$[H_a - (N_z - N_y)\ M_s]\}^{1/2} \qquad (3)$$

where N_x, N_y, N_z are the demagnetizing factors for the ferrite geometry employed.

The slab location is best found experimentally. It has been found that $L/8 < x < L/4$ for maximum differential phase shift. For a given ferrite the amount of phase shift depends on H_i and slab length. The scheme shown in *Figure 2* can be used to increase further the differential phase shift without increasing device length. Here two slabs are placed symmetrically with respect to the center of the waveguide, but oppositely magnetized.
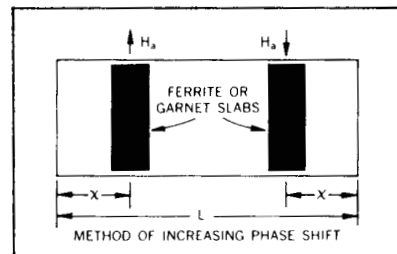

METHOD OF INCREASING PHASE SHIFT

Figure 2

The frequency range of operation may be increased by placing dielectric slabs next to the ferrite or by moving the ferrite from the position of maximum differential phase shift.

For high power applications differential phase shifters are usually designed with a flat slab against the top waveguide wall. This results in increased cooling because of the large area of contact between the ferrite and waveguide wall. The optimum location for this geometry is x = L/4. As shown in *Figure 3*, more than one slab may be employed. Other advantages of this geometry are (1) decreased frequency dependence of differential phase shift, and (2) lower dielectric losses.
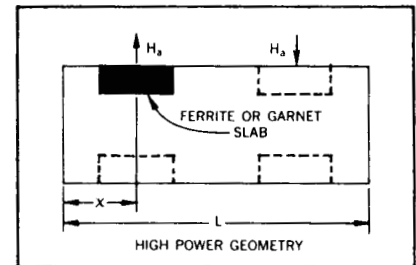

HIGH POWER GEOMETRY

Figure 3

The ratio of differential phase shift to the total attenuation is defined as the figure of merit (F) of the device. A practical formula is:

$$F = \frac{4\omega}{\gamma_{eff}\Delta H} \qquad (4)$$

Narrow resonance linewidth materials will increase the figure of merit. The saturation magnetization ($4\pi M_s$) of the selected material should be such that low field losses do not occur at the frequency of operation.

Summary

The reader may notice a similarity between the design geometry of waveguide gyrators and resonance isolators. Indeed, if the internal static field (H_i) is adjusted for gyromagnetic resonance the gyrator geometries will exhibit good isolator properties.

The selection of the proper ferrite geometry, correct location of the ferrite slab, and choice of a ferrimagnetic material with suitable intrinsic parameters (γ, ΔH, $4\pi M_s$) for the operating frequency desired are the essential factors in gyrator design.

Test for Complex Dielectric Constant

#661 MEASUREMENT PROCEDURES

Introduction

At microwave frequencies the dielectric property (ϵ) or permittivity of ferri-magnets result from the electronic polarizability (α_e) and ionic polarizability (α_i).

Within the temperature—frequency limits of interest to the microwave device engineer, ϵ is essentially constant in microwave ferrimagnetic materials. The residual dielectric losses are taken into account by the complex constant (ϵ^*).

$$\epsilon^* = \epsilon' - j\epsilon'' \qquad (1)$$

where ϵ' is the real part of the permittivity. Energy dissipation can be expressed as $\tan\delta_e = \epsilon''/\epsilon'$. The energy loss is then proportional to ϵ''.

Several methods can be employed to evaluate the ϵ' and ϵ'' of a medium. For microwave ferrimagnetic materials the cavity perturbation technique is gaining general acceptance.

Cavity Method

A TE_{10n} (n odd and 3 or greater) cavity resonant in the X-band region is employed. The loaded Q of the empty cavity should be 2000 or greater. The ferrite sample is in the form of a rod approximately 0.042 inch diameter. It is placed parallel to the microwave electric field in a region of substantially uniform electric and zero microwave magnetic fields. A typical TE_{103} cavity with an
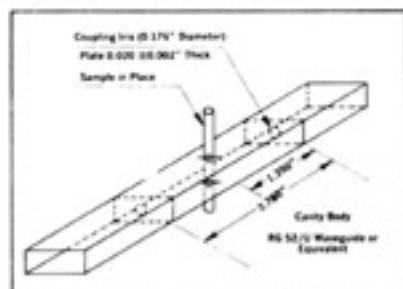

Figure 1

Typical TE_{103} cavity resonant at 9300 mc

empty resonant frequency of 9300 mc is shown in *Figure 1*.

Inserting the sample in the cavity results in (1) a shift of cavity resonant frequency to a lower value, and (2) a reduction of cavity Q. The governing equations are:

$$\frac{\Delta f}{f} = -2(\epsilon' - 1) \cdot \frac{V_s}{V_c} \qquad (2)$$

$$\Delta\left(\frac{1}{Q}\right) = 4\,\epsilon'' \cdot \frac{V_s}{V_c} \qquad (3)$$

where Δf and ΔQ are, respectively, the difference in cavity resonant frequency and cavity Q with and without the sample; f is the resonant frequency of the empty cavity; V_s is the sample volume (within the cavity); V_c is the cavity volume.

It is seen that ϵ' is determined from the cavity resonant frequency shift and ϵ'' found from the reduction of cavity Q.

Measurement

Figure 2 is a schematic diagram of typical equipment required. Power from a suitable unmodulated or amplitude modulated microwave source (A) is run through a variable attenuator (D) and kept at a constant level throughout the measurement with the aid of a directional coupler (E), a crystal detector, and a power indicating meter (F). This constant power is run through a precision variable attenuator (G) to the cavity (H), and the cavity output power is detected and indicated on a suitable meter (I).

Empty Cavity

An attenuation of 3 db is introduced with the precision attenuator. The microwave frequency is adjusted to cavity resonance, as indicated by maximum power output with respect to frequency variation. The indication of the output power level is noted, and the resonant frequency f is measured with a wavemeter, or other suitable means, at (B). The 3 db of attenuation is removed and the two frequencies located at which the output power is the same as at cavity

resonance with the 3 db attenuation in. The separation in frequency of these two half-power points is determined at (B) by a heterodyning technique utilizing a frequency stabilized source (C). The loaded Q of the cavity is then given by $f/\Delta f_{1/2}$ where $\Delta f_{1/2}$ is the frequency separation of the half-power points.

Alternatively, instead of the 3 db of attenuation specified above, a larger amount, α decibels may be used. If Δf is the separation of the two frequencies at which the output power without attenuation is the same as the output power at cavity resonance with the α decibels of attenuation inserted, the Q is given by:

$$Q = \frac{f}{\Delta f}\left(10^{\alpha/10} - 1\right)^{1/2} \qquad (4)$$

By choosing a value of α sufficiently large, it is possible to make the measurement of Δf with a precision wavemeter, eliminating the need of the heterodyning technique.

Sample in Cavity

Repeat the measurements of f and Q. The change in f is the desired Δf, and the change in 1/Q is the desired Δ (1/Q).

The microwave magnetic field is a minimum, but not precisely zero at the sample location. This can introduce magnetic loss into the measurement. A suitable magnetic bias can be applied to the ferrite to avoid this loss contribution.

Reference

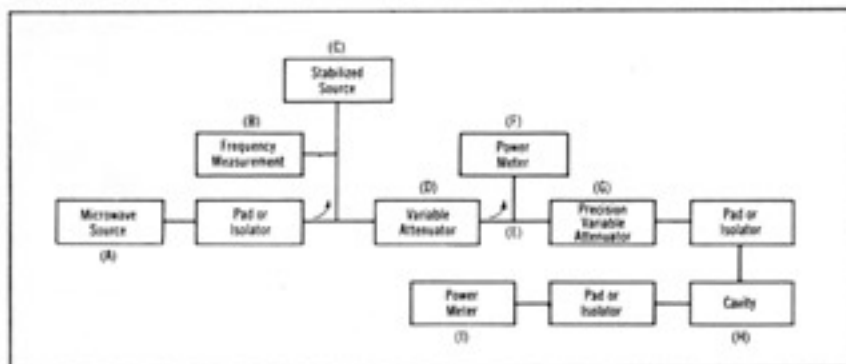American Society for Testing and Materials (ASTM) tentative standard C525-63T.

Figure 2

Diagram of typical equipment set up

Test for Line Width and Gyromagnetic Ratio

#662 MEASUREMENT PROCEDURES

Introduction

At a constant microwave frequency ($\omega = 2\pi f$), ferrimagnets exhibit electromagnetic energy absorption that is a function of the internal static magnetic field (H_i). Maximum absorption occurs when the precession frequency and direction of the elementary magnetic dipoles equals that of the incident microwave magnetic field. The magnitude of H_i (H_r) required to obtain maximum absorption—the ferromagnetic resonance condition—can be computed from the equation:

$$\omega = \gamma_{eff} H_r \qquad (1)$$

where γ_{eff} is the effective gyromagnetic ratio. For a spherical test specimen H_i is independent of the material magnetization and may be taken as equal to the applied DC magnetic field.

The ferrimagnetic resonance line width (ΔH) is defined as the separation of the two H_i values at which the power absorbed by the ferrimagnet is equal to $\frac{1}{2}$ the maximum absorption.

Cavity Method

A TE$_{10n}$ (n even) cavity resonant in the X-band region is employed. The loaded Q (Q_o) of the empty cavity should be 2000 or greater. The test sample is a sphere approximately 0.040 inch diameter. The cavity technique requires that the sample be small compared to $\frac{1}{4}$ of the wave length (λ) of the microwave radiation within it:

$$\lambda = 3 \times 10^4/f(\epsilon')^{\frac{1}{2}} \text{ [cm]} \qquad (2)$$

where f is in megacycles and ϵ' is the dielectric constant.

The sample, mounted on a fused silica or equivalent rod, is positioned away from the cavity wall at a point of minimum microwave electric and maximum microwave magnetic field. A typical TE$_{10n}$ cavity is shown in Figure 1.

The absorption in the specimen is measured by determining the changes of power incident on the cavity required to keep the output power from the cavity at a fixed reference level. It is necessary that the microwave frequency be adjusted to cavity resonance for all measurements. The variations in input power may be characterized by the variations of the attenuation inserted between a monitored source and the cavity in order to maintain the reference output level. If α_o is this attenuator
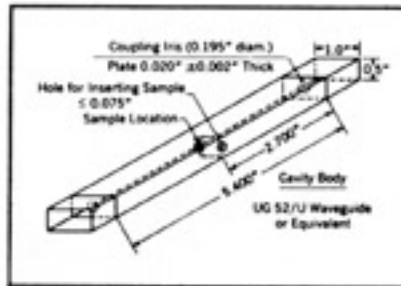

Figure 1
Typical TE$_{10n}$ cavity resonant at 9300 mc

reading in decibels with no sample present, and α_r is this reading for maximum specimen absorption, then the reading corresponding to a specimen absorption of half the resonance value is given by the equation:

$$\alpha_{\frac{1}{2}} = \alpha_o + 20\log2 - 20\log(10^{(\alpha_o - \alpha_{r/m})} + 1) \qquad (3)$$

Measurement

Figure 2 indicates typical equipment required. Power from a suitable microwave source (A) unmodulated or with amplitude modulation, but free of frequency modulation, is fed through a precision variable attenuator (F) to the cavity (G) and the output power is detected and indicated on a suitable meter (H). The power incident on (E) is monitored by directional coupler (D) and a crystal detector. This incident power is kept constant throughout the measurement by variable attenuator (C). The microwave frequency must be adjusted to cavity resonance for all measurements, as indicated by maximum power output with respect to frequency variation. A homogenous adjustable DC magnetic field is applied across the sample region perpendicular to the microwave magnetic field.

The test procedure is: (1) with no specimen present establish an input level α_o measured at (E) on the precision attenuator, and an output level measured at (H). Take this output level as a reference for the remaining measurements. Insert specimen into cavity and vary external magnetic field until the point of maximum specimen absorption is found, as indicated by minimum transmission. Now determine the microwave frequency f, and magnetic field H_r. Thus, f may be measured with a wave meter at (B), and H_r by a rotating coil fluxmeter, etc. The gyromagnetic ratio may be computed by means of Eq. 1. This characteristic may also be given in terms of $g_{eff} = \gamma_{eff} \cdot 2mc/e$, (MKS units).

(2) Determine the attenuation, α_r, required to obtain the reference output level at resonance. Compute the attenuation, $\alpha_{\frac{1}{2}}$, required to obtain the reference output level at the half-power points of specimen absorption from Eq. 3. Insert this amount of attenuation with the precision attenuator, and determine the magnetic field at the two points at which the output reaches the reference value. The difference in the magnetic fields at these two points is the ferrimagnetic resonance line width, ΔH.

(3) The value of ΔH and H_r obtained from these measurements must, in addition to Eq. 2, satisfy the equation:

$$\alpha_o - \alpha_r \cong 20\log(1 + 0.06\, Q_o \Delta H/H_r) \qquad (4)$$

If Eq. 4 is not satisfied, then the sphere diameter must be reduced until the loss difference meets the above requirement.

Reference

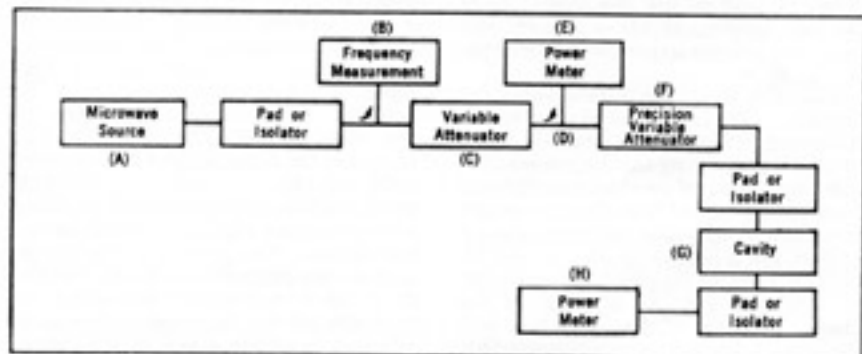American Society for Testing and Materials (ASTM) tentative standard C524-63T.

Figure 2
Diagram of typical equipment set up

Test for Saturation Magnetization

#663 MEASUREMENT PROCEDURES

Introduction

The room temperature saturation magnetization ($4\pi M_s$) of a ferrimagnet is an intrinsic characteristic that is important to the microwave device engineer. He utilizes the saturation magnetization as a design parameter that enters into the initial selection of a ferrimagnetic material for microwave device applications. Typical ferrimagnets exhibit values of $4\pi M_s$ between 300 and 5000 gauss.

Static or low frequency methods are generally employed to measure $4\pi M_s$. The technique described below for the measurement of $4\pi M_s$ has been gaining general acceptance.

Magnetometer Method

The test specimen is a sphere approximately 0.100 inch diameter. When placed in a uniform strong D.C. magnetic field, the sphere becomes uniformly magnetized in a direction parallel to the applied field. External to the sphere the field resulting from this magnetization is exactly that of a magnetic dipole located at the center of the sphere oriented parallel to the magnetization. The strength of this dipole field is proportional to the magnetic moment of the sphere, that is, to M_sV, where V is the volume of the sphere.

If R_1 is the reading for the strength of the dipole field of one sphere of magnetization M_1 and volume V_1, and R_2 is the reading for a second standard sphere (say nickel) of magnetization M_2 and volume V_2, then

$$\frac{R_1}{R_2} = \frac{M_1V_1}{M_2V_2} = \frac{M_1d_1^3}{M_2d_2^3} \quad (1)$$

where d_1 and d_2 are the diameters of the two spheres. If M_2 is known, this equation permits experimental determination of M_1.

Figure 1 shows an arrangement for measuring the saturation magnetization of spheres of ferrimagnets. Such a device is called a vibrating sample magnetometer. By means of an electromechanical transducer (A) and tube (B), the sample is vibrated vertically between pickup coils (C) in a horizontal D.C. magnetic field. A suitable frequency of vibration may be 100 cps. As a result of the changing linkage of the dipole flux with the coils, a signal is induced in the coils at the vibration frequency. The coil arrangement shown is one of several
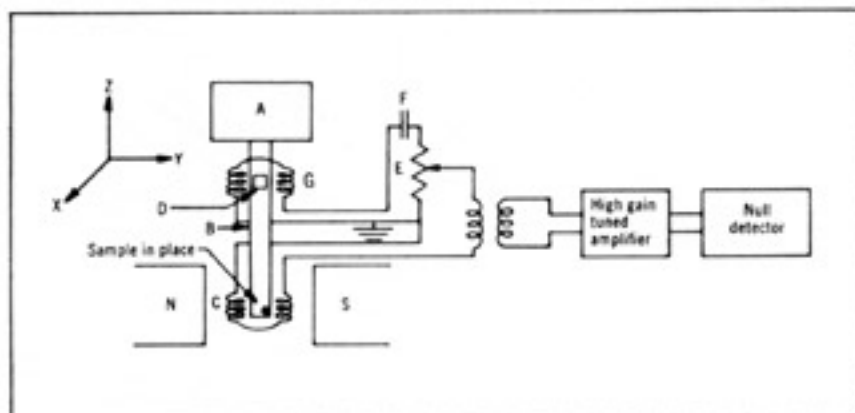

Figure 1

Diagram of typical vibrating sample magnetometer set up

satisfactory ones. In this case the two coils are connected in series opposition with respect to stray fields; the signal voltages in the two coils will then add. The size of this "specimen signal" is proportional to the magnetic moment of the ferrimagnet under test.

A small D.C. permanent magnet (D) is mounted in the tube outside the D.C. magnetic field and situated between another set of pickup coils (G). This magnet is oriented so that its magnetic moment lies on the line connecting the centers of the two coils. A suitable means is provided for selecting an adjustable fraction of the "reference signal" from these coils such that the specimen signal is balanced by a measured fraction of the reference signal. One means of accomplishing this is shown in the figure. The fraction of the reference signal used is chosen by the precision potentiometer (E) and the reading of the potentiometer dial is proportional to the fraction. This signal is combined 180° out of phase with the specimen signal by means of the transformer. The capacitor (F) resonates the inductance of the reference coils, thereby avoiding an undesirable phase difference between the specimen and reference signals applied to the transformer. The strength of the dipole field is thus proportional to the reading R of the potentiometer dial when the fraction of the reference voltage is adjusted to obtain a null in the output of the amplifier. The amplifier is tuned to the vibration frequency.

Measurement

(a) Attach the specimen at the end of the rod and cause it to vibrate perpendicular to the D.C. magnetic field. To minimize dependence on the specimen position, center the specimen with respect to the coils by positioning for a minimum of specimen signal with respect to motion in the Y direction and for a maximum with respect to motion in the X and Z directions. Determine the reading R corresponding to the fraction of the reference signal required to balance out the specimen signal.

(b) The measurement of saturation magnetization requires that the specimen be saturated. For most microwave ferrites, a satisfactory criterion for saturation is that a decrease in the applied D.C. magnetic field by 25 percent shall result in no more than a 1 percent decrease in the indication, R.

(c) The $4\pi M_s$ of the unknown ferrite specimen may then be calculated from Equation 1. A suitable material for the standard specimen is pure nickel. The saturation induction of pure nickel at room temperature is 6070 gauss. This value applies to a nonporous specimen of density 8.90 g/cm³.

References

American Society for Testing and Materials (ASTM) tentative standard C527—63T.

Foner, S., "Versatile and Sensitive Vibrating-Sample Magnetometer," Rev. Sci. Instr., Vol. 30, 1959, pp. 548-557.

Test for Hysteresis Loop Properties

#664 MEASUREMENT PROCEDURES

Introduction

The hysteresis loop of ferrimagnets employed in logic and memory core applications has been intensively studied during the past fifteen years. A rectangular hysteresis loop, providing two stable oppositely directed remanent magnetization states, is the major engineering feature of these materials.

Recently, the microwave device engineer has utilized the rectangular loop property exhibited by certain microwave ferrimagnets in the design of a number of digital or "latching" ferrite phase shifters. These are currently finding use in high power, electronically scanned radar antenna arrays.

Measurement of the dynamic hysteresis loop characteristics of microwave ferrimagnets can be used for design and quality control purposes. A convenient method of making these measurements by means of an oscilloscope loop tracer is described below.
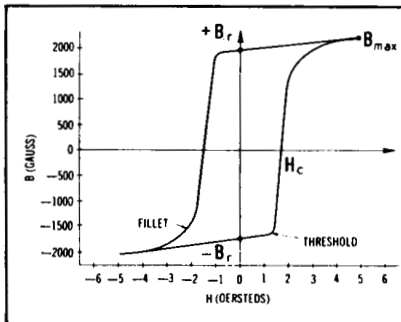

Figure 1

Typical hysteresis loop of a microwave ferrimagnet used in digital phase shifters

Oscilloscope Method

Figure 2 shows a typical measuring circuit. It includes a means for impressing upon the vertical input of the CRO a signal which is proportional to the flux density (B) in the test specimen; and upon the horizontal input of the CRO a signal which is proportional to the magnetizing force (H) acting on the specimen under test.

The primary circuit consists of a signal source, a winding of N_p turns on the test specimen, and a resistor, R_p.
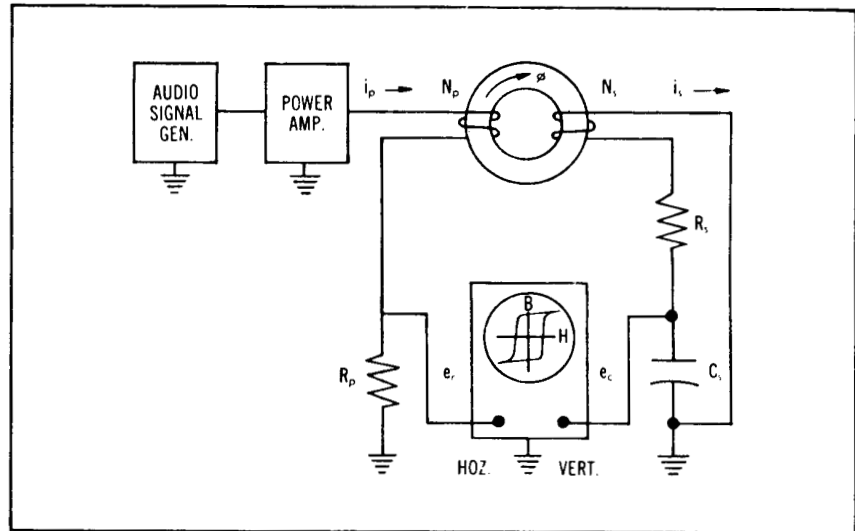

Figure 2

Diagram of dynamic hysteresis loop equipment

The instantaneous voltage drop (e_r) across R_p is applied to the horizontal deflection terminals of the CRO. e_r is related to the magnetizing force (H) by the equation:

$$e_r = \frac{R_p \, lm}{0.4 \, \pi \, N_p} \bullet H \qquad (1)$$

where lm is the mean length of the test specimen magnetic path.

The secondary circuit contains a winding of N_s turns on the test specimen, and an RC integrating network. The instantaneous voltage (e_c) developed across the capacitor is applied to the vertical deflection terminals of the CRO. If $R_s >> 1/\omega C_s$ (app. 250:1), the voltage drop across C_s is related to the magnetic flux density (B) in the test specimen by the equation:

$$e_c = \frac{N_s \, A}{10^8 \, R_s \, C_s} \bullet B \qquad (2)$$

where A is the active cross sectional area of the specimen.

Measurement

Equations (1) and (2) indicate that the pattern displayed on the CRO will represent the dynamic hysteresis loop of the test specimen if the CRO amplifier bandwidths are adequate. For rectangular loop ferrimagnets the amplifiers should be capable of handling up to the 20th harmonic of the test frequency.

The hysteresis loop properties of interest may be read directly from the CRO screen and a photograph made for permanent records. These include data on the coercive force (H_c), remanent flux density (B_r), and squareness ratio defined as B_r/B_{max} where B_{max} is the maximum flux density obtained at the highest value of magnetizing force employed. A typical dynamic hysteresis loop obtained by the oscilloscope method is shown in *Figure 1*. A sharp and well defined threshold gives rise to a distinct value of H that will produce the onset of magnetic flux switching. A small fillet is instrumental in minimizing the amount of energy required for switching. The time required for the magnetic flux to switch from $-B_r$ to $+B_r$ is inversely proportional to the magnetizing force (for $H \geq 2H_c$). When switching time data is required, pulse techniques are generally employed.

Reference

H. F. Storm, "Magnetic Amplifiers", J. Wiley, New York 1955, pp. 53-58.

Test for Spin Wave Line Width

#665 MEASUREMENT PROCEDURES

Introduction

Microwave device engineers have known for some time that ferrimagnetic materials exhibit nonlinear loss characteristics at high levels of peak microwave power. In general, as shown in *Figure 1*, the high power effects appear as: (1) a saturation of the ferromagnetic resonance line width, and (2) the appearance of a subsidiary absorption peak at values of d.c. magnetic field below that required for the main resonance.
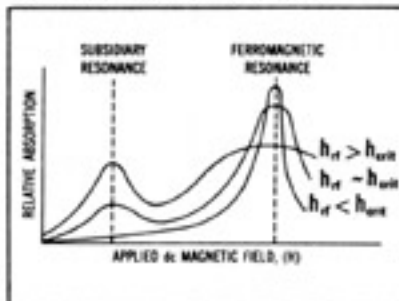

Figure 1
Subsidiary absorption and premature saturation

Present theory suggests that these high power effects arise from power-dependent coupling between the so-called uniform mode of magnetic precession, which is driven by the applied magnetic microwave field (h_{rf}), and certain spin wave modes which become excited if h_{rf} exceeds the instability threshold (h_{crit}). The saturation of the main resonance is caused by spin waves which have the same frequency as that of the h_{rf} field. Other spin waves having a frequency of one-half the signal frequency are responsible for the subsidiary absorption peak.

In recent years, material scientists have preferred to measure the power handling capacity of ferrimagnets by comparing their non-linear thresholds, employing the "parallel pump instability."

Cavity Method

A TE_{10n} (n even) 9300 mc transmission cavity of known characteristics is employed. The test sample is a sphere approximately 0.080 inch diameter, and is positioned away from the cavity wall at a point of minimum microwave electric and maximum microwave magnetic field. In parallel pumping, the d.c. magnetic field (H) is applied parallel to h_{rf}. The value of H field required for the minimum instability threshold is approximately:

$$H = \frac{\omega}{2|\gamma eff|} \quad (1)$$

The magnetic microwave field required for the onset of instability is given by the equation:

$$h_{crit} = \frac{\omega \, \Delta H_k}{|\gamma eff| \, 4\pi M_s} \quad (2)$$

where

ω = operating frequency ($2\pi f$)
γ = gyromagnetic ratio
$4\pi M_s$ = saturation magnetization
ΔH_k = spin wave line width

Since there is, at present, no way of calculating ΔH_k of a polycrystal ferrimagnet, h_{crit} must be found experimentally.

The onset of ferrimagnet nonlinearity can be observed quite easily by noting the distortion of the trailing edge of a high power pulse after transmission through the test cavity, as shown in *Figure 2*. The critical value of h_{rf} can be determined from a knowledge of the test cavity parameters using the equation (MKS units):

$$(h_{rf})^2 = \frac{P_{diss} \, Q_u}{\omega_o \mu_o \frac{V}{4} \left(\frac{\lambda_g}{\lambda}\right)^2} \quad (3)$$

where

P_{diss} = microwave power dissipated in the cavity without the ferrimagnet.
Q_u = the unloaded Q of the cavity.
V = volume of the cavity.
λ_g = cavity wave length
λ = free space wave length
μ_o = free space permeability
ω_o = cavity resonant frequency

Measurement

Figure 3 indicates typical equipment required. Pulsed power from a tunable magnetron (A) is fed through a ferrite
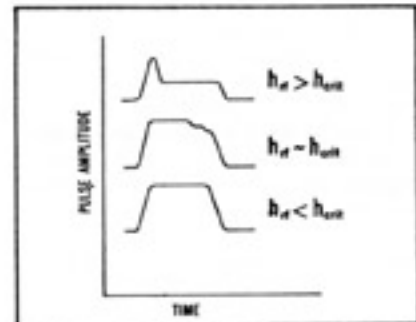

Figure 2
Pulse deterioration at onset of subsidiary resonance

isolator (B) and a power divider (C). The unused power is dissipated in load (D). The average power incident on the test cavity (E) is measured with the decoupled power circuit (F). The transmitted pulse is monitored at the decoupled CRO circuit (G). The d.c. magnetic field is adjusted with the aid of equation (1) to cause pulse deterioration at a minimum value of incident power. The corresponding value of microwave magnetic field ($h_{rf} \sim h_{crit}$) is then calculated from equation (3), which allows ΔH_k to be calculated from equation (2).

Reference

J. F. Ollom and W. H. von Aulock, "Measurement of Microwave Ferrites at High Signal Levels", I.R.E. Transactions on Instrumentation, Vol. 1-9, Sept. 1960, pp 187-193.
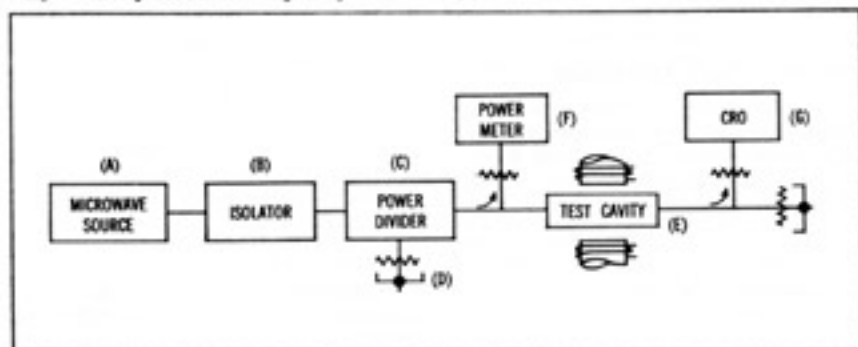

Figure 3
Diagram of typical equipment set up

Test for Switching Coefficients

#666 MEASUREMENT PROCEDURES

Introduction

The rectangular loop property exhibited by certain microwave ferrimagnets is utilized in the design of a number of digital or "latching" ferrite phase shifters. Tech-Briefs No. 664 described a measurement technique to obtain the coercive force (H_c), remanent flux density (B_r), and squareness ratio (R_s) of rectangular loop ferrimagnets. Another useful parameter of these materials, obtained experimentally as a constant of proportionality between magnetizing force and speed of magnetic flux reversal, is known as the switching coefficient (S_w).

Figure 1

Diagram of typical equipment set up

The time required for the magnetic flux to switch from $-B_r$ to $+B_r$ in a toroidal core is inversely proportional to the magnetizing field (H), for amplitudes of H greater than approximately twice the coercive force. Current theory suggests that the magnetic dipoles are reversed or switched in this region by a non-uniform rotation mechanism. A convenient method of measuring the switching coefficient is described below.

Oscilloscope Method

A typical measuring circuit is shown in *Figure 1*. Three separate coils are placed around a thin-wall toroidal specimen. They comprise: (1) a block winding through which a 10 μsec duration current pulse (i_b) of constant amplitude, equal to about ten times the specimen coercive force, is passed; (2) a read winding for a 10 μsec duration current pulse (i_r), controllable in amplitude from about one to ten times the specimen

coercive force; and (3) a readout winding to obtain the output voltage waveform on a CRO screen at point A; or if followed by an integrating network, to obtain the magnetic flux waveform at point B.

Alternate block and read pulses are applied approximately 100 times per second. As the read pulse magnitude is varied, the switching time (t_s) is measured as the 10% points of the output voltage waveform at A; or as the 10% to 90% points of the magnetic flux waveform at B. Values of S_w obtained from output voltage are about 1.5 times greater than those obtained from mag-

netic flux measurements. A preferred method has not been established; therefore the technique of measurement should always be specified.

Figure 2

Typical plot of switching time for a microwave ferrimagnet used in digital phase shifters

$$S_w \equiv \frac{\Delta H}{\Delta \frac{1}{t_s}} \ (oe \cdot \mu sec)$$

Measurement

The dependence of the switching time on the magnetizing field ($H = Ni_r/lm$, where lm is the mean toroid circumference) is most clearly presented by plotting $1/t_s$ as a function of H. When this is done a linear curve is obtained, as shown in *Figure 2*. The experimental relationship may be adequately represented by the equation:

$$S_w = t_s (H - H_o) \qquad (1)$$

H_o and S_w are constants for a given ferrimagnet. The threshold field strength (H_o) is slightly larger than the coercive force of the ferrimagnet and may be termed the threshold for non-uniform rotation flux reversal.

In general, both S_w and H_o decrease with increasing temperature. Typical values of S_w for rectangular loop ferrimagnets, obtained from the output voltage waveform, range between 0.5 and 1.5 oe·μsec. The switching coefficient (S_w) can be considered as the additional field strength in excess of H_o required to switch the magnetic flux between $-B_r$ and $+B_r$ in one microsecond. Thus, a small value of S_w denotes a ferrimagnet with a rapid pulse response. For materials with the same H_o (or same coercive force) a decrease in S_w will result in a faster switching time at a given H field.

Application

In the design of latching ferrite phase shifters the digital bit geometry and switching speed are dictated by system requirements. H_o and S_w are of use to the microwave device engineer because they enter into the calculation of switching power needed to meet the system specifications.
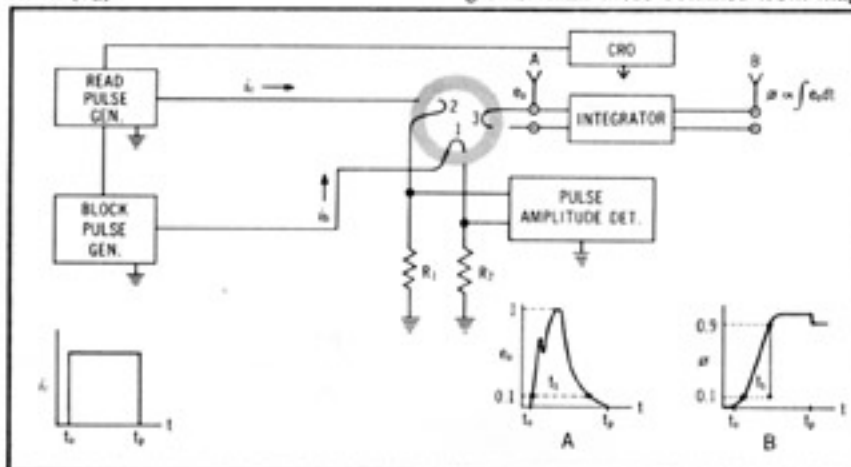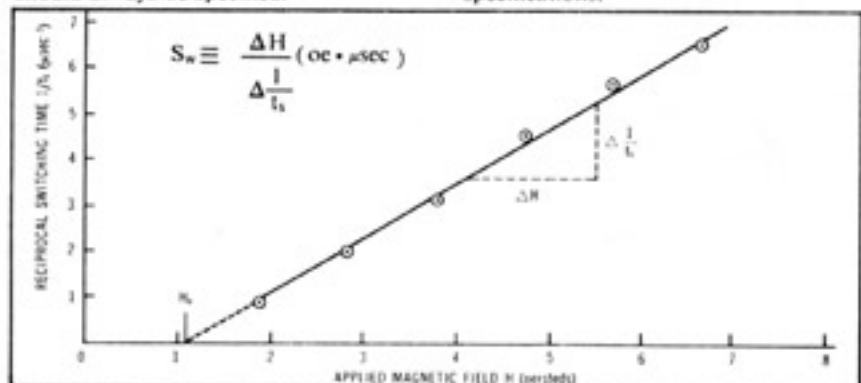
Trans-Tech
Ceramics and Advanced Materials